

POLYMERS AND PEPTIDES ATTACHED TO TERMINALLY  
FUNCTIONALIZED SELF-ASSEMBLED MONOLAYERS:  
SYNTHESIS, CHARACTERIZATION, AND  
MOLECULAR ARCHITECTURE

By

KENTIN L. ALFORD

A thesis submitted in partial fulfillment of  
the requirements for the degree of

MASTER OF SCIENCE IN CHEMISTRY

WASHINGTON STATE UNIVERSITY  
Department of Chemistry

DECEMBER 2005

To the Faculty of Washington State University:

The members of the Committee appointed to examine the thesis of  
KENTIN L. ALFORD find it satisfactory and recommend that it be accepted.

---

Chair

---

---

## **ACKNOWLEDGMENT**

The successful completion of this thesis is due to various contributions from a multiple of individuals. I am eternally grateful to Dr. Glen E. Fryxell for his guidance and willingness to help me be successful. I may never be able to fully express my gratitude. I also appreciate the contributions and periodic encouragement from Dr. William D. Samuels. I am fortunate and thankful to have had the opportunity to work and collaborate with a number of colleagues relating to this research: Kevin Simmons, Dr. Peter C. Rieke, Dr. Manish M. Shah, Roger Voise, Kirk Bigelow, and Marisol Avila.

I would like to thank Associated Western Universities for the fellowship opportunity at Battelle, Pacific Northwest National Laboratories (PNNL), under which this research opportunity was possible. I would also like to acknowledge and thank the United States Army Armament Research Development & Engineering Center (ARDEC), Battelle's Laboratory Directed Research Division, and Battelle Memorial Institute for their financial support for this research and the development of new self-assembled monolayer technologies.

To my family and friends, I thank you for your unwavering support and encouragement. A special thanks to my mother and father for consistently reminding me that I am capable of many things. Finally, to my wife Randee, I am forever grateful for your patience, understanding, and endless support.

POLYMERS AND PEPTIDES ATTACHED TO TERMINALLY  
FUNCTIONALIZED SELF-ASSEMBLED MONOLAYERS:  
SYNTHESIS, CHARACTERIZATION, AND  
MOLECULAR ARCHITECTURE

by Kentin L. Alford, M.S.  
Washington State University  
December 2005

**ABSTRACT**

Chair: Kirk Peterson

Covalent attachment of a material to a solid surface is desirable for a wide variety of applications; molecular recognition studies, sensor design, composite material synthesis or surface property manipulation. The use of terminally functionalized self-assembled monolayers (SAMs) as a foundation upon which to build chemically elaborate interfacial architectures was examined. To this end, peptides, oligonucleotides, oligomers, polymers, initiators and curing agents have been anchored to various SAM interfaces and their behavior examined. Ellipsometry, fluorescence, wetting contact angle measurements and electron microscopy (among others) were routinely employed to monitor attachment of these materials to the monolayer interface. Some of the useful properties (antimicrobial activity, composite material enhancement, interfacial wettability control, etc.) of these functionalized organic thin films will be summarized.

# TABLE OF CONTENTS

ACKNOWLEDGMENT.....	iii
ABSTRACT.....	iv
LIST OF TABLES.....	xi
LIST OF FIGURES.....	xviii
1 INTRODUCTION.....	1
1.1 Antimicrobials.....	2
1.2 Oligonucleotides.....	3
1.3 Composite Materials.....	4
1.4 References.....	5
2 SELF-ASSEMBLED MONOLAYER BACKGROUND.....	6
2.1 Brief Background of SAM Chemistry.....	7
2.2 Methodology of Self-Assembled Monolayers.....	9
2.3 Surface Cleansing Treatment to Increase Reactivity.....	13
2.4 Characterization of SAM Formation.....	14
2.4.1 Ellipsometry.....	15
2.4.2 Contact Wetting Angle.....	16
2.4.3 Scanning Electron Microscopy.....	18
2.4.4 Fluorescence.....	19
2.5 References.....	19
3 PEPTIDES AND ENZYMES.....	23

3.1	Introduction.....	23
3.2	Objective and Background.....	23
3.3	Results and Discussion .....	24
3.3.1	Experiment 1: $\beta$ -Amyloid and Catalase Attachment to NCO SAM on Silicon Wafers.....	24
3.3.2	Experiment 2: Various Peptide Attachment to Silicon Treated Substrates	30
3.4	Conclusions.....	30
4	ANTIMICROBIALS .....	31
4.1	Introduction.....	31
4.2	Objective and Background.....	32
4.2.1	E. coli Cell Viability .....	32
4.2.2	AMC Microscope Imaging .....	33
4.2.3	Ellipsometry and Contact Wetting Angle Measurements.....	33
4.2.4	Absorbance Measurements (Antimicrobial Wafers Inoculated with E. coli Bacteria)	33
4.2.5	Antimicrobials.....	34
4.3	Results and Discussion .....	36
4.3.1	Experiment 1: Antimicrobials Attached to Silicon Wafers Treated with Isocyanatopropyl Triethoxysilane (NCO).....	36
4.3.2	Experiment 2: Antimicrobials Attached to Silicon Wafers Treated with Isocyanatopropyl Triethoxysilane (NCO) - repeat .....	43

4.3.3	Experiment 3: Attachment and Effectiveness of a Variety of Antimicrobials on Silicon Wafers.....	46
4.4	Conclusions.....	49
4.4.1	E. coli cell viability.....	49
4.4.2	AMC Microscope Imaging.....	50
4.4.3	Ellipsometry, Contact Wetting Angle and Optical Density Measurements	50
4.4.4	Absorbance measurements.....	51
4.5	References.....	52
5	OLIGONUCLEOTIDES.....	53
5.1	Introduction.....	53
5.2	Objective and Background.....	53
5.3	Results and Discussion.....	54
5.3.1	Ellipsometry and Contact Angle Measurement of Silicon Wafers Before and After SAM Attachment.....	54
5.3.2	Experiment 2: Fmly 2.1 - 2.4 Nucleotide Attachment on Treated Silicon in a Glass Vial.....	58
5.3.3	Experiment 3: Fmly 2.1 - 2.4 Nucleotide Attachment on Treated Silicon Using a Modified Well Plate.....	66
5.3.4	Experiment 4: SBH 3.1 - 3.12 Oligonucleotide Attachment to a Silicon Treated Substrate Using a Modified Well Plate.....	70

5.3.5	Experiment 5: Wetting Properties of Silicon Wafers with a Fluorescently Labeled Protein .....	76
5.3.6	Experiment 6: Fluorescein-Labeled SBH Oligonucleotides on NCO Treated Silicon Wafers Using a Modified Well Plate .....	81
5.3.7	Experiment 7: Re-establishing the Wettability of Silicon Wafers Using DMF: H <sub>2</sub> O (5:2) as a Solvent.....	85
5.3.8	Experiment 8: A Fluorescein Labeled Oligonucleotide (SBH 3.1) on Treated and Untreated Silicon Wafers to Verify Covalent Attachment .....	87
5.3.9	Experiment 9: Repeat of Fluorescein Labeled SBH 3.1 Oligonucleotide on Treated and Untreated Silicon Wafers.....	92
5.3.10	Experiment 10: Attachment of SBH 3.1 and 3.10 Oligonucleotides With a Fluorescent Label on 3 x 1 Inch Silicon Wafers.....	97
5.3.11	Experiment 11: Attachment of SBH 3.1 and 3.10 Oligonucleotides (no label) on 3 x 1 Inch Silicon Wafers .....	100
5.4	Conclusion .....	102
6	COMPOSITES.....	103
6.1	Introduction.....	103
6.2	Methodology.....	107
6.3	General Procedure.....	107
6.3.1	Procedure for Fabrication of SAMs on Glass Fabrics .....	107
6.3.2	Panel Fabrication <sup>100</sup> .....	108
6.3.3	Test Specimen Part Fabrication <sup>100</sup> .....	110



6.3.4	Testing <sup>101</sup> .....	111
6.4	Results and Conclusions .....	125
6.5	References.....	128
7	EXPERIMENTAL SECTION .....	129
7.1	General SAM Deposition Procedure .....	129
7.2	Enzymes and Proteins .....	130
7.2.1	Experiment 1 .....	130
7.2.2	Experiment 2.....	130
7.3	Antimicrobials.....	131
7.3.1	Materials .....	131
7.3.2	Antimicrobial Preparation and Attachment .....	131
7.3.3	Experimental Detail .....	132
7.4	Oligonucleotides .....	136
7.4.1	Experiment 1 .....	136
7.4.2	Experiment 2.....	137
7.4.3	Experiment 3.....	137
7.4.4	Experiment 4.....	138
7.4.5	Experiment 5.....	139
7.4.6	Experiment 6.....	140
7.4.7	Experiment 7.....	141
7.4.8	Experiment 8.....	142
7.4.9	Experiment 9.....	143

7.4.10	Experiment 10.....	143
7.4.11	Experiment 11.....	144

## LIST OF TABLES

Table 3.3.1A: Silicon wafer ellipsometry ( $\text{\AA}$ ) and wetting contact angle (degrees) measurements prior to any treatment or cleaning in isopropanol (number of measurements vary). Wafers 1 and 2 were wafers removed from racks which were to be cleansed with isopropanol, KOH, and then $\text{HNO}_3$ for subsequent NCO SAM deposition. Solution A and Solution B were two separate NCO solutions prepared for comparison purposes. ....	25
Table 3.3.1B: Silicon wafer ellipsometry ( $\text{\AA}$ ) and contact angle (degrees) measurements after NCO attachment. Solution A was used for the deposition (refer to Table 3.3.1A). Wafers 1 and 2 were wafers removed from racks which were cleansed with isopropanol, KOH, $\text{HNO}_3$ and then exposed to Solution A for NCO SAM deposition. ....	26
Table 3.3.1C: Silicon wafer ellipsometry ( $\text{\AA}$ ) and contact angle (degrees) measurements after doping in $\beta$ -Amyloid solution (1-2 mg $\beta$ -Amyloid in 10 mL water). ....	26
Table 3.3.1D: Silicon wafer ellipsometry ( $\text{\AA}$ ) and contact angle (degrees) measurements after doping in Catalase solution ( $\sim$ 1 mL Catalase in $\sim$ 10 mL of water). Water spots dispersed droplets unevenly and in an unordered, random shape that hindered accurate wetting angle measurements. ....	27
Table 3.3.1E: Silicon wafer ellipsometry measurement averages for Tables 3.3.1 - 4. Measurements for thickness recorded in $\text{\AA}$ . Overall average is the average of both sample measurements (Wafer 1 and 2) obtained. The exception is the overall	

average for Prior to treatment - Solutions A and B. In this case, the overall average is calculated using both Wafer 1 and 2 from Solution A and B. Thus, the overall average is the average of all four wafers. .... 27

Table 3.3.1F: Silicon wafer contact wetting angle measurement averages for Tables 3.3.1A – D. Units for wetting angles are in degrees. Overall average is the average of both sample measurements (Wafer 1 and 2) obtained. The exception is the overall average for Prior to treatment - Solution A and B. In this case, the overall average is calculated using both Wafer 1 and 2 from Solution A and B. Thus, the overall average is the average of all four wafers. .... 28

Table 3.3.1G: Difference values for treated and untreated silicon samples after attachment of  $\beta$ -Amyloid and Catalase. Value used to calculate thickness difference ( $\text{\AA}$ ) for both samples was 32.4  $\text{\AA}$ , which is the overall thickness average after NCO attachment. Value used to calculate contact angle difference is 64.9 degrees, which is also the overall wetting angle (degrees) average after NCO attachment. .... 28

Table 3.3.1H: Average  $\beta$ -Amyloid and Catalase Enzyme Ellipsometry ( $\text{\AA}$ ) and Contact Wetting Angle (degrees) Measurements..... 29

Table 4.3.1A: Antimicrobial SAM ellipsometry measurements on antimicrobial coated silicon wafers with NCO SAM as the attaching linker ( $\text{\AA}$ ). .... 37

Table 4.3.1B: Optical density absorbance measurements of the solution of antimicrobial-coated silicon wafers at 600 nm after inoculation with E. coli-TSB solution at various time intervals. .... 42

Table 4.3.1C: Ellipsometry measurements ( $\text{\AA}$ ) on antimicrobial coated silicon wafers with NCO SAM as the attaching linker after being inoculated with E. coli bacteria in a 37° Celsius water bath with continuous shaking over a 29 hour period. Measurements taken after a 29 hour period.....	43
Table 4.3.2A: Ellipsometry ( $\text{\AA}$ ) results on NCO coated silicon wafers after ~3.5 hour SAM deposition time.....	44
Table 4.3.2B: Static contact angle (degrees) results on NCO coated silicon wafer after ~3.5 hour SAM deposition time.....	45
Table 4.3.2C: Ellipsometry measurements ( $\text{\AA}$ ) of antimicrobial coated silicon wafers with NCO SAM as the attaching linker. Deposition time 18 hours.....	45
Table 4.3.2D: Optical density absorbance measurements at 600 nm on antimicrobial coated silicon wafers at various time intervals (Hours:Minutes) after inoculation with E.Coli-TSB solution . Absorbance measurements conducted on the E.Coli-TSB solution. Control samples (#1 and #2) are blank silicon wafers with no treatment (SAM addition or cleansing). (N/V: No Value. Measurement not taken).....	45
Table 4.3.2E: Ellipsometry measurements ( $\text{\AA}$ ) on antimicrobials attached to NCO coated silicon wafers after inoculation in E. coli-TSB solution 5 hours. (N/V: No Value-measurement not taken; N/D: No Data-value not returned from instrument due to signal loss). .....	46
Table 4.3.3A: Ellipsometry measurements ( $\text{\AA}$ ) on NCO coated silicon wafers after 4 hour SAM deposition time.....	47

Table 4.3.3B: Ellipsometry measurements ( $\text{\AA}$ ) of antimicrobial coated silicon wafers with NCO SAM as the attaching linker. Deposition time was 22 hours. Antimicrobial was bound to NCO SAM on silicon wafer.....	48
Table 4.3.3C: Optical density absorbance measurements at 600 nm on antimicrobial coated silicon wafers at various time intervals (Hours:Minutes) after inoculation with E. coli-TSB solution. Absorbance measurements conducted on the E. coli-TSB solution.....	48
Table 4.3.3D: Ellipsometry measurements ( $\text{\AA}$ ) on antimicrobials attached to NCO coated silicon wafers after inoculation in E. coli-TSB solution 6 hours. (N/D: No Data. Value not returned from instrument due to signal loss).....	49
Table 5.3.1A: Silicon Wafer Ellipsometry and Wetting Contact Angle Measurements Prior to any Treatment or Cleaning in Isopropanol* .....	55
Table 5.3.1B: Silicon Wafer Ellipsometry and Contact Angle Measurements After Isopropanol, Nitric Acid, and Potassium Hydroxide Washes and Drying in Nitrogen Stream* .....	56
Table 5.3.1C: Silicon Wafer Ellipsometry and Wetting Contact Angle Measurements After Isocyanatopropyl Triethoxysilane/Toluene Solution and Drying on Nitrogen Gas Stream.....	56
Table 5.3.1D: Silicon Wafer Ellipsometry Measurement ( $\text{\AA}$ ) Averages from Tables 5.3.1A through C.....	57
Table 5.3.1E: Silicon Wafer Wetting Contact Angle Measurement (degrees) Averages from Tables 5.3.1A through C.....	57

Table 5.3.2A: Fmly 2.1 - 2.4 Nucleotide sample, molecular weight, mass of sample, concentration of solution, and nucleotide sequence. ....	59
Table 5.3.2B: Silicon Ellipsometry Measurements (Å) after Treatment with Isocyanatopropyl Triethoxysilane and Nitrogen Drying. ....	61
Table 5.3.2C: Silicon Contact Wetting Angle Measurements (degrees) after Treatment with Isocyanatopropyl Triethoxysilane and Nitrogen Drying. ....	61
Table 5.3.2D: Sample Fmly 2.1 Ellipsometry Measurements (Å). Sample 1 rinsed with deionized water and nitrogen dried. Sample 2 only nitrogen dried. ....	62
Table 5.3.2E: Sample Fmly 2.2 Ellipsometry Measurements (Å). Units in Å. Sample 1 rinsed with deionized water and nitrogen dried. Sample 2 only nitrogen dried. ....	62
Table 5.3.2F: Sample Fmly 2.3 Ellipsometry Measurements (Å). Sample 1 rinsed with deionized water and nitrogen dried. Sample 2 only nitrogen dried. ....	63
Table 5.3.2G: Sample Fmly 2.4 Ellipsometry Measurements (Å). Sample 1 rinsed with deionized water and nitrogen dried. Sample 2 only nitrogen dried. ....	63
Table 5.3.3A: Fmly 2.1 - 2.4 Nucleotide Sample Ellipsometry Measurements (Å) on Cleansed Silicon Wafers without SAM Attachment. Samples were rinsed with deionized water and dried with nitrogen. ....	67
Table 5.3.3B: Fmly 2.1 - 2.4 Nucleotide Sample Ellipsometry Measurements (Å) on Treated Silicon Wafers with SAM Attachment. Samples were rinsed with deionized water and dried with nitrogen. ....	68
Table 5.3.4A: Oligonucleotide Sample Number and Sequence. ....	72

Table 5.3.4B: Molecular Weight, Mass and Concentration of Oligonucleotide Samples. .....	72
Table 5.3.4C: Ellipsometry Measurements (Å) for Oligonucleotide Samples Prior to Fluorescence Measurements. These samples were not rinsed with deionized water. They were only nitrogen dried.....	73
Table 5.3.4D: Ellipsometry measurements (Å) after being analyzed on FluorImager in deionized water.....	73
Table 5.3.5A: Sequence of Fluorescein-labeled protein attached to silicon wafers.....	77
Table 5.3.5B: Concentration of Fluorescein Sample Solutions.....	77
Table 5.3.5C: Fluorescein excitation and emission wavelengths (nm). ....	77
Table 5.3.6A: Oligonucleotide Sample Name, Molecular Weight, Sequence, and Total Sample Mass.....	82
Table 5.3.6B: Oligonucleotide Sample Total nmoles, Solution Concentration and Total nmoles in 20 and 40 µL Aliquot Samples.....	82
Table 5.3.6C: Oligonucleotide Sample Concentration per square mm in Sample Wells for 20 and 40 µL Aliquot Samples.....	83
Table 5.3.11A: SBH 3.1 and 3.10 Mass (mg) and Concentration (µg/µL). ....	100
Table 5.3.11B: Attachment of SBH 3.1 and 3.10 Average Ellipsometry Measurements (Å) after two consecutive washings with deionized water for 5 minutes with continuous shaking.....	101
Table 6.1A: Contact Wetting Angle Measurements (in degrees) for Monolayer Coated Substrates.....	106



Table 6.3.4.1A: Flexural Modulus Data including sample identification (Id), width, thickness, and flexural modulus (dynes/cm <sup>2</sup> ) and (psi) values.....	113
Table 6.3.4.2A: Short beam shear data. Sample identification, width, thickness, load at failure, displacement maximum load, strain at maximum load, apparent shear strength values and description of break information included.....	116
Table 6.3.4.3A: Tensile Test Data (1/4" R Notched Specimens). Sample identification (Id), width, thickness, sample area (inch <sup>2</sup> ), maximum load, maximum stress, modulus, mean, standard error (S.E.), median, standard deviation (st. dev.), sample variance (variance), range, minimum and maximum sample range, sum and sample count values given.....	119
Table 7.3.3.1A: Antimicrobial Solution Concentration.....	133
Table 7.3.3.1B: Ellipsometry measurements on Silicon Wafers As-Received.....	134
Table 7.3.3.1C: Ellipsometry measurements on Silicon Wafers after Cleansing.....	134
Table 7.3.3.1D: Static Contact Angle measurements on Silicon Wafers after Cleansing .....	134
Table 7.3.3.1E: Ellipsometry measurements on NCO Wafers .....	134

## LIST OF FIGURES

Figure 1A: A 3-demisional space-filling model of a SAM bound to a surface. The red spheres represent a non-hydrolyzable terminal-end group. The blue and green spheres represent a carbon and hydrogen atoms, respectively. The gray spheres represent a silicon atom bound to the surface (gray rectangle). (Figure obtained from Dr. Glen E. Fryxell, Battelle, Pacific Northwest National Laboratory.) .....	2
Figure 2A: Diagram involving the self-assembly of monolayers spontaneously attaching to a hydroxylated surface in an ordered, smooth, thin film. The red spheres are the reactive, polar end groups which interact with the hydroxylated surface. The yellow spheres are the non-reactive terminal group. (Figure obtained from Dr. Glen E. Fryxell, Battelle, Pacific Northwest National Laboratory.).....	6
Figure 2.1A: Steps involved during the self-assembly of monolayers onto a substrate and the reactions which take place. Steps in order of occurrence: hydrolysis, hydrogen bonding, condensation, and then bond formation. ....	9
Figure 2.2A: Chemical reaction of a hydrated silicon surface with silane molecules depicting reactive end groups (X), which reacts, and cross-links with the silicon surface resulting in the derivatized surface.....	10
Figure 2.2B: Description of Silane-based monolayer chemistry. Driving force behind self-assembly from an energetic perspective: van der Waals interactions, head groups/surface interactions, terminal functionality, and siloxane linkages are shown. ....	12

Figure 2.3A: Reaction mechanism of an isocyanate with a primary amine to form an urea linkage. In this reaction, R1 represents the silane bound to an inorganic substrate and R2 represents a carbon chain (singly bonded to the amine). ..... 14

Figure 2.4.2A: Example of contact wetting angle for a hydrophobic, non-wetting surface (left) and a hydrophilic, wetting surface (right). The high contact angle of the hydrophobic surface represents a “beading” of the liquid on the surface..... 18

Figure 4.2.5A: Chemical structures of the four antimicrobials used: Tetracycline, Polymyxin  $\beta$ , Kanamycin, and Nalidixic Acid. .... 35

Figure 4.3.1A: AMC Microscope image of Kanamycin coated silicon wafer after exposure to E. coli-TSB solution 5 hours. .... 38

Figure 4.3.1B: AMC Microscope image of Kanamycin coated silicon wafer after exposure to E. coli-TSB solution 29 hours. .... 39

Figure 4.3.1C: AMC Microscope image of Polymyxin  $\beta$  coated silicon wafer after exposure to E. coli-TSB solution 5 hours. .... 39

Figure 4.3.1D: AMC Microscope image of Polymyxin  $\beta$  coated silicon wafer after exposure to E. coli-TSB solution 29 hours. .... 40

Figure 4.3.1E: AMC Microscope image of Tetracycline coated silicon wafer after exposure to E. coli-TSB solution 5 hours. .... 40

Figure 4.3.1F: AMC Microscope image of Tetracycline coated silicon wafer after exposure to E. coli-TSB solution 29 hours. .... 41

Figure 4.3.1G: AMC Microscope image of NCO-coated silicon wafer (control) after exposure to E. coli-TSB solution 29 hours. .... 41

Figure 5.3.2A: Chemical structures of the four nucleotides in DNA, including Uradine (RNA). The sugar group is attached, but without the phosphate bound to the hydroxyl group on the sugar. .... 59

Figure 5.3.2B: Sample nucleic acid chemical structure and bonding formation for the four various nucleotides labeled T, G, C, A, respectively. Software Development Lab website at <http://dlab.reed.edu/projects/vgm/vgm/VGMProjectFolder/VGM/RED/RED.ISG/chem2.html> ..... 60

Figure 5.3.2C: Blank silicon wafer control (far left) and Fmly samples 2.1 and 2.2 (middle and far right, respectively)..... 64

Figure 5.3.2D: Blank silicon wafer control (far left) and Fmly samples 2.3 and 2.4 (middle and far right, respectively)..... 65

Figure 5.3.3A: Fmly sample 2.1 (upper right corner) and 2.2-2.4 (bottom row, left to right). Fmly control samples 2.1 and 2.2 (top left) is labeled  $\frac{1}{2}$  and Fmly control samples 2.3 and 2.4 (top middle) is labeled  $\frac{3}{4}$ ..... 69

Figure 5.3.4A: FluorImager image of SBH samples 3.1-3.6 shown left to right, top to bottom. Samples dried under ambient air. .... 74

Figure 5.3.4B: FluorImager image of SBH samples 3.7-3.12 shown left to right, top to bottom. Samples dried under ambient air. Samples SBH 3.9 and 3.11 were washed in deionized water prior to imaging. .... 75

Figure 5.3.5A: Fluorescence image of a Fluorescein-labeled  $\beta$ -Amyloid 20 mer attached to a cleansed silicon wafer (1 and 3) and a NCO treated silicon wafer (2 and 4) using

a high sensitivity scan on a FluorImager SI. Fluorescein-labeled  $\beta$ -Amyloid 20 mer wafer samples 1 and 2 were dissolved in a water solution, whereas wafer samples 3 and 4 were dissolved in a DMF solution. On each wafer there are various aliquot sizes deposited onto the secured silicon surface (0.5-25  $\mu$ L). ..... 78

Figure 5.3.5B: Fluorescence image of a Fluorescein-labeled  $\beta$ -Amyloid 20 mer attached to a clean silicon wafer (1 and 3) and a NCO treated silicon wafer (2 and 4) using a high sensitivity scan on a FluorImager SI after being washed with solvent (DMF or deionized water). Fluorescein-labeled  $\beta$ -Amyloid 20 mer wafer samples 1 and 2 were dissolved in a water solution, whereas wafer samples 3 and 4 were dissolved in a DMF solution. On each wafer there are various aliquot sizes deposited onto the secured silicon surface (0.5-25  $\mu$ L). ..... 79

Figure 5.3.6A: FluorImager image of SBH oligomers 3.1, 3.4, 3.7, 3.10 and 3.12 labeled with Fluorescein using a normal sensitivity scan. 20  $\mu$ L aliquots (in 5:2 DMF:water solutions) on cleansed silicon wafers..... 83

Figure 5.3.6B: FluorImager image of SBH oligomers 3.1, 3.4, 3.7, 3.10 and 3.12 labeled with Fluorescein using a normal sensitivity scan. 40  $\mu$ L aliquots (in 5:2 DMF:water solutions) on NCO treated silicon wafers. .... 84

Figure 5.3.7A: FluorImager image of Fluorescein labeled SBH oligonucleotides 3.1, 3.4, 3.7, 3.10, and 3.12 covalently tethered to NCO treated silicon wafers. Various aliquot sizes are visible on each wafer (5.0 to 0.10  $\mu$ L top to bottom). Samples were dissolved in a DMF/water (5:2) solution and secured to a 96-well plate using tape prior to aliquot deposition and imaging. .... 86

Figure 5.3.8A: FluorImager image of Fluorescein-labeled SBH 3.1 oligonucleotide on silicon wafers. Dry labeled samples 1 and 2 are cleansed wafers while labeled samples 3 and 4 are NCO treated wafers. A 2.0  $\mu$ L aliquot is visible on each wafer using a normal sensitivity scan in ambient air. .... 88

Figure 5.3.8B: FluorImager image of Fluorescein-labeled SBH 3.1 oligonucleotide on silicon wafers after a 5 mL DMF/water (5:2) washing. Dry labeled samples 1 and 2 are cleansed wafers while labeled samples 3 and 4 are NCO treated wafers. A 2.0  $\mu$ L aliquot is visible on each wafer using a normal sensitivity scan in ambient air. .... 89

Figure 5.3.8C: FluorImager image of Fluorescein-labeled SBH 3.1 oligonucleotide on silicon wafers after a 20 mL DMF/water (5:2) washing. Dry labeled samples 1 and 2 are cleansed wafers while labeled samples 3 and 4 are NCO treated wafers. A 2.0  $\mu$ L aliquot is visible on each wafer using a normal sensitivity scan in ambient air. .... 90

Figure 5.3.9A: FluorImager image of Fluorescein-labeled SBH 3.1 oligonucleotide on silicon wafers. Dry labeled samples 1 and 2 are cleansed wafers while labeled samples 3 and 4 are NCO treated wafers. A 2.0  $\mu$ L aliquot is visible on each wafer using a normal sensitivity scan in ambient air. .... 93

Figure 5.3.9B: FluorImager image of Fluorescein-labeled SBH 3.1 oligonucleotide on silicon wafers after a ~5 mL DMF: water (5:2) washing. Dry labeled samples 1 and 2 are cleansed wafers while labeled samples 3 and 4 are NCO treated wafers. A 2.0  $\mu$ L aliquot is visible on each wafer using a normal sensitivity scan in ambient air. 94

Figure 5.3.9C: FluorImager image of Fluorescein-labeled SBH 3.1 oligonucleotide on silicon wafers after a 20 mL DMF: water (5:2) washing. Dry labeled samples 1 and

2 are cleansed wafers while labeled samples 3 and 4 are NCO treated wafers. A 2.0  $\mu$ L aliquot is visible on each wafer using a normal sensitivity scan in ambient air. 95

Figure 5.3.10A: FluorImager image of Fluorescein-labeled SBH oligonucleotides 3.1 and 3.10 on silicon wafers producing a 3 x 2 array which alternates from SBH 3.1 to SBH 3.10. The left 3x1 inch wafer sample is cleansed while the right 3x1 inch wafer sample is a NCO treated wafer. 2.0  $\mu$ L aliquot “dots” are visible on each wafer using a normal sensitivity scan in ambient air..... 98

Figure 5.3.10B: FluorImager image of Fluorescein-labeled SBH oligonucleotides 3.1 and 3.10 on silicon wafers producing a 3 x 2 array which alternates from SBH 3.1 to SBH 3.10 after a 20 mL DMF/water (5:2) washing. The left 3x1 inch wafer sample is cleansed while the right 3x1 inch wafer sample is a NCO treated wafer. 2.0  $\mu$ L aliquot “dots” are visible on each wafer using a normal sensitivity scan in ambient air. .... 99

Figure 6.3.1A: Silicon surface derivatized with reactive ends of a SAM molecule, which reacts and cross-links with thermoset materials..... 108

Figure 6.3.2A: Interaction of the epoxy resin with the untreated vs. treated surfaces... 109

Figure 6.3.2B: Interaction of cured epoxy matrix with untreated versus treated surfaces. .... 110

Figure 6.3.4.1A: Flexural modulus average values. .... 114

Figure 6.3.4.1B: Flexural modulus average values including maximum and minimum bars..... 114

Figure 6.3.4.1C: Flexural modulus average values including +/- standard deviation error bars.....	115
Figure 6.3.4.2A: Short beam shear average values (psi). .....	117
Figure 6.3.4.2B: Short beam shear average values (psi) including +/- standard deviation error bars. ....	117
Figure 6.3.4.2C: Short beam shear average values (psi) including maximum and minimum bars. ....	118
Figure 6.3.4.3A: Comparison of Modulus and Strength.....	120
Figure 6.3.4.3B: Tensile Modulus. ....	121
Figure 6.3.4.3C: Scanning electron microscopy (SEM) of Greige Fiber tensile fracture. ....	122
Figure 6.3.4.3D: Scanning electron microscopy (SEM) of Commercial Treatment tensile fracture. ....	123
Figure 6.3.4.3E: Scanning electron microscopy (SEM) of ECH SAM tensile.....	123
Figure 6.3.4.3F: Scanning electron microscopy (SEM) of NCO SAM tensile.....	124
Figure 6.3.4.3H: Scanning electron microscopy (SEM) of GLY SAM tensile fracture. ....	125
Figure 6.4A: Load transfer stress distributions in a single fiber embedded in a matrix material and subjected to an axial load. ....	126



## **Dedication**

*For my Parents and Grandparents, with the hope that I have made them proud*

*and*

*to my nephews, nieces, and children, that they may struggle to do the same.*

# CHAPTER ONE

## 1 INTRODUCTION

Covalent attachment of molecules to a solid surface is desirable for a wide variety of applications: molecular recognition studies, sensor design, composite material synthesis or surface property manipulation, pharmaceutical drug discovery, integrated circuits, environmental remediation, heavy metal recovery/removal, and lubricants.<sup>1</sup> An avenue by which to covalently attach molecules to a solid surface is by use of a self-assembled monolayer.

Self-assembled monolayers have been proven to spontaneously attach in an ordered, smooth, thin film on surfaces such as gold and silicon. The use of terminally functionalized self-assembled monolayers (SAMs) as a foundation upon which to build chemically elaborate interfacial architectures was examined. To this end, anchoring of peptides, enzymes, oligonucleotides, pharmaceuticals, oligomers, polymers, initiators and curing agents to various SAM interfaces was accomplished and their behavior examined. Ellipsometry, fluorescence, and contact wetting angle measurements were commonly employed to monitor attachment of these materials to the monolayer interface. Some of the useful properties (antimicrobial activity, composite material enhancement, interfacial wettability control, etc.) of these functionalized organic thin films will be summarized. A 2-dimensional space filling model of a SAM covalently bound to a surface representing a dense monolayer is shown in Figure 1A.

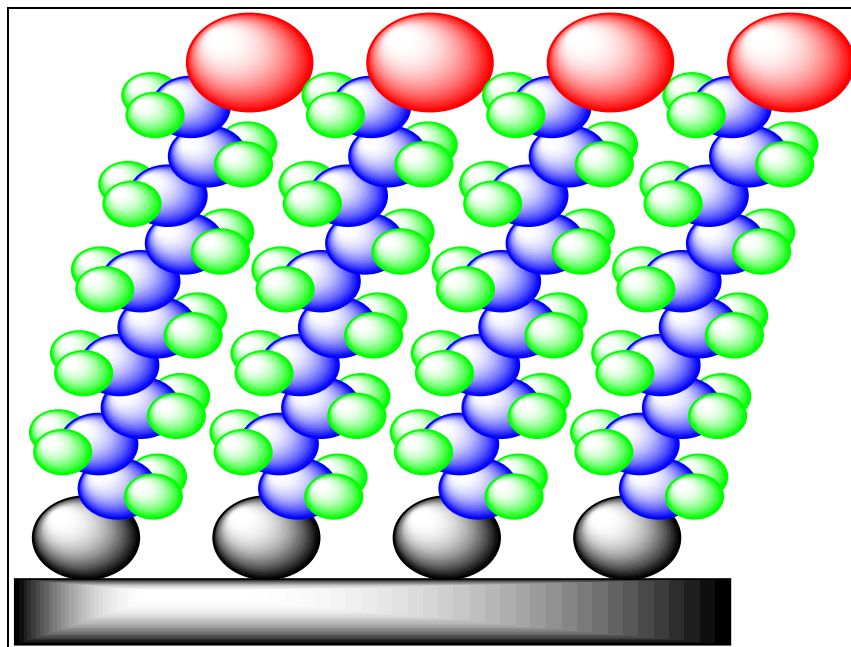


Figure 1A: A 3-demisional space-filling model of a SAM bound to a surface. The red spheres represent a non-hydrolyzable terminal-end group. The blue and green spheres represent a carbon and hydrogen atoms, respectively. The gray spheres represent a silicon atom bound to the surface (gray rectangle). (Figure obtained from Dr. Glen E. Fryxell, Battelle, Pacific Northwest National Laboratory.)

## 1.1 Antimicrobials

Medical devices such as catheters, prosthetics, implants, and other medically invasive devices have certain infection risks associated with them. Hence, infection rates related to these products have continued to rise despite efforts to decrease them.<sup>2-8</sup>

The goal of this study was to impart antimicrobial activity to a surface for possible application to medical devices. To accomplish this goal, demonstrating that it was possible to install an appropriate monolayer to a surface (silicon wafer) and use this monolayer to bind and/or release various antimicrobial agents (phenols, pharmaceuticals, and peptides) was

necessary. A silicon wafer was chosen as the substrate because of the very uniform surface, the extensive SAM studies performed on silicon, and due to the fact that it was a good model to use for proof of concept and allowed ready characterization.

The results will show that antimicrobial activity was demonstrated for some of the agents tested. It will also show that antimicrobial activity required physical contact with the bacterium.

## **1.2 Oligonucleotides**

A sensing array composed of a multitude of biological molecules serving as specific receptor sites has garnered a great deal of attention recently.<sup>9</sup> This concept evolved from the idea of using combinatorial synthetic chemistry approaches to create very large-scale libraries of receptor molecules and to screen the population for enhanced binding activity of individual members of a target of interest. Possible applications for large-scale arrays include sequencing by hybridization, DNA based sensors, medical diagnostics, and nucleic acid oligomer libraries for screening ligand binding.

The objective of this work was to tether oligonucleotides onto a solid flat surface with a low background intrinsic fluorescence. Silicon wafers were selected as the solid surface to attach oligonucleotides because of its extremely low background fluorescence and high uniformity allowing easy detection and characterization. Another advantage of silicon wafers is that they also have low background chemiluminescence. Thus, fluorescent and chemiluminescent labels can be used during DNA-DNA hybridization. The results describe the investigation on the method for covalent attachment of oligonucleotides using isocyanatopropyl triethoxysilane (NCO). Ellipsometry, contact angle, and fluorescence confirmed attachment of the oligonucleotides. The developed method could be made adaptable to automated liquid

handling systems (such as Biomek 2000) to create an array. Retention of bioactivity, strong biorecognition properties, and physically stable arrays are important for constructing biomolecular sensors on surfaces.

### **1.3 Composite Materials**

The use of composite materials is desirable because of the lightweight of the materials and the ability to enhance composite material strength and toughness. However, delamination has been the major cause of structural failure in glass/polymer composites. Delamination is a two-component problem: 1) poor interfacial adhesion from the dissimilarity of the two materials; and 2) incomplete wetting of the glass surface by the thermoset resin, which leads to weak interaction from minimal interfacial contact surface. Other failures in composites such as fiber breakage, matrix cracking, and fiber-matrix debonding also contribute to structural failure. These failures could be reduced, however, if a compliant fiber-matrix interface were synthesized that would increase the load transfer between the fibers and decrease the internal stresses. It has been found that self-assembled monolayers can greatly increase the bond strength between the fiber and the resin matrix of a composite material.<sup>10</sup>

The goal pertaining to the composite materials was to modify the covalent interface of glass fibers (or other reinforcing fibers) to induce strong, uniform, defect-free adhesion between the fibers' surfaces and the polymer matrix. It is hypothesized that a SAM can modify the fiber interface to make it both more wettable (by the polymer phase) and capable of covalently bonding to the polymer molecules. It can create a receptive, hydrophobic interface that the thermoset resin (or polymer precursors) would wet more effectively, leading to a higher contact surface area and more efficient adhesion. To accomplish this task, a SAM tailored to the specific

matrix was covalently bound to the glass fiber surface, followed by fabrication of the glass fibers, and testing of the specimens using contact angle measurements, flexural modulus measurements, short beam shear and tensile testing. Scanning Electron Microscopy (SEM) was also used to obtain surface morphology of the specimens using a non-surface treated glass fiber, commercially available surface-treated glass fiber, and various SAM-treated glass fibers after exposure to the epoxy resin.

#### 1.4 References

1. Whitesides, George M. *Self-Assembling Materials*, Scientific American, Sept. 1995, 146 – 149.
2. Zhang, X.; Whitbourne, R.; Richmond, R. D.; *Antiinfective Coatings for Indwelling Medical Devices*, Medical Plastics and Biomaterials, 1997, Nov./Dec., 16 – 23.
3. Michele L. Pearson. *The Epidemiology of Device-Related Infections*, Surfaces in Biomaterials Foundation, 1997, 71 - 72.
4. Merritt, Katherine. *Studies on Implant Site Infections: Tale of a Journey*, Surfaces in Biomaterials Foundation, 1997, 74 – 78.
5. Martens, Leslie V. *The Nature and Significance of Microbial Contamination of the Dental Unit Waterlines and Potential Solutions*, Surfaces in Biomaterials Foundation, 1997, 80 - 81.
6. Daroulche, Rabih O. *In-Vivo Efficacy of Antiinfective Orthopaedic Devices*, Surfaces in Biomaterials Foundation, 1997, 83 - 84.
7. Tobin, E. J.; Bricault, R. J.; Karimy, H. F.; Barry, J. E.; Tweden, K. S.; Holmberg, W. R.; Simon, B.; *Silver Based Coatings for Improved Infection-Resistance in Medical Devices*, Surfaces in Biomaterials Foundation, 1997, 86 - 90.
8. Baggs, R. B.; Stalls, S.; Ventura, D.; Zhang, X.; *Cellular Adhesion Study on Urinary Catheters with Hydrophillic Coating*, Surfaces in Biomaterials Foundation, 1997, 108 – 110.
9. Cahill, Dolores J. *Protein and Antibody Arrays and their Medical Applications*, Journal of Immunological Methods, 2001, 250, 81-91.
10. Simmons, K.; Fryxell, G.E.; Samuels, W.; Voise, R.; Alford, K. L.; *Interfacial Chemical Control for Enhancements of Composite Material Strengths*, Pacific Northwest National Laboratory, 1998.

## CHAPTER TWO

### 2 SELF-ASSEMBLED MONOLAYER BACKGROUND

Under appropriate reaction conditions, self-assembled monolayers (SAMs) are known to spontaneously attach in an ordered, smooth, thin film on surfaces such as gold and silicon. They can be defined as molecular assemblies that are formed spontaneously when substrates are immersed into a solution of a surface-active molecules in an appropriate solvent.<sup>11,12</sup> A diagram portraying self-assembly of molecules onto a surface is shown below in Figure 2A.

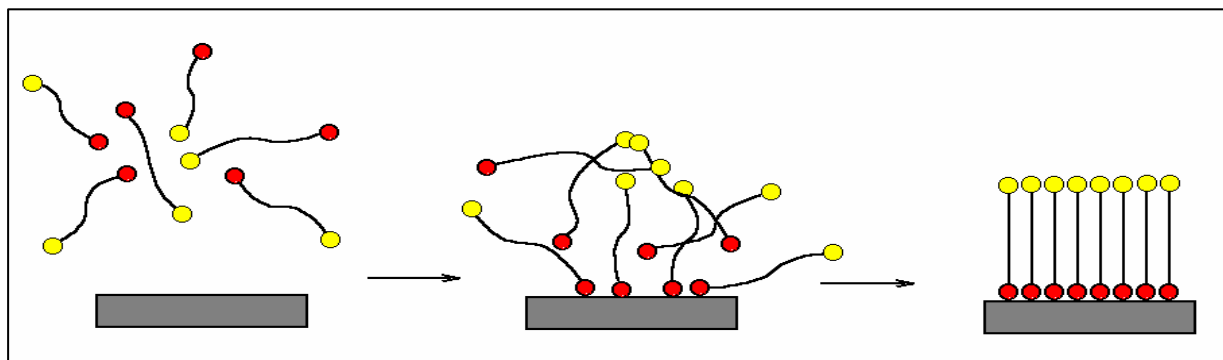


Figure 2A: Diagram involving the self-assembly of monolayers spontaneously attaching to a hydroxylated surface in an ordered, smooth, thin film. The red spheres are the reactive, polar end groups which interact with the hydroxylated surface. The yellow spheres are the non-reactive terminal group. (Figure obtained from Dr. Glen E. Fryxell, Battelle, Pacific Northwest National Laboratory.)

SAMs can offer direct access for preparation of organic functionalized surfaces.<sup>13</sup> Controlling the terminus of the monomer can modify the surface properties of the SAM and can serve as an excellent foundation upon which to build more complex molecular architectures. There are a large number of terminal functionalities commercially available for SAM preparation. These can range from simple primary amines and alcohols to bulky aromatics and

epoxides.<sup>14</sup> Employing organic synthesis in the laboratory can also change the terminal functionality.

Most of the literature relating to self-assembled monolayers over the last 20 years involves alkyl thiols on gold substrates.<sup>15</sup> Nuzzo and Allara published the first paper in this area in 1983.<sup>16</sup> They found that dialkyldisulfides form oriented monolayers on gold surfaces. Since this publication, it has been found that sulfur compounds coordinate very strongly to various substrates such as gold<sup>17-26</sup>, silver<sup>27</sup>, platinum<sup>28</sup>, and copper<sup>29-31</sup>, among others.

There are many other types of self-assembled monolayer methods that have been published as well. Some of these are organosilicon on hydroxylated surfaces (such as silicon, aluminum, and glass)<sup>15,32-43</sup>, fatty acids on glass<sup>44</sup>, carboxylic acids on aluminum oxide<sup>45-47</sup>, and alcohols and amines on platinum.<sup>28</sup> For the studies investigated in this thesis, the primary focus was on organosilicon self-assembled monolayers on hydroxylated silicon wafer surfaces.<sup>22,23</sup> This surface was chosen due to the covalent tethering of the SAM to the surface and the silane-silane cross-linking leading to a robust monolayer structure.

## 2.1 Brief Background of SAM Chemistry

As previously stated, SAMs are known to spontaneously organize into ordered, supramolecular assemblies on ceramic oxide surfaces (e.g. silica). This technique was used to attach an organosilane to a single crystal silicon wafer, creating the SAM. Generally, an organosilane shows two classes of functionality.





The R group is a nonhydrolyzable organic radical that has a functionality that allows the coupling agent to bond with organic polymers and resins. The organosilanes used in these experiments have only one organic substituent. The X group is involved in the reaction with the inorganic substrate. The X group is a hydrolyzable group in which the bond between the silicon atom and the X group in coupling agents is replaced by a bond between the silicon atom and the inorganic substrate.

Reactions involving organosilanes consist of four steps. First, hydrolysis takes place on the surface resulting in the labile X groups attached to the silicon atom being hydrolyzed. The hydrolyzed organosilane,  $(\text{HO})_3\text{SiR}$ , then hydrogen bonds to the surface, but can “crab-walk” around during the self-assembly stage. Condensation then takes place to form oligomers. Last, a covalent linkage is formed with the substrate along with loss of water. There is usually only one bond at the interface from each silicon of the organosilane to the substrate surface. The remaining silanol groups are either bonded to other coupling agent silicon atoms or in free form. Water for hydrolysis may come from several sources. It may be on the substrate surface, added, or come from the atmosphere. It may also be generated *in situ* by dissolving chlorosilanes in excess alcohol. The steps involved during the self-assembly process are shown below in Figure 2.1A.

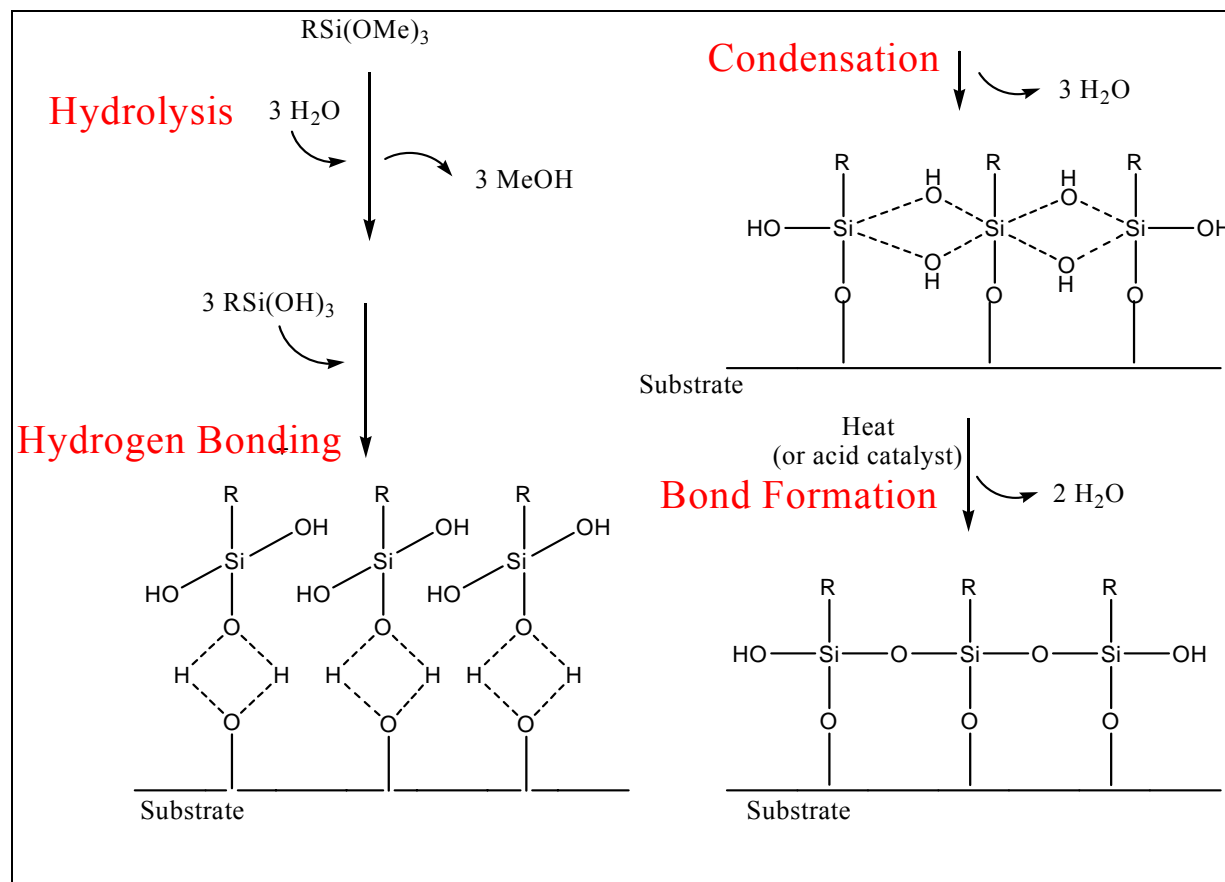


Figure 2.1A: Steps involved during the self-assembly of monolayers onto a substrate and the reactions which take place. Steps in order of occurrence: hydrolysis, hydrogen bonding, condensation, and then bond formation.

## 2.2 Methodology of Self-Assembled Monolayers

As stated previously in Chapter 2.1, an organosilane shows two classes of functionality, R and X. The X group is typically either chlorine or an alkoxy group with a by-product of HCl or an alcohol, respectively. The bond between the silicon atom and the X group in coupling agents is ultimately replaced by a bond between the silicon atom and the inorganic substrate. Although the reaction kinetics vastly favors the chloride substituent, the use of a trialkoxysilane as the

anchor was chosen to avoid the HCl by-product because HCl catalyzes undesired side reactions.

Figure 2.2A shows a basic chemical reaction for making a SAM.

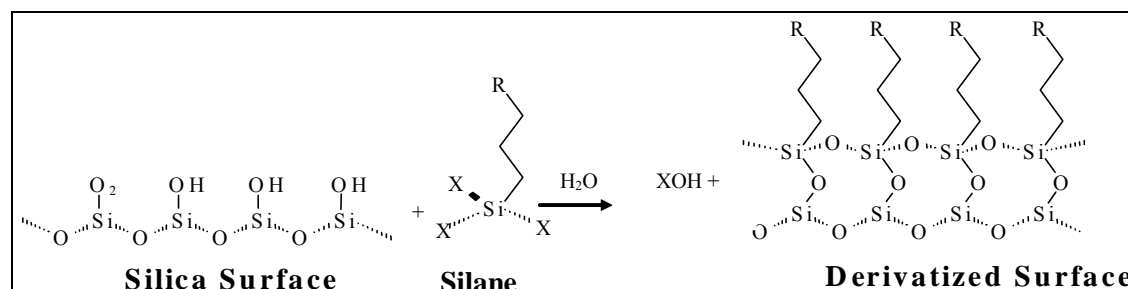


Figure 2.2A: Chemical reaction of a hydrated silicon surface with silane molecules depicting reactive end groups (X), which reacts, and cross-links with the silicon surface resulting in the derivatized surface.

The driving force for self-assembly is the interaction between the head group and the surface and the associative forces between the monomer molecules. In the case of simple alkyl thiols on gold (or alkyl silanes on silicon) the principle attractive forces are Van der Waals forces between the hydrocarbon chains. For more complex molecular systems, these attractive forces can also include hydrogen bonding, dipole-dipole interactions, coulombic attraction, metal-ligand interactions, or any combination of the above.

In a typical procedure for making self-assembled monolayers, a hydroxylated surface is placed in an organic solvent with an organosilane. Water for hydrolysis may come from several sources. It may be on the substrate surface, added, or come from the atmosphere. It may also be generated *in situ* by dissolving chlorosilanes in excess alcohol. However, it is best to add a specific amount, as this is the only way that the chemist can control stoichiometry and avoid bulk polymerization of the silane.

This technique was used to attach various organosilanes to a single crystal silicon wafer. As noted above, it is pertinent that the substrate surface be fully hydroxylated and hydrated. This is necessary for bonding between the silicon atom and the substrate to occur with the exception that an organosilane (R-Si-OH) can still hydrogen bond to a Si-O-Si bridge.

The driving force behind self-assembly can be broken into three parts when considering an energetic point of view: head groups, intramolecular forces, and terminal functionality. The head group is the most important because it involves the most exothermic reaction (~40-45 kcal/mol for thiolate on gold).<sup>48</sup> This is due to chemisorption of the head groups to the substrate surface and allows for “pinning” of the head group to specific sites on the surface (Figure 2.2B). Due to the exothermic head group/substrate interaction, the molecules will attempt to occupy every available site and thus push together molecules that have already absorbed. This is a basic conclusion presented by Ulman and others who study alkyl thiols on gold.<sup>49</sup> The van der Waals interaction of a hydrocarbon chain is about 1.5 kcal/mol per CH<sub>2</sub> or about 27 kcal/mol for an octadecyl (C<sub>18</sub>).<sup>49</sup> If hydrogen bonds were also calculated into the equation (~5 kcal/mol) or dipole-dipole interactions, then the head group chemistry becomes less dominant.

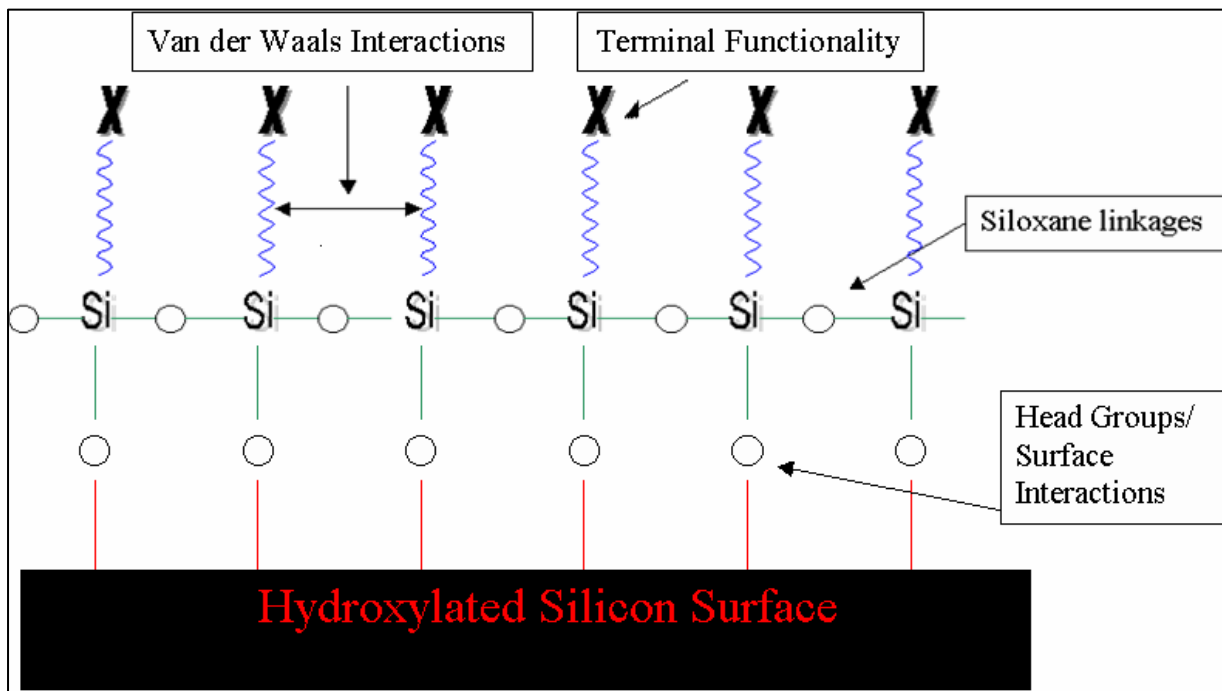


Figure 2.2B: Description of Silane-based monolayer chemistry. Driving force behind self-assembly from an energetic perspective: van der Waals interactions, head groups/surface interactions, terminal functionality, and siloxane linkages are shown.

The second driving force behind self-assembly is van der Waals interactions between the alkyl chains. Although not as exothermic, van der Waals interactions are the main forces in the case of simple alkyl chains. However, if there is a bulky polar group substituted into the alkyl chain, there also is a long-range electrostatic interactions that, energetically, may be more important than van der Waals attractions. The third molecular component is the terminal functionality and the energies associated with this functionality vary. In the case of a simple methyl group, this value typically is at the order of a few kcal/mol.<sup>49</sup>

Organosilanes on silicon wafers were chosen for these experiments for many reasons. The main contributing factors were the silicon surface, bond formation, price and availability.

The uniform, atomically smooth surface of single crystal silicon wafer makes it an excellent choice for characterization of smooth thin films. It can also be easily hydroxylated, which is helpful for self-assembly to occur. A covalent bond to a surface was another factor that needed to be addressed and the Si-O-Si covalent bond satisfied this need. The availability and reasonably low cost associated with silicon wafers also aided in the decision to use them as substrates.

A silicon wafer has a native oxide surface layer composed of silanols, siloxane linkages, and silicon dioxide. A schematic of a native silicon surface was shown previously in Figure 2.2A. The silanol (SiOH), siloxane linkages (Si-O-Si), and silicon dioxide (SiO<sub>2</sub>) were depicted.

### 2.3 Surface Cleansing Treatment to Increase Reactivity

Isopropyl alcohol (IPA) or chloroform (CHCl<sub>3</sub>) can be used to clean the silicon surface and the polypropylene holder of oils and possible surface impurities prior to SAM formation.<sup>50</sup> Plasma treatments have also been used to clean the surface as well.<sup>51</sup> This is also done to increase the surface reactivity of the silicon surface.

A mild base wash can be used to break the Si-O-Si bond to leave a Si-O<sup>-</sup> ion at the surface. Potassium hydroxide (KOH) was used to accomplish this because the K<sup>+</sup> ion does not bind tightly to the silicon surface. A mild acid wash can then be used to protonate the Si-O<sup>-</sup> ions. In this study, nitric acid (HNO<sub>3</sub>) was used because of its oxidizing power. Thus, if the KOH treatment leaves behind any “bald spots” of bare Si in the SiO<sub>2</sub> layer, then the HNO<sub>3</sub> would oxidize the Si to SiO<sub>2</sub>.

Once the SAM is covalently attached to the surface, it is possible to then take advantage of the reactivity of the terminal functionality. As mentioned previously, this monolayer consists of one terminal substituent, which commonly was an isocyanate. Ammonia and primary and

secondary amines will form substituted ureas when added to isocyanates<sup>52</sup> while alcohols (R'OH) will form carbamates (substituted urethanes) when added to isocyanates.<sup>53</sup> A reaction mechanism can be found below in Figure 2.3A.

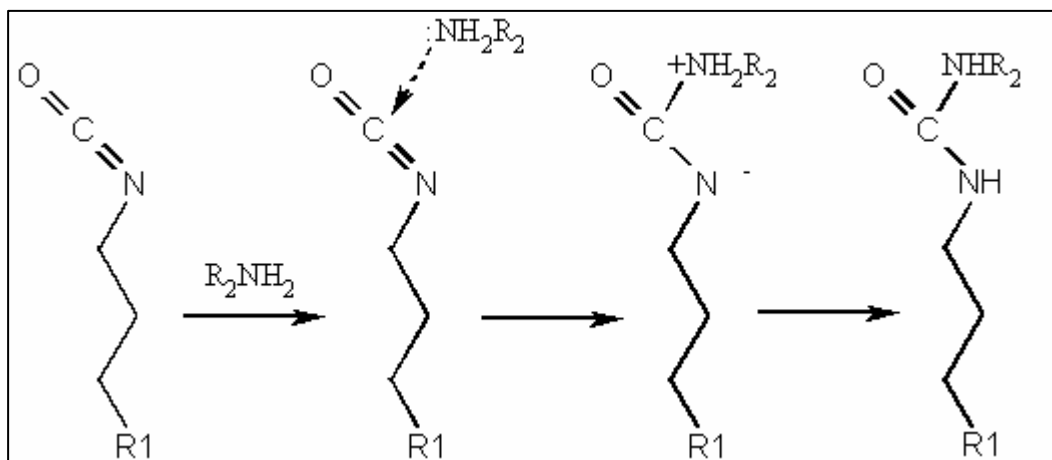


Figure 2.3A: Reaction mechanism of an isocyanate with a primary amine to form an urea linkage. In this reaction, R1 represents the silane bound to an inorganic substrate and R2 represents a carbon chain (singly bonded to the amine).

## 2.4 Characterization of SAM Formation

There are many analytical tools that can be used to analyze thin film properties and surface characteristics: Ellipsometry, contact wetting angle, Scanning Electron Microscopy (SEM), and fluorescence will be discussed in further detail in this section. Analysis of film properties, such as thickness and uniformity, can be determined by ellipsometry, plasmon-surface polarization (PSP), x-ray reflection, and x-ray standing waves.<sup>54</sup> Ellipsometry was the most useful optical technique for the determination of film thickness in these studies because,

unlike the other techniques, the skill and time needed to obtain measurements is not as labor-intensive and the sensitivity of the measurement is comparable.

One method for characterizing the chemical behavior of a surface is to measure its wettability. This can be done using a solvent such as water, pH buffers or non-volatile organic solvents, as a way of gauging the different components (acid/base properties, permanent dipole moment, polarizability) of the overall interfacial wettability.<sup>55,56</sup> The most common of these measurements is contact angle and surface tension.

Surface morphology of thin films can be determined using Scanning Electron Microscopy (SEM) which allows for surface imaging to detect structure on films or surfaces with a resolution of 5–15 nm and magnifications of up to 300,000x.<sup>57</sup> A common technique to determine surface coverage of molecules on a surface is to bind a fluorescent-marker onto the molecules and then scan the surface for fluorescence. Covalent bonding of a fluorescent-labeled oligonucleotide to a self-assembled monolayer could be verified by using fluorescence spectroscopy.

For this research, the use of ellipsometry, contact wetting angle, SEM, and fluorescence to verify covalent attachment of the SAMs and/or molecule(s) of interest on the silicon substrate was chosen. The reasons for choosing these four analytical tools and their benefits are summarized below.

#### 2.4.1 Ellipsometry

To analyze film thickness, ellipsometry was chosen because it is a common optical technique used to determine film thickness and refractive index of thin homogeneous films.<sup>58-61</sup> An ellipsometer is an optical instrument that measures the changes in the state of polarization of



collimated beams of monochromatic polarized light caused by reflection from the surface of materials. This allows for the measurement of a transparent film thickness. For more details on ellipsometry, refer to reference from Ultrathin Organic Films.<sup>62</sup> A Gaertner Ellipsometer using GC6A Single Layer Absorption (GC10141) program was used in these experiments.

Ellipsometry has some advantages over other methods for measuring film thickness such as:

1. Measurements can be made in optically transparent environments such as air or liquids.
2. Capable of measuring film thicknesses at least an order of magnitude smaller than can be measured by other methods such as interferometry.
3. Doesn't require special conditions such as vacuum, heat or electron bombardment which may change the optical properties of the surface, but can make measurements under these conditions if desired.
4. Permits determination of the index of refraction of thin films of unknown thickness, whereas interferometry and reflectometry does not.

For these reasons, ellipsometry was used to measure the uniformity and thickness of the thin films.

#### 2.4.2 Contact Wetting Angle

In many cases it has been observed that a liquid placed on a solid will not wet it, but remains as a drop with a definitive angle of contact between the liquid and the solid phases. Since different solid surfaces have varying wetting properties, it is possible to use this phenomenon to verify the wettability of a material surface both prior to, and after, exposure to covalent attachment of the SAM and to correlate this to the surface energy.

The contact angle is a rough measure of the surface energy of a material. Wetting is typically defined as having a contact angle value of  $0^\circ$  (or close to zero) between the liquid and solid phase such that the liquid spreads over the solid easily. Non-wetting can be defined as having a liquid that does not wet a surface completely. It forms an angle greater than  $90^\circ$  so that the liquid beads (“balls up”) and can run off the surface easily (see Figure 2.4.2A). Hence, when a surface and a liquid both have a contact angle of  $0^\circ$ , then the surface-free energy of both materials is equal.<sup>56</sup> Contact angle measurements using different solvents (liquids) can be used to evaluate wetting properties, uniformity, surface-free energy, and information on surface order.

Some of the advantages of using contact wetting angle measurements are:

1. The quality and uniformity of stable monolayers can be estimated from wetting measurements.
2. Wetting is the most sensitive measure of surface composition and structure<sup>43</sup>.
3. It is a non-destructive, reproducible analytical tool.

Static contact angle measurements will provide in this investigation a sensitive measure of surface changes in chemical composition and structure. A NRL C.A. Goniometer Model #100-00 115 was used in these experiments to determine static contact wetting angle.

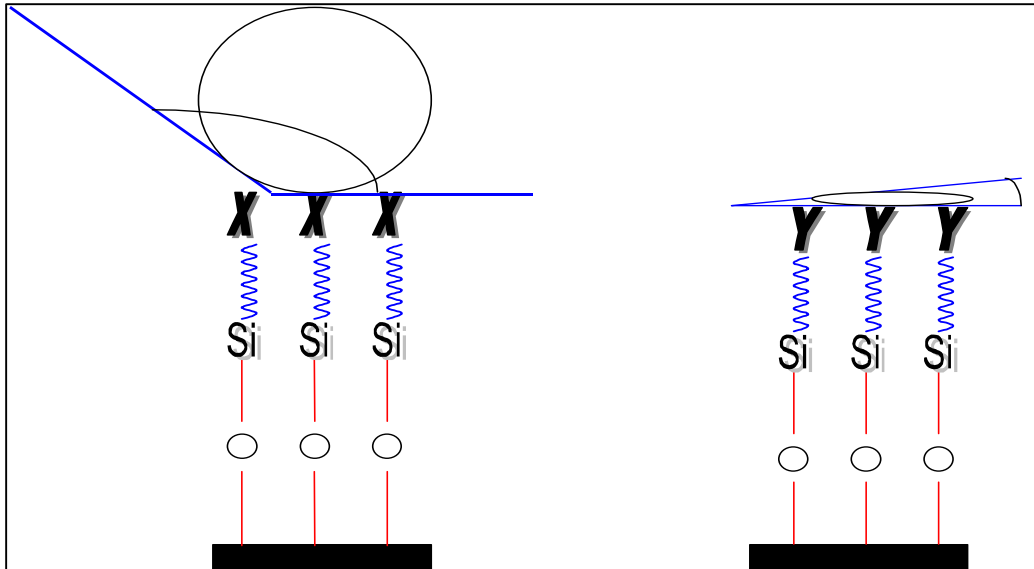


Figure 2.4.2A: Example of contact wetting angle for a hydrophobic, non-wetting surface (left) and a hydrophilic, wetting surface (right). The high contact angle of the hydrophobic surface represents a “beading” of the liquid on the surface.

### 2.4.3 Scanning Electron Microscopy

Scanning electron microscopy produces fundamental details as to the surface morphology, defects, and patterns of a solid sample. A focused beam of electrons is used to scan a surface and the intensity of the scattered secondary electrons is monitored. The intensity of the secondary electron production varies at each point on the sample surface and provides the quality of the image, which is dependant upon having a high intensity of signal. The contrast in the image is a result of scattering from dissimilar surface areas as a result of geometry differences. Images are sharp at both high and low points on the surface and very dark and light areas emphasize detail. This method will provide a good understanding as to surface morphology.

#### 2.4.4 Fluorescence

Fluorescence spectroscopy measurements permit detection of covalent attachment of fluorescent-labeled oligonucleotides to SAMs. A complex is considered to be luminescent if it emits light after it has been electronically excited by the absorption of radiation. Rapidly decaying luminescence is traditionally called fluorescence. Fluorescence occurs when an excited state of the same multiplicity as the ground state decays radiatively into the ground state. This transition is commonly fast; on the order of milliseconds to nanoseconds.

Fluorescence spectroscopy was chosen as an analytical tool during the oligonucleotide studies. Determining the thickness of the covalently bound oligonucleotide to the SAM surface was not possible in all experiments due to the nature of the experiment (explained in more detail in Chapter Five, Oligonucleotides). Therefore, an alternate means by which to quantify the amount of molecules on the surface was needed. Hence, oligonucleotides labeled with fluorescein (fluorescent label) were used to verify covalent attachment to the SAM surface.

#### 2.5 References

11. Zisman, W.A. *Adv. Chem. Ser.* 1964, 43, 1.
12. Bigelow, W.C.; Pickett, D.L.; Zisman, W.A. *Journal Colloid Interface Science*, 1946, 1, 513.
13. Fryxell, G. E.; Rieke, P. C.; Wood, L. L.; Engelhard, M. H.; Williford, R. E.; Graff, G. L.; Campbell, A. A.; Wiacek, R. J.; Lee, L.; Halverson, A.; *Nucleophilic Displacements in Mixed Self-Assembled Monolayers*, *Langmuir*, 1996, 12, 21, 5064- 5075.
14. Silicon Compounds Register and Review, 5th Edition. United Chemical Technologies Inc., 1993.
15. Sagiv, Jacob, *Organized monolayers by adsorption. 1. Formation and structure of oleophobic mixed monolayers on solid surfaces*, *J. Am. Chem. Soc.*, 1980, 102, 92-98.
16. Nuzzo, R.G.; Allara, D.L.; *Adsorption of bifunctional organic disulfides on gold surfaces* *J. Am. Chem. Soc.*, 1983, 105, 4481 - 4483.

17. Bain, C.D.; Troughton, E.B.; Tao, J.-T.; Evall, J.; Whitesides, G.M.; Nuzzo, R.G.; *Formation of monolayer films by the spontaneous assembly of organic thiols from solution onto gold*, J. Am. Chem. Soc., 1989, 111, 321 - 335.
18. Porter, M.D.; Bright, T.B.; Allara, D.L.; Chidsey, C.E.D.; *Spontaneously organized molecular assemblies. 4. Structural characterization of n-alkyl thiol monolayers on gold by optical ellipsometry, infrared spectroscopy, and electrochemistry*, J. Am. Chem. Soc., 1987, 109, 3559 - 3568.
19. Whitesides, G.M.; Laibinis, P.E.; *Wet chemical approaches to the characterization of organic surfaces: self-assembled monolayers, wetting, and the physical-organic chemistry of the solid-liquid interface*, Langmuir, 1990, 6, 87 - 96.
20. Chidsey, C.E.D.; Loiacono, D.N.; *Chemical functionality in self-assembled monolayers: structural and electrochemical properties*, Langmuir, 1990, 6, 3, 682 - 691.
21. Nuzzo, R.G.; Dubois, L.H.; Allara, D.L.; *Fundamental studies of microscopic wetting on organic surfaces. 1. Formation and structural characterization of a self-consistent series of polyfunctional organic monolayers*, J. Am. Chem. Soc., 1990, 112, 558 - 569.
22. Bain, C.D.; Whitesides, G. M.; *Formation of monolayers by the coadsorption of thiols on gold: variation in the length of the alkyl chain*, J. Am. Chem. Soc., 1989, 111, 7164 - 7175.
23. Strong, L.; Whitesides, G.M.; *Structures of self-assembled monolayer films of organosulfur compounds adsorbed on gold single crystals: electron diffraction studies*, Langmuir, 1988, 4, 546 - 558.
24. Chidsey, C.E.D.; Liu, G.-Y.; Rowntree, P.; Scoles, G. Journal of Chemical Physics, 1989, 91, 4421.
25. Rubinstein, I.; Steinberg, S.; Tor, Y.; Shanzer, A.; Sagiv, J. Nature 1988, 332, 426.
26. Nuzzo, R.G.; Fusco, F.A.; Allara, D.L.; *Spontaneously organized molecular assemblies. 3. Preparation and properties of solution adsorbed monolayers of organic disulfides on gold surfaces*, J. Am. Chem. Soc., 1987, 109, 2358 - 2368.
27. Ulman, A. Journal of Material Ed. 1989, 11, 205.
28. Troughton, E.B.; Bain, C.D.; Whitesides, G. M.; Nuzzo, R.G.; Allara, D.L.; Porter, M.D.; *Monolayer films prepared by the spontaneous self-assembly of symmetrical and unsymmetrical dialkyl sulfides from solution onto gold substrates: structure, properties, and reactivity of constituent functional groups*, Langmuir, 1988, 4, 365 - 385.
29. Stewart, K.R.; Whitesides, G.M.; Godfried, H.P.; Silvera, I.F. Surface Science 1986, 57, 1381.
30. Blackman, L.C.F.; Dewar, M.J.S.; Hampson, H. Journal of Applied Chem. 1957, 7, 160.
31. Blackman, L.C.F.; Dewar, M.J.S. Journal Chem. Soc. 1957, 171.
32. Tilman, N.; Ulman, A.; Penner, T.L.; *Formation of multilayers by self-assembly*, Langmuir 1989, 5, 101 - 111.
33. Tilman, N.; Ulman, A.; Schildkraut, J.S.; Penner, T.L.; *Incorporation of phenoxy groups in self-assembled monolayers of trichlorosilane derivatives. Effects on film thickness, wettability, and molecular orientation*, J. Am. Chem. Soc., 1988, 111, 6136 - 6164.
34. Netzer, L.; Sagiv, J.; *A new approach to construction of artificial monolayer assemblies*, J. Am. Chem. Soc., 1983, 105, 674 - 676.
35. Netzer, L.; Sagiv, J.; Iscovici, R. Thin Solid Films, 1983, 99, 235.
36. Netzer, L.; Sagiv, J.; Iscovici, R. Thin Solid Films, 1983, 100, 67.

37. Maoz, R.; Sagiv, J.; *Penetration-controlled reactions in organized monolayer assemblies. 2. Aqueous permanganate interaction with self-assembling monolayers of long-chain surfactants*, Langmuir 1987, 3, 1045 - 1051.
38. Maoz, R.; Sagiv, J. Thin Solid Films 1985, 132, 135.
39. Maoz, R.; Sagiv, J. Journal of Colloid Interface Science 1984, 101, 201.
40. Cohen, S.R.; Naman, R.; Sagiv, J.; *Thermally induced disorder in organized organic monolayers on solid substrates*, Journal of Physical Chemistry, 1986, 90, 3054 - 3056.
41. Gun, J.; Sagiv, J.; Iscovici, R. Journal of Colloid Interface Science, 1984, 101, 201.
42. Gun, J.; Sagiv, J. Journal of Colloid Interface Science, 1986, 112, 457.
43. Finklea, H.O.; Robinson, L.R.; Blackburn, A.; Richter, B.; Allara, D.; Bright, T.; *Formation of an organized monolayer by solution adsorption of octadecyltrichlorosilane on gold: electrochemical properties and structural characterization*, Langmuir, 1986, 2, 239 - 244.
44. Chen, S.H.; Frank, C.F.; *Infrared and fluorescence spectroscopic studies of self-assembled n-alkanoic acid monolayers*, Langmuir 1989, 5, 978 - 987.
45. Allara, D.L.; Nuzzo, R.G.; *Spontaneously organized molecular assemblies. 1. Formation, dynamics, and physical properties of n-alkanoic acids adsorbed from solution on an oxidized aluminum surface*, Langmuir 1985, 1, 45 - 52.
46. Allara, D.L.; Nuzzo, R.G.; *Spontaneously organized molecular assemblies. 2. Quantitative infrared spectroscopic determination of equilibrium structures of solution-adsorbed n-alkanoic acids on an oxidized aluminum surface*, Langmuir 1985, 1, 52 - 66.
47. Ogawa, H.; Chihera, T.; Taya, K.; *Selective monomethyl esterification of dicarboxylic acids by use of monocarboxylate chemisorption on alumina*, J. Am. Chem. Soc., 1985, 107, 1365 - 1369.
48. Dubois, L.H.; Zegarski, B.R.; Nuzzo, R.G. Proc. National Academy of Science, USA 1987, 84, 4739.
49. Nuzzo, R.G.; Korenic, E.M.; Dubois, L.H.; Journal of Chemical Physics, 1990, 93, 767.
50. Tarasevich, B.J.; Rieke, P.C.; Liu, J.; *Nucleation and Growth of Oriented Ceramic Films onto Organic Interfaces*, Chem. Mater., 1996, 8, 292 - 300.
51. Ron, H.; Rubinstein, I.; *Alkanethiol Monolayers on Preoxidized Gold. Encapsulation of Gold Oxide under an Organic Monolayer*, Langmuir, 1994, 10, 4566 - 4573.
52. March's Advanced Organic Chemistry, Smith, M.B.; March, J., 5<sup>th</sup> Edition, Wiley-Interscience, page 1191 and 1261.
53. March's Advanced Organic Chemistry, Smith, M.B.; March, J., 5<sup>th</sup> Edition, Wiley-Interscience, page 1182 - 1183, and 1257.
54. Ultrathin Organic Films, Abraham Ulman. MRS Bull, 1995.
55. Rieke, Peter C. Journal of Crystal Growth, 1997, 182, 472-484.
56. Wettability, John C. Berg. Marcel Dekker, Inc., New York, 1993, 74-148.
57. CRC Handbook of Chemistry and Physics, 76<sup>th</sup> Edition, CRC Press, 1995.
58. Wasserman, S.R.; Whitesides, G.M.; Tidswell, I.M.; Ocko, B.M.; Pershan, P.S.; Axe, J.D.; *The structure of self-assembled monolayers of alkylsiloxanes on silicon: a comparison of results from ellipsometry and low-angle x-ray reflectivity*, J. Am. Chem. Soc., 1989, 111, 5852-5261.
59. Ellipsometry and Polarized Light, Azzam, R.M.A.; Bashara, N.M., North-Holland Publishing Co., Amsterdam, 1977.

60. McCrackin, F.L.; Passaglia, E.; Stromberg, R.R.; Steinberg, H.L.; J. Res. Natl. Bur. Stand. Sect A. 1963, 67, 636.
61. Luzinov, I.; Julthongpiput, D.; Liebmann-Vinson, A.; Cregger, T.; Foster, M. D.; Tsukruk, V. V.; *Epoxy-Terminated Self-Assembled Monolayers: Molecular Glues for Polymer Layers*, Langmuir, 2000, 16, 504 - 516.
62. Ultrathin Organic Films. Abraham Ulman. MRS Bull, 1995, page 2.

## **CHAPTER THREE**

### **3 PEPTIDES AND ENZYMES**

#### **3.1 Introduction**

For proof of concept,  $\beta$ -Amyloid (proteinaceous fibrils) and Catalase (enzyme) were studied for future experiments relating to the covalent attachment of antimicrobials, as well as oligonucleotides, to silicon wafer substrates. These experiments were conducted to establish a baseline of understanding and to determine if the self-assembled monolayer chemistry would work for various peptides and enzymes using isocyanatopropyl triethoxysilane (NCO) SAM.

#### **3.2 Objective and Background**

$\beta$ -amyloid (proteinaceous fibrils) and Catalase (enzyme) were studied for future experiments relating to antimicrobial and oligonucleotide covalent attachment to silicon wafer substrates via a self-assembled monolayer. These experiments would demonstrate proof of concept that covalent attachment of  $\beta$ -amyloid and Catalase to a self-assembled monolayer on a silicon wafer substrate was possible. The objective of these experiments was to use a single crystal silicon wafer as a substrate to covalently bind isocyanatopropyl triethoxysilane (NCO) in solution, which becomes the SAM. The terminal functionality on the NCO SAM was then used to bind Catalase and  $\beta$ -Amyloid 20 mer to the SAM via a urea linkage. The analytical techniques employed to verify covalent attachment of the SAM to the silicon surface and the SAM terminus to peptide or enzyme linkages in these experiments were ellipsometry and contact angle



measurements. These were performed in order to determine the initial SAM monolayer thickness, covalent attachment of the enzyme or peptide to the SAM by ellipsometry, and wetting characteristics of the SAM and enzyme or peptide interface.

### **3.3 Results and Discussion**

#### **3.3.1 Experiment 1: $\beta$ -Amyloid and Catalase Attachment to NCO SAM on Silicon Wafers**

As stated previously in Chapter 2 and in Section 3.2, the addition of the SAM and molecule of interest (peptide or enzyme) was verified by ellipsometry and static contact angle measurements. The silicon wafer wetting characteristics (contact angle) and oxide thickness layer (ellipsometry) was first determined on the bare, native silicon wafer substrate (Table 3.3.1A). Measurements for the NCO SAM addition (Table 3.3.1B) and following  $\beta$ -Amyloid (Table 3.3.1C) or Catalase (Table 3.3.1D) addition followed this. The differences from ellipsometry and wetting contact angle measurements from Table 3.3.1E and F suggest that both the  $\beta$ -Amyloid 20 mer and Catalase samples successfully attached to the SAM surface. This can be seen in the drastic contact angle differences ( $\sim 19$  degrees for  $\beta$ -Amyloid and  $\sim 36$  degrees for Catalase) and also in the increased optical thickness of the enzyme and peptide attached to the silicon substrate due to monolayer and peptide, or enzyme, addition ( $\sim 11$  Å for  $\beta$ -Amyloid and  $\sim 49$  Å for Catalase).

Table 3.3.1A: Silicon wafer ellipsometry ( $\text{\AA}$ ) and wetting contact angle (degrees) measurements prior to any treatment or cleaning in isopropanol (number of measurements vary). Wafers 1 and 2 were wafers removed from racks which were to be cleansed with isopropanol, KOH, and then  $\text{HNO}_3$  for subsequent NCO SAM deposition. Solution A and Solution B were two separate NCO solutions prepared for comparison purposes.

Measurement #	Thickness ( $\text{\AA}$ )				Angle (Degrees)			
	Solution A		Solution B		Solution A		Solution B	
	Wafer 1	Wafer 2	Wafer 1	Wafer 2	Wafer 1	Wafer 2	Wafer 1	Wafer 2
1	30	31	30	30	21	21.25	24	22
2	30	31	31	30	20.5	21	23	21
3	27	30	31	29	21	21.25	24	23
4	27	30	30	29	20.5	21	22	23
5	31	30	31	28	21	21.75	24	21.5
6	31	30	32	30	20	21.25	20	20
7	29	27	31	29	-	-	-	-
8	28	27	27	28	-	-	-	-
9	-	-	26	28	-	-	-	-
10	-	-	27	34	-	-	-	-
11	-	-	28	29	-	-	-	-
12	-	-	34	27	-	-	-	-

Table 3.3.1B: Silicon wafer ellipsometry (Å) and contact angle (degrees) measurements after NCO attachment. Solution A was used for the deposition (refer to Table 3.3.1A). Wafers 1 and 2 were wafers removed from racks which were cleansed with isopropanol, KOH, HNO<sub>3</sub> and then exposed to Solution A for NCO SAM deposition.

Measurement #	Thickness (Å)		Angle (Degrees)	
	Wafer 1	Wafer 2	Wafer 1	Wafer 2
1	33	32	64	67
2	32	32	59	63
3	33	32	62	65
4	34	32	70	68
5	37	33	65	68
6	32	32	64	64
7	32	32	66	62
8	32	32	66	66
9	32	32	-	-
10	31	31	-	-

Table 3.3.1C: Silicon wafer ellipsometry (Å) and contact angle (degrees) measurements after doping in  $\beta$ -Amyloid solution (1-2 mg  $\beta$ -Amyloid in 10 mL water).

#	Thickness (Å)		Angle (Degrees)	
	Wafer 1	Wafer 2	Wafer 1	Wafer 2
1	66	41	45.5	47
2	42	39	43	46
3	42	39	-	47
4	42	39	45	47
5	42	42	47	49
6	45	40	47	41
7	55	48	-	-
8	41	40	-	-
9	40	39	-	-
10	47	44	-	-

Table 3.3.1D: Silicon wafer ellipsometry (Å) and contact angle (degrees) measurements after doping in Catalase solution (~1 mL Catalase in ~10 mL of water). Water spots dispersed droplets unevenly and in an unordered, random shape that hindered accurate wetting angle measurements.

#	Thickness (Å)		Angle (Degrees)	
	Wafer 1	Wafer 2	Wafer 1	Wafer 2
1	91	82	29	25
2	109	70	36	26
3	75	69	24	32
4	70	73	23	26
5	67	94	27	36
6	68	93	30	33
7	71	77	-	28
8	81	99	-	30
9	76	88	-	-
10	82	99	-	-

Table 3.3.1E: Silicon wafer ellipsometry measurement averages for Tables 3.3.1 - 4. Measurements for thickness recorded in Å. Overall average is the average of both sample measurements (Wafer 1 and 2) obtained. The exception is the overall average for Prior to treatment - Solutions A and B. In this case, the overall average is calculated using both Wafer 1 and 2 from Solution A and B. Thus, the overall average is the average of all four wafers.

	Wafer 1	Wafer 2	Overall
Prior to treatment- Solution A	29.1	29.5	29.4
Prior to treatment- Solution B	29.8	29.3	
After NCO treatment	32.8	32.0	32.4
β-Amyloid 20 mer	46.2	41.1	43.7
Catalase	79.3	84.4	81.9

Table 3.3.1F: Silicon wafer contact wetting angle measurement averages for Tables 3.3.1A – D. Units for wetting angles are in degrees. Overall average is the average of both sample measurements (Wafer 1 and 2) obtained. The exception is the overall average for Prior to treatment - Solution A and B. In this case, the overall average is calculated using both Wafer 1 and 2 from Solution A and B. Thus, the overall average is the average of all four wafers.

	<b>Wafer 1</b>	<b>Wafer 2</b>	<b>Overall</b>
Prior to treatment- Solution A	20.7	22.2	21.6
Prior to treatment- Solution B	22.8	21.8	
After NCO treatment	64.5	65.4	64.9
$\beta$ -Amyloid 20 mer	45.5	46.2	45.9
Catalase	28.2	29.5	28.8

Table 3.3.1G: Difference values for treated and untreated silicon samples after attachment of  $\beta$ -Amyloid and Catalase. Value used to calculate thickness difference ( $\text{\AA}$ ) for both samples was 32.4  $\text{\AA}$ , which is the overall thickness average after NCO attachment. Value used to calculate contact angle difference is 64.9 degrees, which is also the overall wetting angle (degrees) average after NCO attachment.

	<b>Thickness (<math>\text{\AA}</math>)</b>		<b>Angle (Degrees)</b>	
	<b>Wafer 1</b>	<b>Wafer 2</b>	<b>Wafer 1</b>	<b>Wafer 2</b>
$\beta$ -Amyloid 20 mer	13.8	8.7	-19.4	-18.7
Catalase	46.9	52	-36.7	-35.4

Table 3.3.1H: Average  $\beta$ -Amyloid and Catalase Enzyme Ellipsometry ( $\text{\AA}$ ) and Contact Wetting Angle (degrees) Measurements.

<b>Sample Description</b>	<b>Average Thickness (<math>\text{\AA}</math>)</b>	<b>Average Contact Angle (Degrees)</b>
Silicon wafer	29.4	21.6
Silicon wafer + SAM	32.4	64.9
Silicon wafer + SAM + $\beta$ -Amyloid	43.6	45.3
Silicon wafer + SAM + Catalase	81.8	28.8

Average ellipsometry and varying contact angle measurements in Table 3.3.1H show the positive attachment of the enzymes to the NCO terminated SAM by conversion of the isocyanate with the addition of the amine terminus to a urea. The large thickness difference between  $\beta$ -Amyloid and Catalase may be due to irregular drying of the silicon wafer after submersion in solution. The varying wetting measurements obtained when comparing the four samples verifies attachment of Catalase and  $\beta$ -Amyloid. Ellipsometry measurement differences between the Catalase and  $\beta$ -Amyloid samples may be due to the fact that the Catalase molecular structure is larger than  $\beta$ -Amyloid.

Another possible explanation for the thickness difference is that water spots were noticeable on the Catalase samples which resulted in uneven drying during nitrogen blowing. Considering that the water “spots” were a contributor to the thickness measurements, a close inspection of the data suggests that the average thickness after Catalase deposition would be around 70  $\text{\AA}$  (oxide layer, SAM, and Catalase); which would suggest an increase in surface thickness of at least 30  $\text{\AA}$ .

### 3.3.2 Experiment 2: Various Peptide Attachment to Silicon Treated Substrates

The overall average ellipsometry measurements on the silicon wafers treated with the peptides above increased, varying from 50 to 95 Å after being placed in water or DMF solution. The contact wetting angle also changed from ~31 degrees to between 55 and 70 degrees.

These experiments were repeated over a span of 30 days and often the same peptide solution was re-used. A regression was noticed in the average peptide thickness on the SAM treated silicon substrate. This could be due to a reduction in the amount of solute available for interaction with the SAM since only a few milligrams of each peptide was utilized. However, the overall average contact wetting angles varied little throughout the experiments.

## 3.4 Conclusions

The average ellipsometry measurements for the NCO treated wafer,  $\beta$ -Amyloid 20 mer treated wafer, and the Catalase treated wafer were 32.4, 43.7 and 81.9 Å, respectively. The respective average contact angle measurements were 64.9, 45.9 and 28.8 degrees. The difference in ellipsometry and contact angle measurements suggests that both samples attached successfully to the NCO treated surface, proving that the NCO SAM is a viable option for attaching primary or secondary amine-terminated peptides or enzyme.

## **CHAPTER FOUR**

### **4 ANTIMICROBIALS**

#### **4.1 Introduction**

Medical devices such as catheters, prosthesis, implants, and other invasive devices have become an integral part of modern day medical care; in spite of that, they have certain infection risks associated with them. Some of these risks include bloodstream infection, urinary tract infection, pneumonia, and surgical site infection. Despite technological advances in the materials, design, and manufacturing used for these devices, infection continues to be a frequent and serious complication. Furthermore, infection rates related to these products have also continued to rise despite efforts to decrease them<sup>2-8</sup>.

The significance of obtaining an antimicrobial agent that would release from a surface after being exposed to a bacterium could reduce infection sites as well as decrease the frequency in which a medical device may have to be replaced. On the other hand, a surface that covalently binds an antimicrobial to the surface could significantly lower, or eliminate, the number of sites in which a bacterium could adhere to the surface. An important note to mention is if the bacterium were to adhere to the surface, it would be necessary for the antimicrobial agent to: 1) kill the bacterium or 2) not allow for bacterial colonies to form.

The goal of these experiments was to impart antimicrobial activity to a surface for application to medical devices. Accomplishing this goal required demonstrating that it was possible to install an appropriate monolayer (SAM with an isocyanate-terminus- NCO) to a



surface (silicon wafer) and use this to covalently bind and/or release various antimicrobial agents (phenols, pharmaceuticals, and peptides) over time. A silicon wafer was chosen as the substrate because of the very uniform surface, the extensive SAM studies performed on silicon, and due to the fact that it is a good model to use for proof of concept.

The results will show that various antimicrobials agents were successfully covalently attached to the silicon surface via a SAM linkage and that antimicrobial activity was demonstrated for some of the antimicrobial agents tested. It will also show that antimicrobial activity required physical contact with the bacterium.

## **4.2 Objective and Background**

The following outlines experiments involving covalent bonding of various antimicrobial agents onto silicon substrates via attachment of a self-assembled monolayer. Various techniques and experiments were conducted to determine the viability, reliability and effectiveness of antimicrobial agents on silicon substrates when inoculated with a gram negative strand of *Escherichia coli* (*E. coli*) bacteria. The following is a brief list and description of the experiments performed.

### **4.2.1 *E. coli* Cell Viability**

Optical density measurements (absorbance) at 600 nm were performed to verify that the bacteria was alive and reproducing in the tryptic soy broth (TSB) solution inoculated with *E. coli* prior to submersion of an antimicrobial-coated silicon wafer with an aliquot of inoculated *E. coli*

solution. Optical density measurements were measured at 600 nm since this wavelength has been used previously to verify bacterial viability of gram negative strands of E. coli solutions.<sup>63</sup>

#### 4.2.2 AMC Microscope Imaging

Microscope images were taken of antimicrobial-coated silicon wafers before, during, and after being subjected to E. coli bacteria at various time intervals to determine if cell adhesion onto the silicon wafers occurred. Each wafer was washed with deionized water prior to imaging to reduce physisorbed material on the surface.

#### 4.2.3 Ellipsometry and Contact Wetting Angle Measurements

Measurements were made to determine and verify either SAM, antimicrobial, and/or E. coli attachment and thickness of said adhered to the silicon surface at various times during experiments. As stated previously in section 2.4.1, an ellipsometry measurement allows for the thickness determination of an optically transparent thin film. When using a SAM for the covalent attachment of the antimicrobial agent, mapping the progress and success of the film depositions (bare silicon + SAM + antimicrobial + E. coli) by simple thickness determinations is possible. A complete NCO SAM typically has a monolayer thickness of approximately 7-10 Å.

#### 4.2.4 Absorbance Measurements (Antimicrobial Wafers Inoculated with E. coli Bacteria)

Silicon wafers treated with antimicrobial agents were placed in solutions that were inoculated with E. coli and absorbance measurements were performed to follow the amount of bacterial growth, qualitatively, as a function of time at 37° Celsius with constant shaking. More

detail as to the cell viability, microscope imaging, ellipsometry, contact angle, and absorbance measurements can be found in the Experimental Section at the end of this document (Chapter 7).

#### 4.2.5 Antimicrobials

Antimicrobial attachment to silicon wafers was performed using the following different anti-bacterials: Tetracycline, Polymyxin  $\beta$ , Kanamycin, and Nalidixic acid. These particular anti-bacterial agents were used because of their demonstrated effectiveness against gram-negative bacteria, such as *E. coli*, although the path at which these agents “kill” the bacterium may vary (i.e. outside the cell wall versus inside the cell wall). Silicon wafers coated with a monolayer of isocyanatopropyl triethoxysilane (NCO) were used for the covalent attachment of the antimicrobials. As stated previously, the sites at which the antimicrobials can covalently attach to an isocyanate-terminated the SAM are the hydroxyl or alcohol appendages (Nalidixic acid) or amine terminated sites (Tetracycline, Polymyxin  $\beta$ , Kanamycin) of the antimicrobials. Figure 4.2.5A shows the chemical structure of each of the anti-bacterial agents.

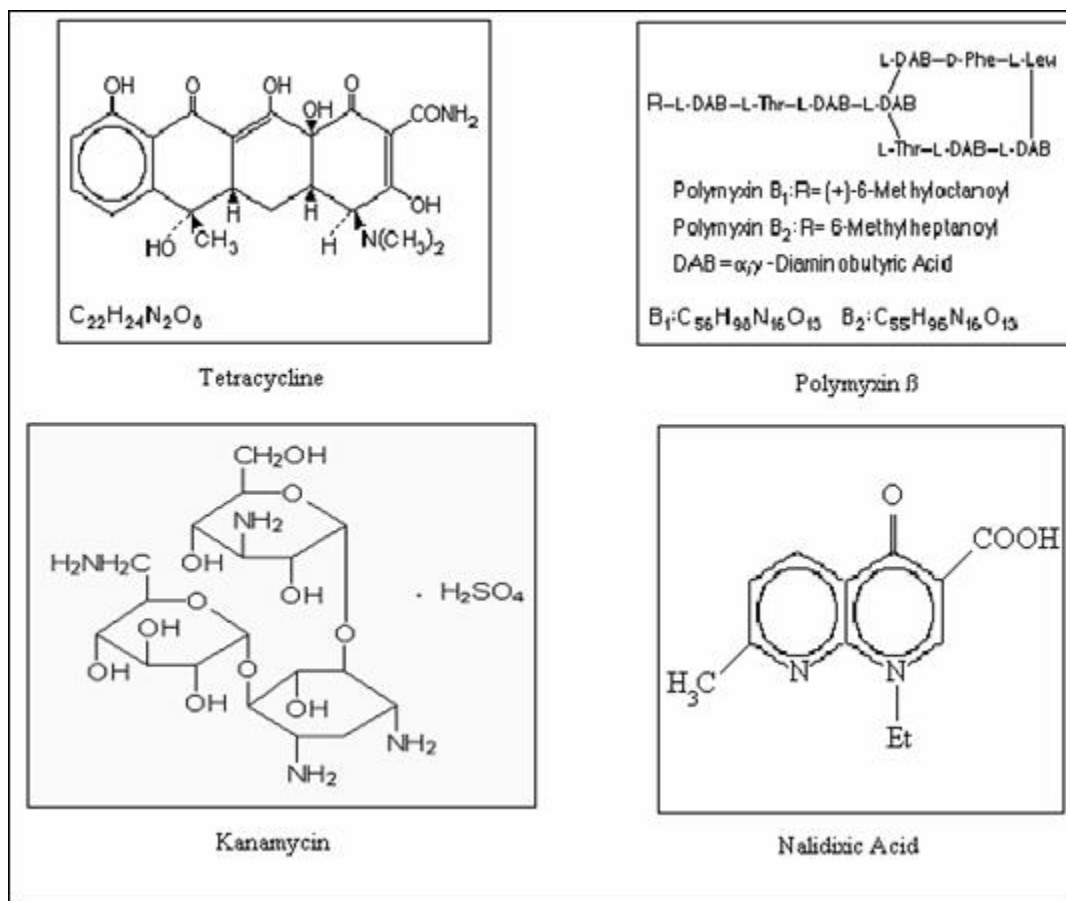


Figure 4.2.5A: Chemical structures of the four antimicrobials used: Tetracycline, Polymyxin  $\beta$ , Kanamycin, and Nalidixic Acid.

Polymyxin  $\beta$  sulfate is an antibiotic complex produced by *Bacillus polymyxa* composed as a mixture of Polymyxins  $\beta_1$  and  $\beta_2$ . It is used to treat infections against gram-negative organisms and is often used in combination with neomycin and is an important allergen in leg ulcer dermatitis.<sup>64</sup> It acts by being a cationic surface active agent, due to its lipophilic and lipophobic ends, that disturbs the integrity of the cell membrane. Kanamycin is an aminoglycoside antibiotic effective against gram-positive and gram-negative organisms.<sup>65</sup> It inhibits protein synthesis by binding to the 30S ribosomal subunit, causing misreading of the mRNA.<sup>65</sup> Tetracyclines possess a wide range of antimicrobial activity against gram-positive and

gram-negative bacteria. The bacterial ribosome is the site of action of Tetracyclines. Access to the ribosomes of gram-negative bacteria is obtained by passive diffusion through hydrophilic pores in the outer cell membrane and then by an energy-dependent active transport system that pumps all Tetracyclines through the inner cytoplasmic membrane.<sup>66</sup> This active transport system may require a periplasmic protein carrier.

Tetracyclines bind specifically to 30 S ribosomes and appear to inhibit protein synthesis by preventing access of aminoacyl tRNA to the acceptor site on the mRNA-ribosome complex.<sup>66</sup> The inhibitory effects of the Tetracyclines can be reversed by washing. This suggests that the reversibly bound antibiotic rather than the small portion of irreversibly bound drug is responsible for the antibacterial action. Nalidixic acid is a synthetic anti-bacterial chemical that is highly effective against gram-negative bacteria such as *E. coli*, *Proteus*, and other gram-negative bacteria.<sup>67</sup> Both active and inactive forms of Nalidixic acid are found in urine.

### **4.3 Results and Discussion**

#### **4.3.1 Experiment 1: Antimicrobials Attached to Silicon Wafers Treated with Isocyanatopropyl Triethoxysilane (NCO)**

This experiment was performed to determine if antimicrobial effectiveness would be altered by covalent attachment of its terminal functionality to the NCO SAM. This initially was a cause for concern since it was not known which chemical constituent of the antimicrobial agent was responsible for the destruction (killing efficiency) of the bacterium or if covalent attachment of the antimicrobial to the surface would alter its efficiency.

Ellipsometry measurements from Table 4.3.1A suggest all of the antimicrobials covalently bonded to the silicon wafers with the possible exception of Kanamycin. A possible explanation for the low thickness results for Kanamycin may be that the molecule is laying flat on the surface. Due the many possible binding sites of the Kanamycin molecule (eleven possible binding sites on Kanamycin), it is possible that the molecule is “pinned” parallel to the surface and not perpendicular to the surface, therefore resulting in a very small (thin) surface thickness.

Table 4.3.1A: Antimicrobial SAM ellipsometry measurements on antimicrobial coated silicon wafers with NCO SAM as the attaching linker (Å).

	1	2	3	4	5	6	7	8	Average	Std. Dev.
NCO + Polymyxin β	46.53	42.83	37.54	39.42	46.79	49.48	42.46	38.42	42.93	4.35
NCO + Tetracycline	49.72	41.43	43.67	38.64	40.21	34.22	32.6	41.69	40.27	5.38
NCO + Kanamycin	31.55	31.27	33.79	35.08	31.02	32.26	35.37	34.13	33.06	1.75
NCO*	28.87	31.46	28.7	28.78	28.71	28.71	28.75	28.79	29.1	0.96

\*Note: These values do not take into consideration the native oxide coating on the silicon wafers. Therefore, these values are a combination of the oxide coating as well as the SAM. Typically, the NCO SAM has a thickness value of 7-10 Å and the oxide coating has a thickness value of 15-20 Å.

After the antimicrobials were covalently bound to the NCO SAM, the wafers were then submersed for 29 hours in an E. coli media and photographed using an AMC microscope after being inoculated for 5 and 29 hours (Figures 4.3.1A-F). From these photographs, it is possible to visibly determine if bacterial adhesion or biofilm growth onto the antimicrobial-coated wafer surface is taking place. The microscope images for the Polymyxin β coated wafer (Figures 4.3.1C and D) revealed no bacterial adhesion to the surface occurred over the 29 hour inoculation period. Conversely, the microscope images for the Kanamycin and Tetracycline coated wafers (Figures 4.3.1A, B, E, and F) may depict evidence of bacterial adhesion to the surface over the 29 hour inoculation period. This is difficult to confirm, however, since the E. coli solution included tryptic soy broth (TSB- a culturing medium used to achieve sufficient

growth of many kinds of microorganisms) and this subsequently may actually be what was adhered to the surface.

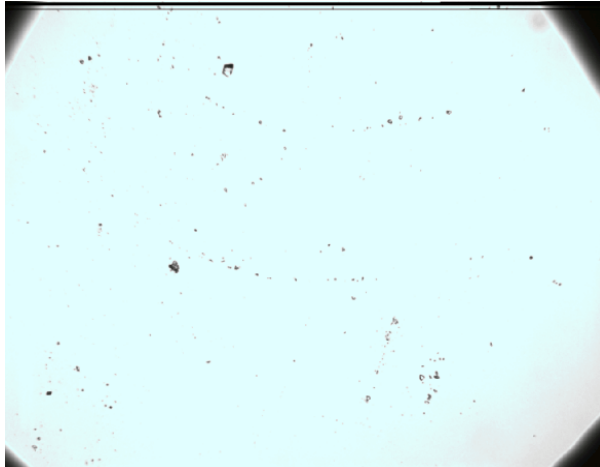


Figure 4.3.1A: AMC Microscope image of Kanamycin coated silicon wafer after exposure to *E. coli*-TSB solution 5 hours.

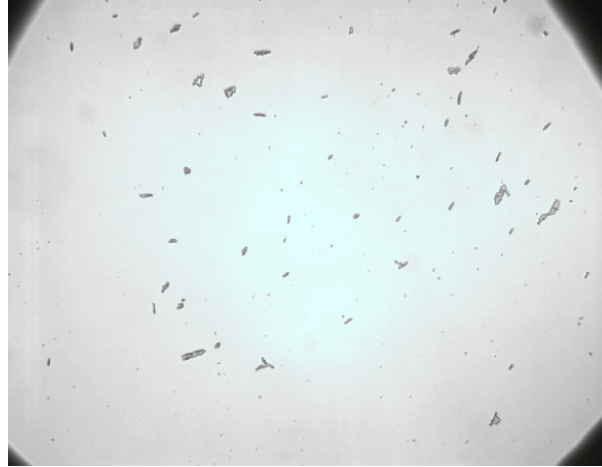


Figure 4.3.1B: AMC Microscope image of Kanamycin coated silicon wafer after exposure to *E. coli*-TSB solution 29 hours.

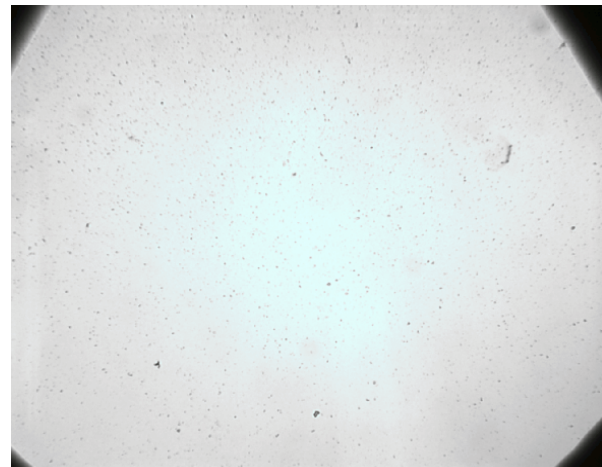


Figure 4.3.1C: AMC Microscope image of Polymyxin  $\beta$  coated silicon wafer after exposure to *E. coli*-TSB solution 5 hours.



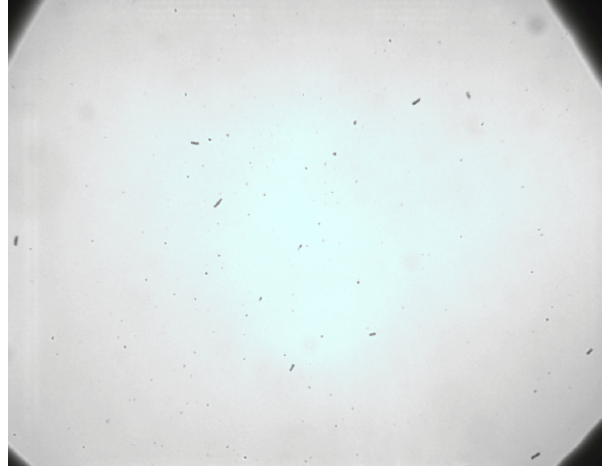


Figure 4.3.1D: AMC Microscope image of Polymyxin  $\beta$  coated silicon wafer after exposure to E. coli-TSB solution 29 hours.



Figure 4.3.1E: AMC Microscope image of Tetracycline coated silicon wafer after exposure to E. coli-TSB solution 5 hours.



Figure 4.3.1F: AMC Microscope image of Tetracycline coated silicon wafer after exposure to *E. coli*-TSB solution 29 hours.



Figure 4.3.1G: AMC Microscope image of NCO-coated silicon wafer (control) after exposure to *E. coli*-TSB solution 29 hours.

Optical density measurements performed on each *E. coli* solution in which an antimicrobial-coated wafer was submersed are shown in Table 4.3.1B. Ellipsometry measurements on the antimicrobial-coated wafer post-exposure for 29 hours are shown in Table 4.3.1C. From these tables the steady increase in solution absorbance (optical density) and the

increase in monolayer thickness suggest that a formation of biofilm growth may be occurring as a function of time. However, as mentioned earlier, images did not support a biofilm addition on the Polymyxin  $\beta$  sample. A possible explanation for the ellipsometric increase can be water absorption onto the antimicrobial-coated wafer after being subjected to the E. coli solution and inadequate drying time. Another possible explanation is that although there was no visible bacterial growth on the antimicrobial-coated wafer surface when viewing the photographs, the E. coli cells or TSB solution may have adhered to the surface regardless of efforts taken to avoid this (i.e. copious washing with water and nitrogen drying). Due to this inconsistency in data, the experiment was repeated. From the photographs obtained it was concluded that the lack of bacterial growth on the surface of the Polymyxin  $\beta$  antimicrobial-coated silicon wafer implies that antimicrobial effectiveness is not altered by covalent attachment to the NCO SAM.

Table 4.3.1B: Optical density absorbance measurements of the solution of antimicrobial-coated silicon wafers at 600 nm after inoculation with E. coli-TSB solution at various time intervals.

<b>ABSORBANCE</b>		
<b>Antimicrobial</b>	<b>5 Hours</b>	<b>29 Hours</b>
Polymyxin $\beta$	0.08279	1.20021
Tetracycline	0.08655	1.01119
Kanamycin	0.00275	1.12098
NCO wafer	0.13832	0.54134
Control	0.05731	1.37091

Table 4.3.1C: Ellipsometry measurements ( $\text{\AA}$ ) on antimicrobial coated silicon wafers with NCO SAM as the attaching linker after being inoculated with E. coli bacteria in a 37° Celsius water bath with continuous shaking over a 29 hour period. Measurements taken after a 29 hour period.

	<b>1</b>	<b>2</b>	<b>3</b>	<b>4</b>	<b>5</b>	<b>6</b>	<b>7</b>	<b>8</b>	<b>Ave</b>	<b>Std. Dev.</b>
Polymyxin $\beta$	77.21	90.34	90.35	115.58	104.00	156.35	77.91	107.22	102.37	25.73
Tetracycline	108.99	79.69	101.29	129.60	94.10	91.56	78.56	93.84	97.20	16.53
Kanamycin	112.50	75.34	80.21	84.78	84.19	81.10	97.25	89.20	88.07	11.84
NCO	152.80	68.04	184.75	117.29	289.36	110.34	91.05	106.07	139.96	70.30

#### 4.3.2 Experiment 2: Antimicrobials Attached to Silicon Wafers Treated with Isocyanatopropyl Triethoxysilane (NCO) - repeat

Experiment 2 (4.3.2) is a repeat of Experiment 1 (4.3.1), with additional antimicrobials (Chloramphenicol and Nalidixic Acid) included and static contact angle measurements were recorded. However, AMC microscope images were not taken. Initial ellipsometric results (Tables 4.3.2A and C) reveal interesting results. When reviewing the data from the tables, it appears that the Tetracycline and Chloramphenicol antimicrobial-coated wafers did not covalently attach to the NCO wafer surface and the Polymyxin  $\beta$  antimicrobial-coated wafer surface had a nominal increase in surface thickness. When comparing the ellipsometric results obtained from Experiment 1 (Table 4.3.1A) to Experiment 2 (4.3.2C) for Polymyxin  $\beta$ , the difference in antimicrobial deposition onto the silicon wafer differs from  $\sim 13 \text{ \AA}$  for Experiment 1 to  $\sim 1.5 \text{ \AA}$  from Experiment 2.

In contrast, the Kanamycin antimicrobial-coated wafer had a significantly larger deposition thickness ( $\sim 2000 \text{ \AA}$ ). Due to the thick deposition, it was assumed that the Kanamycin antimicrobial-coated wafer was not covalently bound to the surface and was actually physisorbed

to the surface. This was verified in the ellipsometric measurements taken on the wafer after inoculation in E. coli-TSB solution for 5 hours (Table 4.3.2E). The overall increase in measured thickness for each antimicrobial-coated wafer after inoculation with E. coli-TSB solution for 5 hours, with the exception of Kanamycin, suggests that the antimicrobial were covalently attached to the NCO SAM. Once again, either a biofilm addition onto the antimicrobial-coated wafer surface or inadequate drying occurred.

Optical density absorbance measurements conducted at 600 nm on antimicrobial-coated wafers at various time intervals after inoculation with E. coli-TSB solution (Table 4.3.2D) verified that the E. coli-TSB solution was viable (Control #1 and 2). It also suggests that the Chloramphenicol and Nalidixic Acid antimicrobial-coated wafers reduced the cell viability (reproduction capability) of the E. coli bacterium over a 5-hour time frame. Since the results of the Chloramphenicol and Nalidixic Acid-coated wafers showed promising results, another experiment was conducted to evaluate the covalent attachment and effectiveness of the antimicrobials.

Table 4.3.2A: Ellipsometry ( $\text{\AA}$ ) results on NCO coated silicon wafers after ~3.5 hour SAM deposition time.

	<b>1</b>	<b>2</b>	<b>3</b>	<b>4</b>	<b>5</b>	<b>6</b>	<b>7</b>	<b>8</b>	<b>Ave</b>	<b>Std. Dev.</b>
Wafer #1	32.22	31.74	33.09	32.78	32.53	32.68	32.77	32.50	32.54	0.41
Wafer #2	34.46	32.11	30.93	32.49	31.94	33.74	33.11	33.74	32.82	1.16

Table 4.3.2B: Static contact angle (degrees) results on NCO coated silicon wafer after ~3.5 hour SAM deposition time.

	1	2	3	4	5	6	Ave	Std. Dev.
Wafer #1	61	61	66	68	66	68	65.0	3.2

Table 4.3.2C: Ellipsometry measurements (Å) of antimicrobial coated silicon wafers with NCO SAM as the attaching linker. Deposition time 18 hours.

	1	2	3	4	5	6	7	8	Ave	Std. Dev.
Polymyxin β	33.97	33.45	35.21	33.2	42.39	26.67	32.33	35.88	34.14	4.35
Tetracycline	35.03	24.66	28.58	30.19	29.05	28.82	28.55	29.4	29.29	2.84
Chloramphenicol	29.49	26.47	28.15	27.74	27.39	19.69	26.75	25.63	26.41	2.96
Nalidixic Acid	46.75	43.72	51.08	50.71	45.97	45.29	53.87	48.24	48.20	3.43
Kanamycin	2024	2045	1456	2208	2073	2234	2234	2105	2047	254

Table 4.3.2D: Optical density absorbance measurements at 600 nm on antimicrobial coated silicon wafers at various time intervals (Hours:Minutes) after inoculation with E.Coli-TSB solution . Absorbance measurements conducted on the E.Coli-TSB solution. Control samples (#1 and #2) are blank silicon wafers with no treatment (SAM addition or cleansing). (N/V: No Value. Measurement not taken)

Sample	2:30	5:00
Control #1	N/V	0.414215
Control #2	N/V	0.412063
NCO wafer	0.788269	0.424819
Polymyxin β	0.021330	0.402328
Tetracycline	-0.046110	0.455718
Chloramphenicol	N/V	0.027465
Nalidixic Acid	0.356384	0.364608
Kanamycin	0.023056	0.434173

Table 4.3.2E: Ellipsometry measurements (Å) on antimicrobials attached to NCO coated silicon wafers after inoculation in E. coli-TSB solution 5 hours. (N/V: No Value-measurement not taken; N/D: No Data-value not returned from instrument due to signal loss).

	1	2	3	4	5	6	7	8	Ave	Std. Dev.
NCO wafer	40.55	43.22	37.81	44.67	44.22	41.73	43.68	43.10	42.37	2.3
Polymyxin β	48.92	49.00	47.64	52.91	47.25	47.95	52.00	51.94	49.70	2.2
Tetracycline	N/V	N/V	N/V	N/V	N/V	N/V	N/V	N/V	N/V	N/V
Chloramphenicol	47.16	43.16	42.77	43.82	28.37	41.94	42.11	42.31	41.46	5.6
Nalidixic Acid	46.62	50.83	53.42	50.47	50.78	50.99	52.81	74.99	53.86	8.8
Kanamycin	1308	N/S	1431	1430	1348	1383	1426	1415	1392	48

### 4.3.3 Experiment 3: Attachment and Effectiveness of a Variety of Antimicrobials on Silicon Wafers

The purpose of this experiment was to reconfirm covalent attachment of various antimicrobial agents to a silicon substrate after attachment of a self-assembled monolayer and to determine (evaluate) its' activity (efficiency). Ellipsometry measurements (Table 4.3.3B) suggest that all the antimicrobial-coated wafers covalently attached to the surface. The Tetracycline and Chloramphenicol-coated wafers again showed little, or no, increase in thickness after antimicrobial deposition which suggests covalent attachment of the antimicrobial to the surface did not occur. As stated in the previous experiment (4.3.2), the optical density measurements (Table 4.3.3C) after inoculation with E. coli-TSB solution for six hours suggest that the E. coli cells are viable. Also, the Chloramphenicol and Tetracycline-coated wafers optical density values were below the control which suggests antimicrobial effectiveness. This is difficult to positively state however, since the optical density measurements for the NCO wafer was in the same range as both antimicrobial-coated wafers (~0.411, ~0.433, and ~0.419 for the NCO, Chloramphenicol, and Tetracycline wafers, respectively). These values are lower than the optical

density values for the control wafer (~0.454), however. In fact, all antimicrobial-coated wafers had lower optical density values in comparison to the control wafer, including a significantly lower value of ~-0.047 for the Nalidixic Acid-coated wafer after 6 hours.

Ellipsometric results after inoculation again suggests that either a biofilm addition onto the antimicrobial-coated wafer surface or inadequate drying occurred (Table 4.3.3D), with the exception of Nalidixic Acid. In this case, the antimicrobial thickness reduced from an average of 71.41 Å (Table 4.3.3B) to 53.27 Å (Table 4.3.3D). This value is somewhat misleading, however. The average antimicrobial thickness after the initial deposition for Nalidixic Acid was calculated using all eight data values obtained including an atypical value of 220.33 Å. The other seven data values obtained were between ~42 and ~65 Å. Thus, if this one data value were removed the resultant average antimicrobial thickness for the initial deposition for Nalidixic Acid would be 50.13 Å. The high thickness measurement is probably due to uneven drying or a particle on the surface during the measurement and is considered to be inaccurate. Thus, the average antimicrobial thickness of 50.13 Å is used for subsequent discussion in Section 4.4.

Table 4.3.3A: Ellipsometry measurements (Å) on NCO coated silicon wafers after 4 hour SAM deposition time.

	<b>1</b>	<b>2</b>	<b>3</b>	<b>4</b>	<b>5</b>	<b>6</b>	<b>7</b>	<b>8</b>	<b>Ave</b>	<b>Std. Dev.</b>
Wafer #1	29.35	30.00	30.10	30.46	32.75	32.87	29.35	32.30	30.90	1.50
Wafer #2	30.39	32.07	32.09	35.47	31.17	30.71	30.21	30.18	31.54	1.76
Overall	-	-	-	-	-	-	-	-	31.22	1.62



Table 4.3.3B: Ellipsometry measurements ( $\text{\AA}$ ) of antimicrobial coated silicon wafers with NCO SAM as the attaching linker. Deposition time was 22 hours. Antimicrobial was bound to NCO SAM on silicon wafer.

	<b>1</b>	<b>2</b>	<b>3</b>	<b>4</b>	<b>5</b>	<b>6</b>	<b>7</b>	<b>8</b>	<b>Ave</b>	<b>Std. Dev.</b>
Polymyxin $\beta$	37.01	39.57	38.36	41.43	35.89	44.84	42.56	44.69	40.54	3.39
Tetracycline	27.61	35.28	30.22	28.88	33.11	28.81	32.26	29.73	30.74	2.59
Chloramphenicol	27.53	28.30	27.38	28.66	31.97	28.46	66.40	25.86	33.07	13.58
Nalidixic Acid	42.22	52.96	65.41	50.17	220.33	44.43	48.18	47.56	71.41	60.58
Kanamycin	132.66	132.28	228.52	134.95	134.74	132.52	129.23	130.43	144.42	34.04

Table 4.3.3C: Optical density absorbance measurements at 600 nm on antimicrobial coated silicon wafers at various time intervals (Hours:Minutes) after inoculation with E. coli-TSB solution. Absorbance measurements conducted on the E. coli-TSB solution.

	1:30	6:00
Control	0.434967	0.454528
NCO wafer	0.369293	0.411163
Polymyxin $\beta$	0.239425	0.436889
Tetracycline	0.435363	0.419998
Chloramphenicol	0.393173	0.433270
Nalidixic Acid	0.295776	-0.047760
Kanamycin	0.420852	0.403839

Table 4.3.3D: Ellipsometry measurements ( $\text{\AA}$ ) on antimicrobials attached to NCO coated silicon wafers after inoculation in E. coli-TSB solution 6 hours. (N/D: No Data. Value not returned from instrument due to signal loss).

	1	2	3	4	5	6	7	8	Ave	Std. Dev.
NCO wafer	40.12	36.27	38.59	37.59	42.00	39.06	N/D	40.41	39.15	1.90
Polymyxin $\beta$	55.02	55.19	58.13	58.06	N/D	59.73	56.16	57.00	57.04	1.72
Tetracycline	42.85	44.94	41.48	43.32	42.93	39.52	43.45	44.28	42.85	1.69
Chloramphenicol	42.78	41.33	39.91	41.82	40.97	40.87	40.22	44.19	41.51	1.41
Nalidixic Acid	49.57	53.56	52.47	53.64	56.84	55.08	53.66	51.31	53.27	2.22
Kanamycin	263.47	154.55	141.55	138.92	357.37	190.15	231.14	142.34	202.44	77.78

## 4.4 Conclusions

### 4.4.1 E. coli cell viability

In all the experiments conducted, there were viability controls performed to verify that the E. coli cells that were in solution were alive and multiplying. These verifications were labeled as “controls” and the only data obtained was absorbance measurements. In all three (3) experiments, the absorbance readings for the controls were consistently equal to or higher than the antimicrobial attached samples. This would suggest that: 1) the E. coli cells in the control experiments are viable and alive since an increasing absorbance measurement represents an increase in E. coli cell density and 2) the antimicrobial-coated wafers either reduces bacterial growth of the solution in general and/or eliminates bacterial adhesion onto the antimicrobial-coated silicon wafers.

#### 4.4.2 AMC Microscope Imaging

It is difficult to determine which of the antimicrobial agents reduced or inhibited cell growth through this technique but it is obvious that there was a noticeable difference in cell adhesion and colony growth to the antimicrobial-coated silicon surfaces throughout the inoculation period. The Polymyxin  $\beta$ -coated wafer displayed the most dramatic visual effect of reducing or inhibiting cell growth while the Kanamycin and Tetracycline-coated wafers both had areas of possible bacterial colonies or cell growth on the surface. Also, when imaging the individual solutions in a transmission scan instead of a reflectance scan, there was no bacterium present in the Polymyxin  $\beta$ -coated wafer solution which would suggest the antimicrobial-coated wafer didn't allow for bacterial adhesion to the surface and/or "killed" the bacterium.

#### 4.4.3 Ellipsometry, Contact Wetting Angle and Optical Density Measurements

From Experiment 1 (4.3.1) the antimicrobials which showed attachment onto the NCO-coated silicon surface were Polymyxin  $\beta$  and Tetracycline. Ellipsometric values regarding all antimicrobial-coated wafers increased in thickness after being exposed to *E. coli*. This suggests that bacterial adhesion or biofilm growth onto the surface may have occurred and as a result the antimicrobial agents did not successfully deter the bacteria from adhering to the surface. However, it does appear that the colonies did not "spread" after adhesion. Therefore it is believed that the *E. coli* bacteria were either "killed" or hindered in such a way that after adhesion to the surface took place, the bacteria was incapable of multiplying further.

In Experiment 2 (4.3.2), there was excessive Kanamycin deposition onto the NCO SAM wafer before being exposed to *E. coli* solution. There appeared to be no covalent deposition of

Tetracycline, Chloramphenicol, and possibly Polymyxin  $\beta$  antimicrobials after attachment of the NCO SAM. A possible explanation for this is that either there was no covalent attachment of the antimicrobial or the antimicrobial is in a “laying down” orientation which would cause the thickness measurements to appear thin (Polymyxin  $\beta$  thickness of  $\sim 2$  Å).

When examining Tables 4.3.2C, D, and E, the Tetracycline antimicrobial is more than likely not present. This is assumed since the ellipsometric thickness ( $0$  Å) and optical density measurement ( $\sim 0.455$ ) after a 5 hour exposure is non-existent and higher than the control sample ( $0.414$ ), respectively. On the other hand, the Polymyxin  $\beta$  and Chloramphenicol-coated wafers are probably in the “lay down” orientation. This is concluded since the optical density values ( $\sim 0.402$  and  $\sim 0.027$ , respectively) after exposure to the *E. coli* bacterial solution for 5 hours is lower than the control. Also, the ellipsometric measurements after exposure confirm this conclusion. An increase in film thickness is portrayed in all antimicrobial and control (NCO) wafers after exposure to *E. coli* bacteria, with the exception of Kanamycin. This also may indicate a possible biofilm or bacterial adhesion to the silicon surface.

In Experiment 3 (4.3.3), all antimicrobials had a noticeable deposition except Tetracycline and Chloramphenicol. All ellipsometry measurements increased after exposure to *E. coli* with the exception of Nalidixic acid. This also may indicate a possible biofilm or bacterial adhesion to the silicon surface.

#### 4.4.4 Absorbance measurements

Nalidixic acid had considerably lower absorbance measurements (*E. coli* cell density) than any of the other antimicrobials tested. The antimicrobial-coated wafers that did not appear to have considerable (if any) antimicrobial attachment determined from ellipsometry results fell

within the range that would be expected for a NCO-coated wafer. Since Nalidixic acid had considerably lower absorbance (optical density) measurements and ellipsometry measurements indicate loss of antimicrobial after exposure to E. coli, then it may be assumed that some antimicrobial was either physisorbed and was washed off the surface after being placed in TSB solution. Or it was released after coming into contact with the E. coli bacteria. This may have contributed to the reduction of bacterial growth since there would be a greater interaction probability between the antimicrobial agent and bacteria in solution.

In conclusion, it appears that Nalidixic acid repeatedly reduced the amount of bacterial growth in solution (absorbance measurements) and also displayed a covalent antimicrobial attachment. Chloramphenicol optical density results also suggest that it reduces bacterial growth in solution even though ellipsometric results would imply otherwise.

#### 4.5 References

63. Kallio, P.T.; Tsai, P.S.; Bailey, J.E.; *Expression of Vitreoscilla Hemoglobin Is Superior to Horse Heart Myoglobin or Yeast Flavohemoglobin Expression for Enhancing Escherichia coli Growth in a Microaerobic Bioreactor*, Biotechnol. Prog. 1996, 12, 751 - 757.
64. Physicians' Desk Reference, 53<sup>rd</sup> Edition, 1999, Medical Economics Company, Inc., 1936.
65. The Merck Index, 12<sup>th</sup> Edition, 1996, Medical Economics Company, Inc., 900-901.
66. Physicians' Desk Reference, 53<sup>rd</sup> Edition, 1999, Medical Economics Company, Inc., 1514.
67. Physicians' Desk Reference, 53<sup>rd</sup> Edition, 1999, Medical Economics Company, Inc., 2792.

## **CHAPTER FIVE**

### **5 OLIGONUCLEOTIDES**

#### **5.1 Introduction**

The idea of using biochip arrays to understand biological reactions has become commonplace over past few years. This concept evolved from the idea of using combinatorial synthetic chemistry approaches to create very large-scale libraries of receptor molecules and screen the population for enhanced binding activity of individual members of a target of interest. Possible applications for large-scale arrays include sequencing by hybridization, DNA based sensors, and nucleic acid oligomer libraries for screening ligand binding.

Many factors, such as immobilization chemistries resulting in retention of bioactivity, strong biorecognition properties, and stable arrays, are important for constructing biomolecular arrays on surfaces. The use of liquid solution chemistry of an isocyanatopropyl triethoxy silane linker to tether oligonucleotides was examined and will be discussed.

#### **5.2 Objective and Background**

The objective of this work was to tether oligonucleotides on a solid flat surface with a low background intrinsic fluorescence. Silicon wafers were chosen as the solid surface for attaching oligonucleotides because of its extremely low background fluorescence. Another advantage with silicon wafers is that they also have low background chemiluminescence. Thus, fluorescent and chemiluminescent labels can be used during DNA-DNA hybridization. This

chapter describes the investigation on the method for covalent attachment of oligonucleotides using isocyanatopropyl triethoxysilane (NCO). Attachment was confirmed by two approaches: ellipsometry and fluorescence. In the second approach, attachment of the oligonucleotide was verified using fluorescence measurements of a fluorescently labeled oligonucleotide on the silicon wafers using a FluorImager. The developed method could be made adaptable to automated liquid handling systems, such as Biomek 2000, to create an array.

### **5.3 Results and Discussion**

#### **5.3.1 Ellipsometry and Contact Angle Measurement of Silicon Wafers Before and After SAM Attachment**

To obtain a standard reference before conducting any tests, the thickness of the oxide coating and the wettability characteristics of the silicon wafers were determined. Ellipsometry and static contact wetting angle measurements at two (2) steps during the attachment of isocyanatopropyl triethoxysilane (NCO) to the silicon surface was performed. Measurements were taken on the native silicon wafer substrate prior to cleansing, after cleansing, and again after the covalent attachment of the NCO SAM (Tables 5.3.1A-C).

Four samples were prepared on various dates to compare ellipsometry and contact wetting angle variations. This was done to ensure there were no deviations in procedure or results acquired from experiment to experiment. The average overall thickness measurements of the untreated silicon wafer before SAM attachment on the wafer and after SAM attachment were 29.4 and 32.0 Å, respectively (Table 5.3.1D). The overall averages of the wetting contact angle

measurements were 21.6 and 71.0 degrees, respectively (Table 5.3.1E). It can therefore be assumed that the results are repeatable and reasonable. (It should be noted that the static contact angle measurements conducted on the native silicon wafers after the cleansing step reduces increases the wetting of the surface and decreases the contact angle to below 20 degrees on average.)

The approximate 2.5 Ångstrom increase in thickness suggests that a thin film of linker molecules adhered to the silicon surface. This thickness is consistent with what would be expected for a molecule of this length. Contact wetting angles also fluctuated, confirming that the silicon surface was being restructured.

Table 5.3.1A: Silicon Wafer Ellipsometry and Wetting Contact Angle Measurements Prior to any Treatment or Cleaning in Isopropanol\*

#	9/17		10/2		9/17		10/2	
	Thickness (Å)		Thickness (Å)		Angle (Degrees)		Angle (Degrees)	
	Sample 1	Sample 2	Sample 1	Sample 2	Sample 1	Sample 2	Sample 1	Sample 2
1	30	31	30	30	21	21.25	24	22
2	30	31	31	30	20.5	21	23	21
3	27	30	31	29	21	21.25	24	23
4	27	30	30	29	20.5	21	22	23
5	31	30	31	28	21	21.75	24	21.5
6	31	30	32	30	20	21.25	20	20
7	29	27	31	29	-	-	-	-
8	28	27	27	28	-	-	-	-
9	-	-	26	28	-	-	-	-
10	-	-	27	34	-	-	-	-
11	-	-	28	29	-	-	-	-
12	-	-	34	27	-	-	-	-

\* Data was obtained on September 17 and October 2, 1997 (number of measurements vary).



Table 5.3.1B: Silicon Wafer Ellipsometry and Contact Angle Measurements After Isopropanol, Nitric Acid, and Potassium Hydroxide Washes and Drying in Nitrogen Stream\*

#	Thickness (Å)		Angle (Degrees)	
	Sample 1	Sample 2	Sample 1	Sample 2
1	19	22	19	16
2	19	22	18	19
3	21	22	21	20
4	20	22	20	20
5	20	22	22	20.5
6	20	22	23	21
7	21	22	-	-
8	21	22	-	-
9	20	21	-	-
10	20	20	-	-
11	19	20	-	-
12	19	21	-	-

\*From data obtained on October 2, 1997 (number of measurements vary).

Table 5.3.1C: Silicon Wafer Ellipsometry and Wetting Contact Angle Measurements After Isocyanatopropyl Triethoxysilane/Toluene Solution and Drying on Nitrogen Gas Stream.

#	Thickness (Å)			Angle (Degrees)		
	Sample 1	Sample 2	Sample 3	Sample 1	Sample 2	Sample 3
1	33	32	31	71	66	67
2	31	36	34	64	68	71
3	34	32	30	67	71	74
4	31	33	31	70	71	73
5	31	32	33	66	79	70
6	30	33	31	66	82.5	74
7	31	32	32	80	-	-
8	31	32	32	77	-	-
9	32	32	32	-	-	-
10	29	31	31	-	-	-

\* From data obtained on October 13, 1997 (number of measurements vary).

Table 5.3.1D: Silicon Wafer Ellipsometry Measurement (Å) Averages from Tables 5.3.1A through C.

	<b>Sample 1</b>	<b>Sample 2</b>	<b>Sample 3</b>	<b>Overall Average</b>	<b>Date Obtained</b>
Prior to any treatment	29.13	29.5	-	29.43	9/17
	29.83	29.25	-		10/2
After IPA, HNO <sub>3</sub> , KOH wash	19.92	21.5	-	20.71	10/2
After NCO/toluene addition	31.3	32.5	31.7	31.96	10/13

Table 5.3.1E: Silicon Wafer Wetting Contact Angle Measurement (degrees) Averages from Tables 5.3.1A through C.

	<b>Sample 1</b>	<b>Sample 2</b>	<b>Sample 3</b>	<b>Overall Average</b>	<b>Date Obtained</b>
Prior to any treatment	20.7	21.3	-	21.6	9/17
	22.8	21.8	-		10/2
After IPA, HNO <sub>3</sub> , KOH wash	20.5	19.4	-	20.0	10/2
After NCO/toluene addition	67.3	74.3	71.5	71.0	10/13

Obtaining these values, as well as the data, required numerous trials. As noted in the data and calculation portions of this report, sample dates varied. This was done to compare ellipsometry and contact wetting angle variations over an extended period of time, to confirm that no variations or deviations were experienced from experiment to experiment.

It should also be noted that some data obtained was not used in these calculations due to unforeseen circumstances such as evaporation of solvent or mishandling of silicon wafers. This often resulted in spots covering the silicon surface which interfered with ellipsometry and

contact angle measurements. However, measurements were still performed on these wafers and results were in good agreement to those obtained on properly handled samples.

One variation in the experimental process was performed when obtaining the toluene/isocyanatopropyl triethoxysilane data. In this portion of the process, the silicon wafers were not placed in the reaction kettle and heated but was allowed to stand in the toluene/isocyanatopropyl triethoxysilane solution over a 3 day period. This is ample time for the chemical kinetics for this reaction to occur and did not compromise data.

The data and results obtained in these experiments are accurate to the limits of the instrumentation used. Due to the numerous samples prepared on various days, it can be assumed that these results are repeatable and are reasonable. The overall increase in thickness measurements of approximately 2.5 Å suggests that a thin film of molecules did adhere to the silicon surface when reviewing Table 5.3.1D. Contact wetting angle averages also fluctuated (Table 5.3.1E) which confirms that a restructuring of the silicon surface is occurring.

### 5.3.2 Experiment 2: Fmly 2.1 - 2.4 Nucleotide Attachment on Treated Silicon in a Glass Vial

After confirming the silane linker was covalently attached to the silicon wafer surface from Experiment 5.3.1, the next step was to determine the adsorption ability of certain nucleotide chains on silicon wafers treated with an NCO SAM. This was achieved by dissolving an oligonucleotide in deionized water and covalently attaching it to the SAM via solution chemistry in a glass vial. Four nucleotide samples were diluted in 10 mL of deionized water with varying concentrations and the four nucleotide samples consisted of four different chain configurations (Table 5.3.2A).

Table 5.3.2A: {PRIVATE }Fmly 2.1 - 2.4 Nucleotide sample, molecular weight, mass of sample, concentration of solution, and nucleotide sequence.

Sample	MW (g/mol)	Mass (mg)	Concentration (mg/mL)	Sequence
2.1	2472	24	2.4	5'-TACTACTCG-3'
2.2	2457	21	2.1	5'-CACACTCG-3'
2.3	2487	20	2.0	5'-TACATTTCG-3'
2.4	2456	41	4.1	5'-TACTACTCA-3'

DNA consists of four nucleic acids: Adenine (A), thymine (T), guanine (G), and cytosine (C) (Figure 5.3.2A). The nucleotide structure can be broken down into 2 parts: the sugar-phosphate backbone and the base. All nucleotides share the sugar-phosphate backbone. Nucleotide polymers are formed by linking the monomer units together using an oxygen on the phosphate, and a hydroxyl group on the sugar.

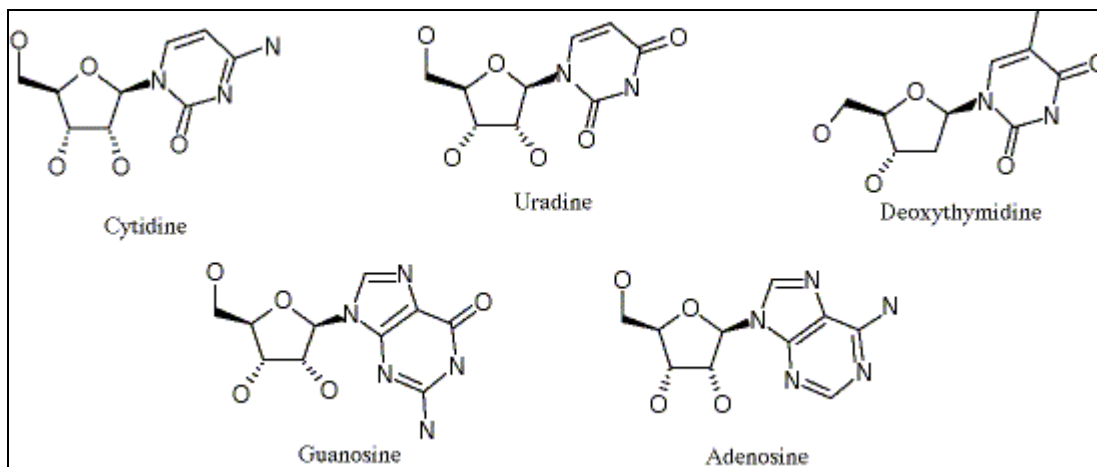


Figure 5.3.2A: Chemical structures of the four nucleotides in DNA, including Uracine (RNA). The sugar group is attached, but without the phosphate bound to the hydroxyl group on the sugar.

A chain of nucleotides can be joined by bonds between phosphate and sugar (= phosphodiester bonds). Adenine, thymine, guanine, and cytosine are capable of being linked

together to form a long chain. The 3'-hydroxyl group on the ribose unit, reacts with the 5'-phosphate group on its neighbor to form a chain (Figure 5.3.2B).

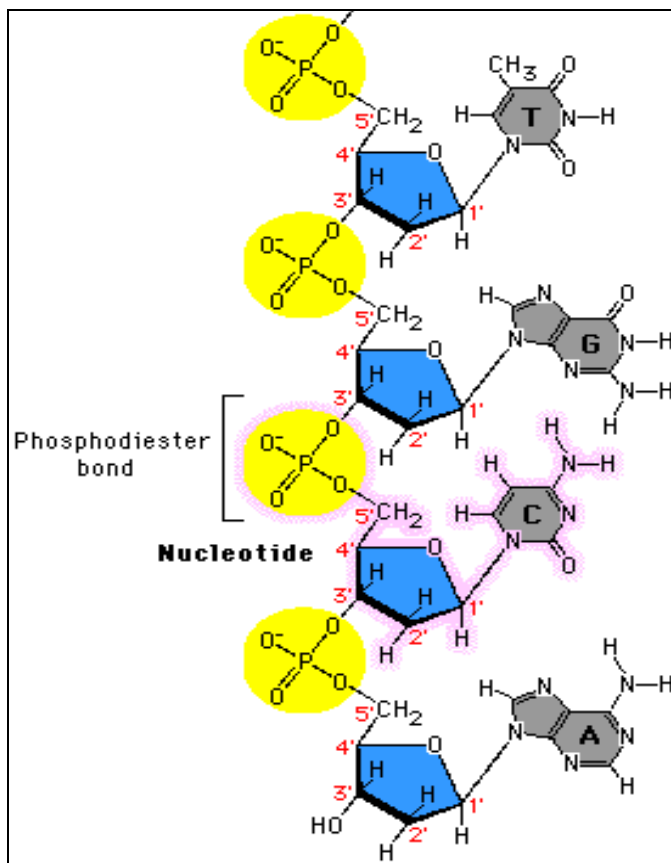


Figure 5.3.2B: Sample nucleic acid chemical structure and bonding formation for the four various nucleotides labeled T, G, C, A, respectively. Software Development Lab website at <http://dlab.reed.edu/projects/vgm/vgm/VGMPProjectFolder/VGM/RED/RED.ISG/chem2.html>

Rinsing the Fmly samples tethered to the NCO linkage on the silicon wafers appeared to have some effect on the thickness measurements (Tables 5.3.2B and C). Although the average thickness values did not fluctuate greatly between the two measurements (with the exception of

Fmly 2.2,  $\sim 8\text{\AA}$ ), the reduction in thickness of the Fmly nucleotide samples after rinsing would suggest that some of the nucleotide was physisorbed to the surface.

Table 5.3.2B: Silicon Ellipsometry Measurements ( $\text{\AA}$ ) after Treatment with Isocyanatopropyl Triethoxysilane and Nitrogen Drying.

#	Sample 1	Sample 2
1	30	30
2	29	33
3	33	34
4	30	31
5	30	31
6	30	40
7	30	31
8	30	33
9	31	31
10	38	31
Ave	31.1	32.5
Std. Dev	2.64	2.92

Table 5.3.2C: Silicon Contact Wetting Angle Measurements (degrees) after Treatment with Isocyanatopropyl Triethoxysilane and Nitrogen Drying.

#	Sample 1	Sample 2
1	60	64
2	66	63
3	65	62
4	61	64
5	65	61
6	68	59
Ave	64.17	62.17
Std. Dev	3.06	1.94

Table 5.3.2D: Sample Fmly 2.1 Ellipsometry Measurements (Å). Sample 1 rinsed with deionized water and nitrogen dried. Sample 2 only nitrogen dried.

#	Sample 1	Sample 2
1	31	36
2	30	27
3	30	26
4	30	40
5	31	35
6	31	27
7	29	28
8	30	32
9	30	32
10	32	32
Ave	30.4	31.5
Std. Dev	0.84	4.58

Table 5.3.2E: Sample Fmly 2.2 Ellipsometry Measurements (Å). Units in Å. Sample 1 rinsed with deionized water and nitrogen dried. Sample 2 only nitrogen dried.

#	Sample 1	Sample 2
1	30	45
2	29	40
3	30	40
4	34	37
5	28	41
6	31	40
7	32	40
8	33	37
9	35	38
10	34	42
Ave	31.6	40
Std. Dev	2.4	2.4

Table 5.3.2F: Sample Fmly 2.3 Ellipsometry Measurements (Å). Sample 1 rinsed with deionized water and nitrogen dried. Sample 2 only nitrogen dried.

#	Sample 1	Sample 2
1	28	39
2	27	28
3	27	30
4	28	33
5	28	28
6	27	29
7	27	28
8	29	29
9	35	36
10	28	28
Ave	28.4	30.8
Std. Dev	2.4	3.9

Table 5.3.2G: Sample Fmly 2.4 Ellipsometry Measurements (Å). Sample 1 rinsed with deionized water and nitrogen dried. Sample 2 only nitrogen dried.

#	Sample 1	Sample 2
1	28	59
2	36	47
3	33	44
4	39	41
5	37	39
6	36	40
7	38	42
8	41	42
9	48	36
10	34	36
Ave	37	42.6
Std. Dev	5.3	6.7

Figures 5.3.2B and C are FluorImager pictures of Fmly samples 2.1 through 2.4, which were dried in air. These samples were placed in a non-fluorescing 6-well plate and imaged with the aliquot “doped” side facing the reader. Figure 5.3.2B shows a blank silicon wafer control (far



left) and Fmly samples 2.1 and 2.2 (middle and far right, respectively). Figure 5.3.2C shows a blank silicon wafer control (far left) and Fmly samples 2.3 and 2.4 (middle and far right, respectively). The numbering system and description for the individual wafers follows:

- 1) Fmly sample rinsed in deionized water and nitrogen dried,
- 2) Fmly sample nitrogen dried only.

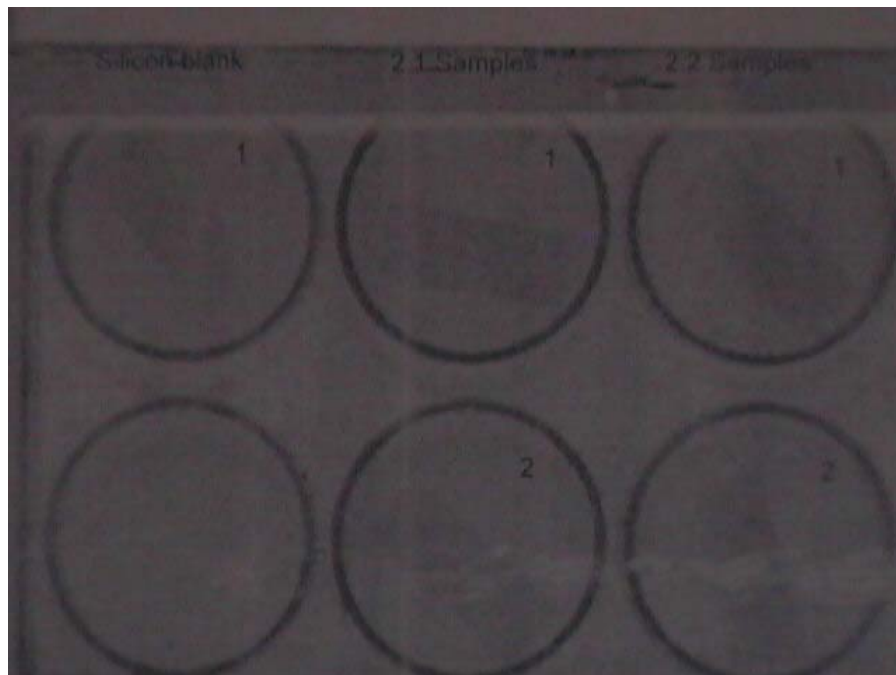


Figure 5.3.2C: Blank silicon wafer control (far left) and Fmly samples 2.1 and 2.2 (middle and far right, respectively).

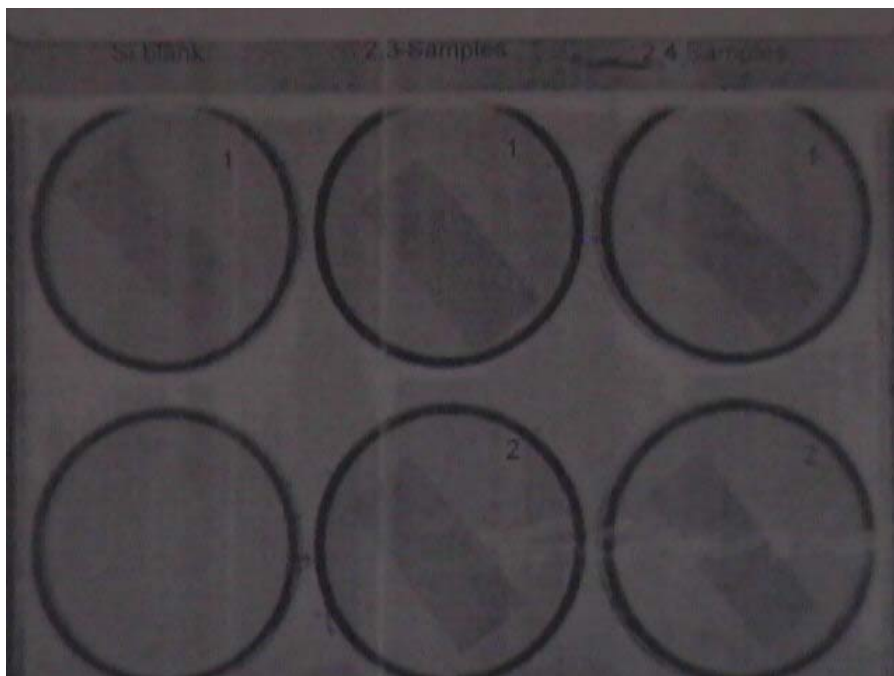


Figure 5.3.2D: Blank silicon wafer control (far left) and Fmly samples 2.3 and 2.4 (middle and far right, respectively).

Fmly 2.1 and 2.3 samples 1 and 2 exhibit no change in ellipsometry measurements suggesting no nucleotide addition. Fmly 2.2 sample 1 also exhibits no change in ellipsometry measurements.

Fmly 2.2 sample 2 did show considerable thickness increases and increased by an average of approximately 9 Å. Fmly 2.4 samples 1 and 2 thickness increased by an average of 6 and 11 Å, respectively. This suggests that nucleotide addition occurred.

In all cases, Samples 1 were rinsed with deionized water and nitrogen dried. Samples 2 were not rinsed with the deionized water but were nitrogen dried.

Possible explanations for the limited absorption of the nucleotides on the silicon wafers could be the amount of sample available for attachment. Fmly 2.4 samples had twice the amount of moles available for attachment than any other sample. This is noticed in the average

ellipsometry increase on both the nitrogen dried and rinsed samples. However, this would not explain why Fmly 2.2 sample 2 exhibited an increase in thickness while Fmly 2.1 and 2.3 showed none.

Perhaps a better explanation for this phenomenon could be that the sample placed in the solvent did not dissolve completely which would have resulted in a more diluted solution and even less possible moles to attach to the treated silicon substrate. If the sample did not dissolve completely, it can also be assumed that the majority of the solute rested at the bottom of the sample solution and would not interact with the silicon wafers.

In all samples rinsed with deionized water and then nitrogen dried, except Fmly 2.4, the ellipsometry measurements were similar to measurements made on the silicon wafers after being treated with the SAM. This would suggest that the nucleotide attachment was not covalently bound. Therefore, the nucleotide is probably only physisorbed to the surface.

### 5.3.3 Experiment 3: Fmly 2.1 - 2.4 Nucleotide Attachment on Treated Silicon Using a Modified Well Plate

Since the ellipsometry measurements had a variation of oligonucleotide attachments according to the data obtained in Experiment 5.3.2, a new approach was implemented. A Corning round bottom 96-cell well plate was modified, which increased both the oligonucleotide sample mass and localized its binding area on the treated silicon surface. It was believed that this new design would help increase the amount of oligonucleotides covalently bound to the silicon surface in the well while decreasing the total volume needed. The stock solution prepared in Experiment 2 was used for this experiment, however, the volume of the oligonucleotide stock

solution needed for each experiment decreased due to the improved design. Silicon wafers treated with a NCO SAM and wafers not treated (cleansed only) were used.

Ellipsometry measurements made on the cleansed silicon wafers (without SAM) after rinsing (Table 5.3.3A) indicated that a thin layer of molecules did not attach covalently to the surface, as expected. Measurements conducted on SAM treated silicon wafers after rinsing (Table 5.3.3B) suggest that a layer of molecules attached to the surface in all four samples, and it can also be assumed that the attachment was covalent. It was noted that an apparent “ring” on the silicon surface was observed when the modified well plate was removed. It appeared that the majority of the sample was located near the edges of the cell wells. This may be attributable to the wettability of the well plate surface.

Table 5.3.3A: Fmly 2.1 - 2.4 Nucleotide Sample Ellipsometry Measurements (Å) on Cleansed Silicon Wafers without SAM Attachment. Samples were rinsed with deionized water and dried with nitrogen.

#	Sample 2.1	Sample 2.2	Sample 2.3	Sample 2.4
1	35	17	35	28
2	37	21	25	26
3	31	21	38	23
4	31	25	36	22
5	46	24	25	25
6	44	21	26	42
7	32	20	22	84
8	33	18	25	372
Ave.	36.13	20.88	29.00	77.75
Std. Dev.	5.9	2.7	6.2	120.7

Table 5.3.3B: Fmly 2.1 - 2.4 Nucleotide Sample Ellipsometry Measurements (Å) on Treated Silicon Wafers with SAM Attachment. Samples were rinsed with deionized water and dried with nitrogen.

#	Sample 2.1	Sample 2.2	Sample 2.3	Sample 2.4
1	67	34	39	34
2	50	36	44	44
3	51	38	43	36
4	45	40	42	36
5	44	43	36	38
6	42	32	36	35
7	47	38	44	34
8	50	34	39	31
Ave.	49.50	36.88	40.38	36.00
Std. Dev.	7.8	3.6	3.3	3.8

FluorImager picture Figure 5.3.3A is of Fmly samples 2.1 through 2.4. Two untreated, but cleansed, silicon wafers were used as controls. Individual aliquots of Fmly 2.1 and 2.2 control samples were labeled 1/2 and Fmly 2.3 and 2.4 were labeled 3 /4. Two wells for each cleansed wafer were used to place the approximate 2.0-mL aliquot into the wells. Figure 5.3.3A also shows Fmly sample 2.1 (upper right corner) and 2.2-2.4 (bottom row, left to right). All samples were dried in air and placed in a non-fluorescing 6-well plate and imaged with the aliquot “doped” side facing upward.

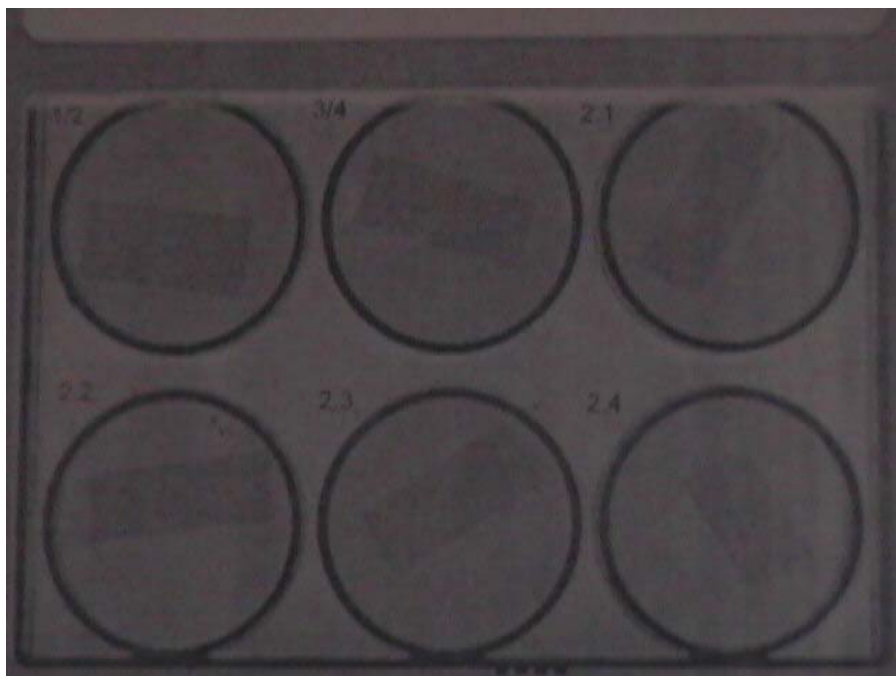


Figure 5.3.3A: Fmly sample 2.1 (upper right corner) and 2.2-2.4 (bottom row, left to right). Fmly control samples 2.1 and 2.2 (top left) is labeled  $\frac{1}{2}$  and Fmly control samples 2.3 and 2.4 (top middle) is labeled  $\frac{3}{4}$ .

Upon inspection of the ellipsometry values obtained in the control samples, it appears that there may be some attachment of Fmly 2.1 and 2.4 to the surface after rinsing (Table 5.3.3A). However, when comparing the standard deviations for Fmly 2.1, this value falls within the expected value for a cleansed silicon wafer obtained in Experiment 1 (5.3.1). Also, further inspection reveals that Fmly 2.4 has an extremely high standard deviation and the average ellipsometry value falls to 28.2 Å when the last two (2) recorded values are disqualified.

Ellipsometry measurements made on the cleansed silicon wafers (without SAM) after rinsing (Table 5.3.3A) indicated that a thin layer of molecules did not attach covalently to the surface. Measurements conducted on SAM treated silicon wafers after rinsing (Table 5.3.3B) suggest that the molecules were covalently attached to the surface in all four samples. It was

noted that an apparent “ring” on the silicon surface was observed when the modified well plate was removed. It appeared that the majority of the sample was located near the edges of the cell wells. This may be attributable to the wettability of the well surface.

Fluorescence measurements obtained also suggest that the Fmly sample bound to the silicon wafers for the control samples were not permanent (covalent) and the associated “rings” were simply physisorbed to the surface.

#### 5.3.4 Experiment 4: SBH 3.1 - 3.12 Oligonucleotide Attachment to a Silicon Treated Substrate Using a Modified Well Plate

Oligonucleotide samples were obtained to reproduce the results obtained from the previous nucleotide experiments (Experiments 5.3.2 and 5.3.3). Twelve oligonucleotide samples, SBH 3.1 - 3.12 (Table 5.3.4A), were used for attachment onto the silicon wafers. These oligonucleotide sample solutions were transferred into the modified well plate cells in a manner similar to that reported in Experiment 5.3.3.

Ellipsometry measurements on the samples not rinsed with deionized water varied in average from 875 to 1850 Å (Table 5.3.4C). These measurements obtained before rinsing with deionized water represent multi-layer attachment. Two samples, SBH 3.9 and 3.11, were washed with deionized water, and the average ellipsometry measurements were 84 and 97 Å, respectively (Table 5.3.4D). This suggests that the thickness of the oligonucleotide molecules covalently bound were about 52 and 65 Å, respectively.

Oligonucleotide length is not a simple, straight-forward calculation and depends on the conformation of the oligonucleotide. For argument sake, it was assumed the oligonucleotides (a single strand) were in a helical conformation (per standard conformation for double stranded

DNA). Base pair spacing under these conditions is 3.4 Å; an oligo of 17 nucleotides (SBH 3.1: 5'-III-ITA-ACT-CGC-CII-II-3') would then be ~58 Å in length, not including the fluorescein at the 5'end (I= Inosine, N= unknown nucleic acid residue). The fluorescein molecule probably is not much more than an additional 3-5 Å in length. In the worst case scenario, if the oligonucleotide is stretched out in a ladder-like conformation, the base pair spacing would be 6.8 Å; therefore a 17mer would be ~116 Å in length.

The oligonucleotide thickness of the two washed samples may suggest that the oligonucleotide is not a single monolayer of molecules and instead is in a multi-layer formation on the surface. Assuming the oligonucleotide for SBH 3.9 (5'-IINI-NICA-ACT-CGC-CNINI-II-3') is in a helical conformation (per standard conformation for double stranded DNA), the length of this molecule would therefore be ~58 Å. If SBH 3.9 is stretched out in a ladder-like conformation, it would have a length of ~116 Å. These calculations took into consideration that the unknown nucleic acid residue (N) length is negligible. From these calculations, it may be inferred that there is only one monolayer of covalently bound oligonucleotides on the silicon surface and it is in a helical conformation.



Table 5.3.4A: Oligonucleotide Sample Number and Sequence.

SBH Sample	Sequence
3.1	5'-III-ITA-ACT-CGC-CII-II-3'
3.2	5'-III-ITA-ACC-CGC-CII-II-3'
3.3	5'-III-ICA-ACT-CGC-CII-II-3'
3.4	5'-NININI-NITA-ACT-CGC-CNINI-NINI-3'
3.5	5'-NININI-NITA-ACC-CGC-CNINI-NINI-3'
3.6	5'-NININI-NICA-ACT-CGC-CNINI-NINI-3'
3.7	5'-IINI-NITA-ACT-CGC-CNINI-II-3'
3.8	5'-IINI-NITA-ACC-CGC-CNINI-II-3'
3.9	5'-IINI-NICA-ACT-CGC-CNINI-II-3'
3.1	5'-NINII-ITA-ACT-CGC-CII-NINI-3'
3.11	5'-NINII-ITA-ACC-CGC-CII-NINI-3'
3.12	5'-NINII-ICA-ACT-CGC-CII-NINI-3'

Table 5.3.4B: Molecular Weight, Mass and Concentration of Oligonucleotide Samples.

SBH Sample	MW (g/mol)	Sample mass (µg)	Conc. (µg/µL)	Conc. (nmol/µL)
3.1	2778.06	380.12	3.801	1.368
3.2	2763.05	293.44	2.934	1.062
3.3	2763.05	655.02	6.55	2.371
3.4	2778.06	293.08	2.931	1.055
3.5	2763.05	184	1.84	0.666
3.6	2763.05	611.21	6.112	2.212
3.7	2778.06	1003.68	10.037	3.613
3.8	2763.05	1276.34	12.763	4.619
3.9	2763.05	905.86	9.059	3.279
3.1	2778.06	1158.04	11.58	4.169
3.11	2763.05	1137.49	11.375	4.116
3.12	2763.05	1138.33	11.383	4.120

Table 5.3.4C: Ellipsometry Measurements (Å) for Oligonucleotide Samples Prior to Fluorescence Measurements. These samples were not rinsed with deionized water. They were only nitrogen dried.

<b>SBH #</b>	<b>1</b>	<b>2</b>	<b>3</b>	<b>4</b>	<b>5</b>	<b>6</b>	<b>7</b>	<b>8</b>	<b>Ave</b>	<b>Std. dev.</b>
3.1	2238	2270	2168	2383	720	2282	741	1953	1844	699
3.2	833	1643	703	638	294	748	2228	777	983	630
3.3	2431	2150	2267	536	579	2277	521	2079	1605	884
3.4	1675	514	581	677	1732	2201	-	-	1230	726
3.5	438	2234	976	2348	84	707	-	-	1131	946
3.6	648	853	492	97	132	232	459	2154	633	667
3.7	520	853	621	2258	697	562	515	707	842	583
3.8	2074	618	636	607	2316	809	2250	293	1200	853
3.9	531	583	562	468	1935	577	1654	2073	1048	705
3.1	2215	524	667	564	703	598	-	-	879	658
3.11	2238	1932	2240	1062	588	1037	514	593	1276	747
3.12	530	599	515	563	2182	2197	2098	702	1173	819

Table 5.3.4D: Ellipsometry measurements (Å) after being analyzed on FluorImager in deionized water.

	<b>SBH 3.9</b>	<b>SBH 3.11</b>
1	44	44
2	51	53
3	66	116
4	90	153
5	85	263
6	47	135
7	68	51
8	108	52
9	176	50
10	0	56
Ave	73.5	97.3
Std dev.	47	71

FluorImager images in Figures 5.3.4A and B are of SBH samples 3.1 through 3.12. Figure 5.3.4A shows SBH samples 3.1 – 3.6, whereas Figure 5.3.4B shows SBH samples 3.7 – 3.12. All samples were dried in air and placed in a non-fluorescing 6-well plate and imaged with the aliquot “doped” side facing upward. Samples were dried in ambient air. Samples SBH 3.9 and 3.11 were washed in deionized water prior to imaging.

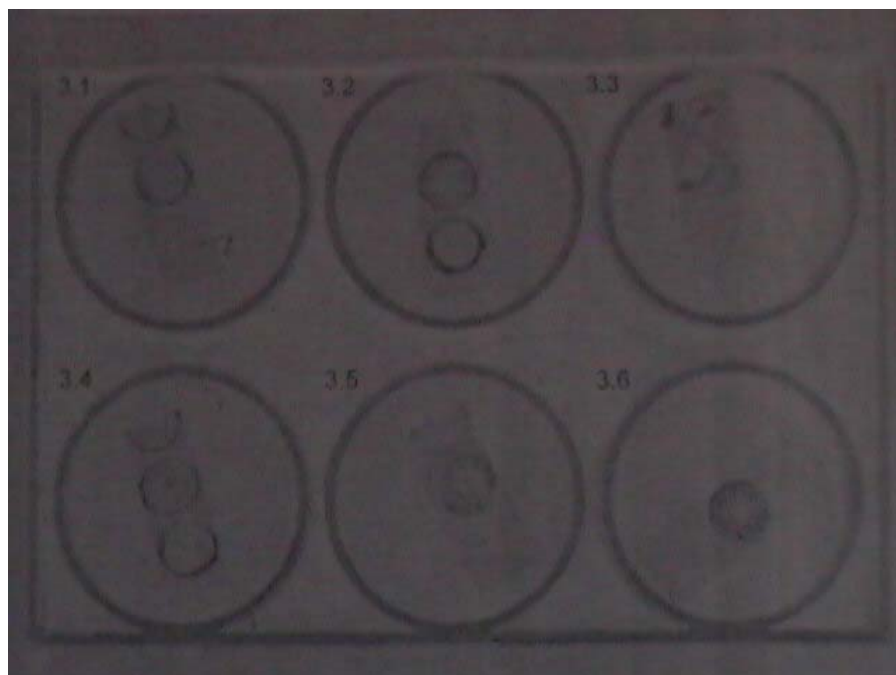


Figure 5.3.4A: FluorImager image of SBH samples 3.1-3.6 shown left to right, top to bottom. Samples dried under ambient air.

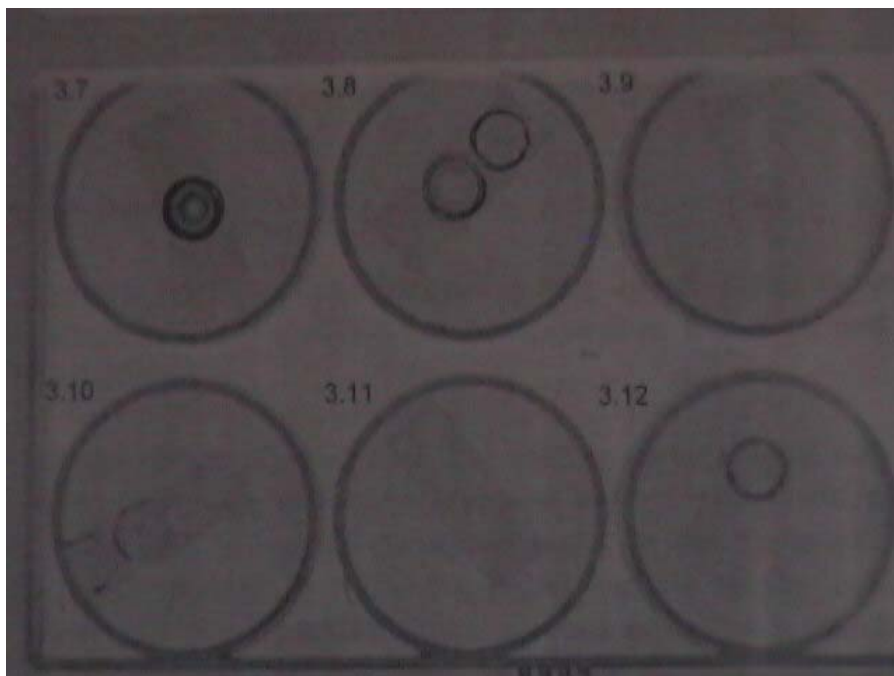


Figure 5.3.4B: FluorImager image of SBH samples 3.7-3.12 shown left to right, top to bottom. Samples dried under ambient air. Samples SBH 3.9 and 3.11 were washed in deionized water prior to imaging.

### **Results and Discussion.**

There are various possible experimental errors which could have occurred during this procedure that may have compromised the data and calculations obtained.

The exact sample mass transferred onto the silicon surface may not be accurate. Since the oligonucleotide samples were in the solid phase, it was necessary to add 100  $\mu\text{L}$  of deionized water to the samples. Centrifugation was needed to force the liquid sample to the bottom of the vial. Each sample had different ammonium salt concentrations; therefore, the exact sample mass transferred onto the surface may differ due to the solubility of the oligonucleotide sample.

Ellipsometry data obtained before fluorescence measurements are not representative of a true monolayer coverage thickness because these measurements only represent the density of the dried sample mass (Table 5.3.4C). Ellipsometry measurements on samples SBH 3.9 and 3.11

(Table 5.3.4D) are a more accurate measurement of monolayer thickness. However, these results are also subject to criticism because the wafers were not rinsed with deionized water. The wafers were simply placed in a water-filled cell well during fluorescence analysis. The wafers were then nitrogen dried and subsequently measured for monolayer thickness using ellipsometry. To obtain a more reliable ellipsometry measurement, the experiment could be repeated with an additional ellipsometry measurement made after a controlled washing with deionized water.

Ellipsometry measurements on the samples not rinsed with deionized water varied from an average of 875 to 1850 Å. Ellipsometry data obtained before fluorescence measurements are not representative of a true monolayer surface coverage thickness because these measurements only represent the density of the dried sample mass. However, two samples, SBH 3.9 and 3.11 were washed with deionized water and the average ellipsometry measurements after washing were 84 and 97 Å, respectively.

The fluorescence measurements obtained may also be skewed slightly. Noting the drying pattern on the silicon surfaces, the “rings” depicting fluorescence must be a “shadowing effect” due to the sample thickness since the oligonucleotide samples did not have a fluorescent tag. Also, after being submersed in the water solution, samples 3.9 and 3.11 had no detectable “shadowing effect”. This would again suggest that the “rings” are in fact merely shadows. It should be noted, however, that it is not known if these samples fluoresce in the emission wavelength of the FluorImager SI.

### 5.3.5 Experiment 5: Wetting Properties of Silicon Wafers with a Fluorescently Labeled Protein

The eventual application of this technique was to develop an array using a Biomek 2000 or equivalent liquid handling system for spotting purposes. It was necessary to know if the

solvent had any effect on the wetting characteristics or bonding capabilities of the SAM surface. It was also decided to begin using fluorescent-labeled molecules to decrease the time required to analyze the silicon wafers. A fluorescent-labeled oligonucleotide was not immediately available; instead a fluorescent-labeled protein was used. Thus, a protein ( $\beta$ -Amyloid 20 mer) with a fluorescent label (fluorescein) was used to determine the fluorescence intensity of fluorescein-tethered  $\beta$ -Amyloid 20 mer attached to a silicon wafer treated with NCO SAM. Various aliquots were spotted directly onto the NCO treated silicon surface without using the modified well plate.

From the FluorImager SI image (Figure 5.3.5A), it is apparent that the untreated silicon surface had irregular drying patterns and large surface-area coverage. This was expected since the wetting of native silicon is appreciably higher than that of NCO-treated wafers (<22 degrees and 71 degrees, respectively). The SAM treated silicon surface localized both sample solutions into small, circular patterns, as expected.

Table 5.3.5A: Sequence of Fluorescein-labeled protein attached to silicon wafers.

Fluorescein - QGTVSFNYPQITK
-----------------------------

Table 5.3.5B: Concentration of Fluorescein Sample Solutions

	Mass of Fluorescein (mg)	Concentration (mg/mL)
Water (1 mL)	1.5	1.5
DMF (1 mL)	4.4	4.4

Table 5.3.5C: Fluorescein excitation and emission wavelengths (nm).

	Excitation	Emission
Fluorescein	490	520

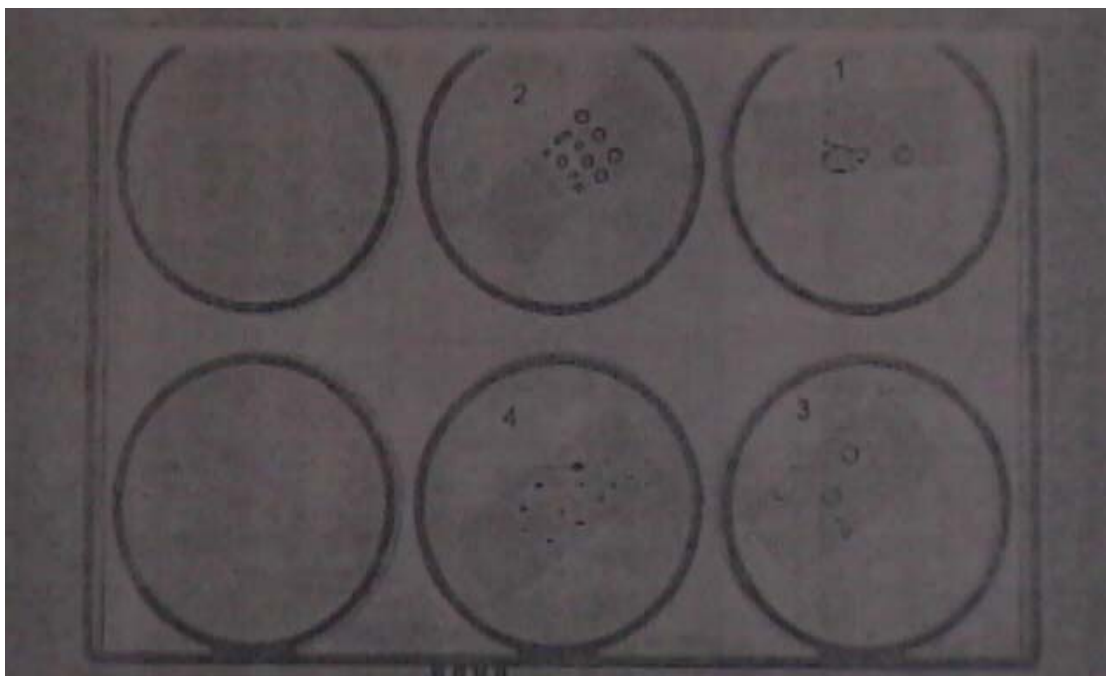


Figure 5.3.5A: Fluorescence image of a Fluorescein-labeled  $\beta$ -Amyloid 20 mer attached to a cleansed silicon wafer (1 and 3) and a NCO treated silicon wafer (2 and 4) using a high sensitivity scan on a FluorImager SI. Fluorescein-labeled  $\beta$ -Amyloid 20 mer wafer samples 1 and 2 were dissolved in a water solution, whereas wafer samples 3 and 4 were dissolved in a DMF solution. On each wafer there are various aliquot sizes deposited onto the secured silicon surface (0.5-25  $\mu$ L).

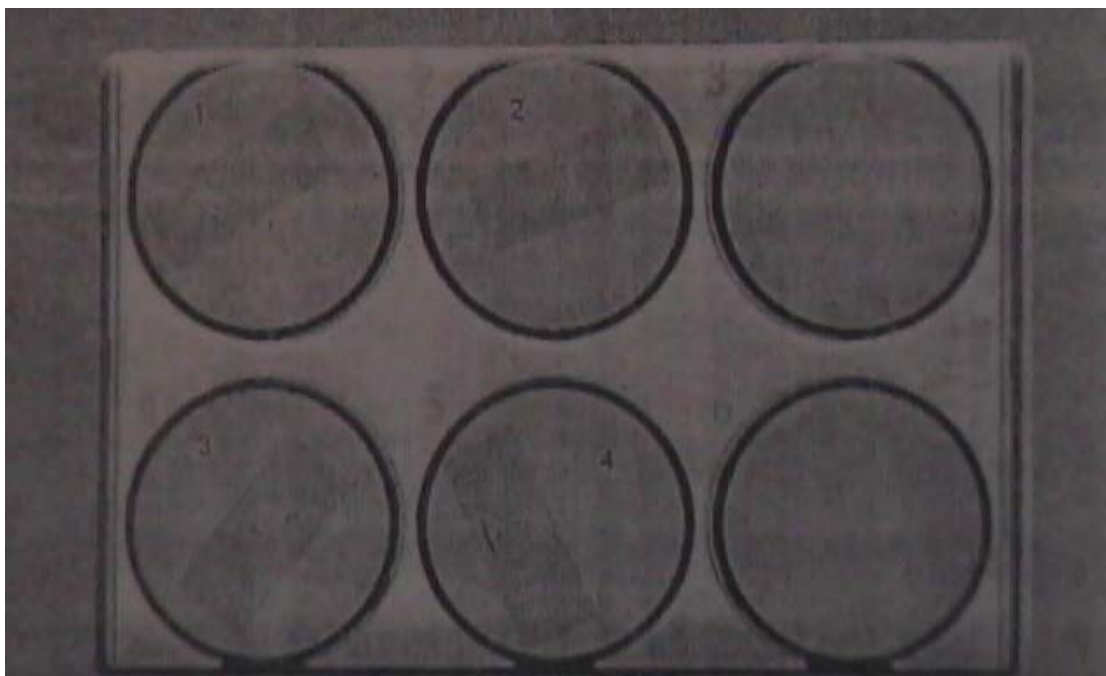


Figure 5.3.5B: Fluorescence image of a Fluorescein-labeled  $\beta$ -Amyloid 20 mer attached to a clean silicon wafer (1 and 3) and a NCO treated silicon wafer (2 and 4) using a high sensitivity scan on a FluorImager SI after being washed with solvent (DMF or deionized water). Fluorescein-labeled  $\beta$ -Amyloid 20 mer wafer samples 1 and 2 were dissolved in a water solution, whereas wafer samples 3 and 4 were dissolved in a DMF solution. On each wafer there are various aliquot sizes deposited onto the secured silicon surface (0.5-25  $\mu$ L).

From Figure 5.3.5A, silicon wafer #1 is a cleansed wafer without the SAM attached (no NCO linker) with water as the solvent. The first aliquot consisted of a 2.5  $\mu$ L drop that resulted in a large spread area. A 1.0  $\mu$ L aliquot was then used which absorbed into the previous droplet. A 0.5  $\mu$ L aliquot was applied to the surface which produced another large coverage area. Three more 0.5  $\mu$ L aliquots were applied from an Eppendorf (2.0  $\mu$ L) in a row but it was very difficult to perform due to the uneven spreading on the surface. This suggests that the silicon surface is very hydrophilic.



Silicon wafer #2 is a NCO treated wafer with water as the solvent. The first aliquot tested was 1.0  $\mu\text{L}$  which produced a small uniform droplet. Two more were placed in the same row and manner. It was not possible to get more than three, 1  $\mu\text{L}$  droplets in a single row (1 cm in width). Four, 0.5  $\mu\text{L}$  aliquots were then placed on the wafer in a row. These were small uniform droplets also. A third row of 0.5  $\mu\text{L}$  aliquots was attempted but the solution appeared to become absorbed into the above row. A fourth row of 0.5  $\mu\text{L}$  aliquots was performed using a 2.0  $\mu\text{L}$  Eppendorf pipet. Five of these droplets were placed in a row although it was difficult to reproduce. A very steady hand and eye was needed.

Silicon wafer #3 is a cleansed wafer without the SAM attached with DMF as the solvent. One, 0.5  $\mu\text{L}$  aliquot covered a very large surface area (approx. 1.5 x 0.5 cm). Three, 0.10  $\mu\text{L}$  aliquots covered an area similar to the 0.5  $\mu\text{L}$  aliquot above.

Silicon wafer #4 is a NCO treated wafer with DMF as the solvent. The first aliquot was a 0.5  $\mu\text{L}$  droplet which spread relatively wide ( $\sim 0.5 \times 0.5$  cm). A 0.25  $\mu\text{L}$  aliquot produced another large area coverage about half the size of the 0.5  $\mu\text{L}$  sample. Three, 0.10  $\mu\text{L}$  aliquots were obtained in a single line (1 cm in width). A few 0.05  $\mu\text{L}$  aliquots were placed on the treated wafer- the size of the droplets is about right for a desired 6 x 6 array.

From Figure 5.3.5B, silicon wafer samples 1 and 2 show no fluorescence detectable after rinsing with deionized water. However, wafer samples 3 and 4 do show some fluorescence although not in the original fluorescing areas (Figure 5.3.5A).

It was expected that wafer samples 1 and 3 would have significant reductions in fluorescence after rinsing since these do not contain a SAM surface in which to covalently bind to. This could be attributed to the fluorescein sample not having an amine group to covalently attach to the SAM surface.

This may also be contributed to a detection limitation after rinsing with the solvent. If the fluorescein is not attached strongly to the SAM or silicon surface, it is possible that the sample "washed" away with the solvent upon rinsing.

It is also possible that the fluorescent label (fluorescein) became quenched before, during or after the rinsing process. This possibility seems to have the most validity since the samples were exposed to direct UV light on various occasions (during placement of the sample into and out of the FluorImager SI, rinsing with nitrogen drying, etc.).

Upon looking at the fluorescence data, it appears that DMF acts as a better "attaching" solvent than does water alone due to the visible increase in fluorescence.

#### 5.3.6 Experiment 6: Fluorescein-Labeled SBH Oligonucleotides on NCO Treated Silicon Wafers Using a Modified Well Plate

From Experiment 5.3.5, it was determined that the DMF solvent localized the sample into distinct, small areas, whereas the water solvent localized most of the sample on the outer portions of the aliquot droplet. Therefore, a ratio of DMF to water that would both maximize the solubility of the oligonucleotide in solution to increase possible attachment and also to enhance the localization of the sample was needed. Ethanol was used as a solvent as well. The modified 96-cell well plate was used to determine if this new solvent ratio would encourage the solute to localize in the middle of the sample aliquot droplet rather than at the edges.

Leakage of samples into bordering wells (Figures 5.3.6A and B) was observed, however, fluorescence on the surface was still visible. Oligonucleotide SBH 3.4, which was partially soluble in ethanol, has a very random drying pattern in both images. However, the other samples tended to have higher fluorescence concentrations in circular patterns regardless of "leaking".

These circles are essentially the same diameters as the well plate holes, which suggest that the solutions are attracted to the well plate sides, thus resulting in a higher fluorescence concentration after drying. It was concluded that a DMF:H<sub>2</sub>O (5:2) solvent was a better choice than DMF, ethanol, or water alone. It was a better solvent for the oligonucleotide and wetted the silicon wafer better.

Table 5.3.6A: Oligonucleotide Sample Name, Molecular Weight, Sequence, and Total Sample Mass.

Sample	Mass (mg)	MW (g/mol)	Sequence
SBH 3.1	1.5776	2778.06	5'-Fluorescein-III-ACT-CGC-CII-II-3'
SBH 3.4	3.10488	2778.06	5'-Fluorescein-NININI-NITA-ACT-CGC-CNINI-NINI-3'
SBH 3.7	3.01104	2778.06	5'-Fluorescein-IINI-NITA-ACT-CGC-CNINI-II-3'
SBH 3.10	2.24808	2778.06	5'-Fluorescein-NINI-ITA-ACT-CGC-CII-NINI-3'
SBH 3.12	0.90092	2763.05	5'-Fluorescein-NINII-ICA-ACT-CGC-CII-NINI-3'

Table 5.3.6B: Oligonucleotide Sample Total nmoles, Solution Concentration and Total nmoles in 20 and 40  $\mu$ L Aliquot Samples

Sample	Total nmol.	nmol / $\mu$ L	nmol in 20 $\mu$ L	nmol in 40 $\mu$ L
SBH 3.1	567.931	0.811	16.227	32.453
SBH 3.4	1117.748	2.235	44.710	89.420
SBH 3.7	1083.966	2.168	43.359	86.717
SBH 3.10	809.302	1.619	32.372	64.744
SBH 3.12	326.087	0.652	13.043	26.087

Table 5.3.6C: Oligonucleotide Sample Concentration per square mm in Sample Wells for 20 and 40  $\mu\text{L}$  Aliquot Samples

Sample	20 $\mu\text{L}$ aliquot (nmol / mm <sup>2</sup> )	40 $\mu\text{L}$ aliquot (nmol / mm <sup>2</sup> )
SBH 3.1	0.504	1.009
SBH 3.4	1.390	2.780
SBH 3.7	1.348	2.696
SBH 3.10	1.006	2.013
SBH 3.12	0.405	0.811

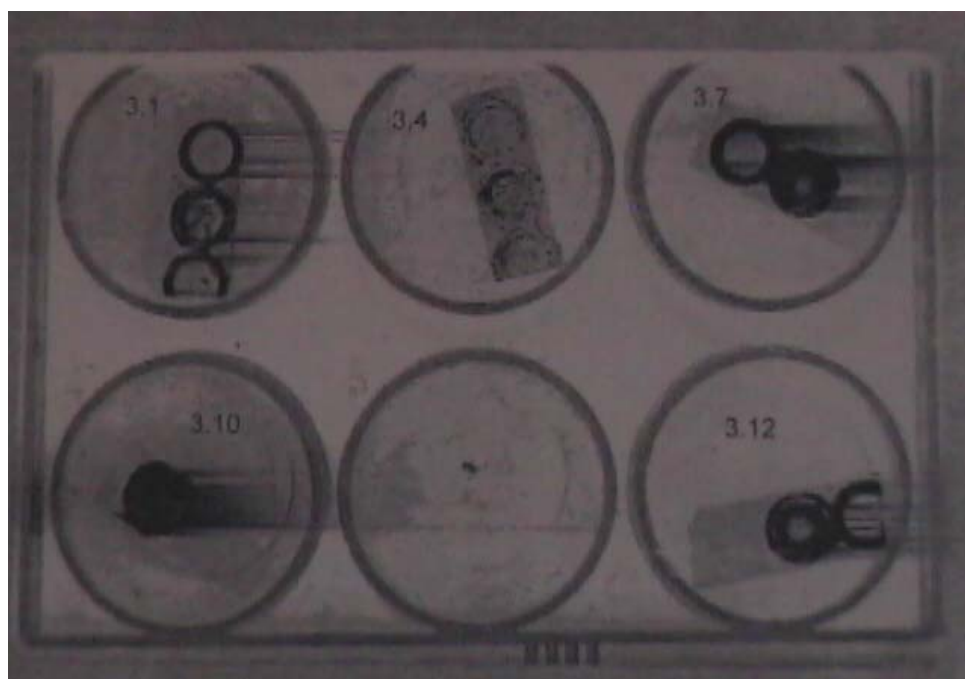


Figure 5.3.6A: FluorImager image of SBH oligomers 3.1, 3.4, 3.7, 3.10 and 3.12 labeled with Fluorescein using a normal sensitivity scan. 20  $\mu\text{L}$  aliquots (in 5:2 DMF:water solutions) on cleansed silicon wafers.

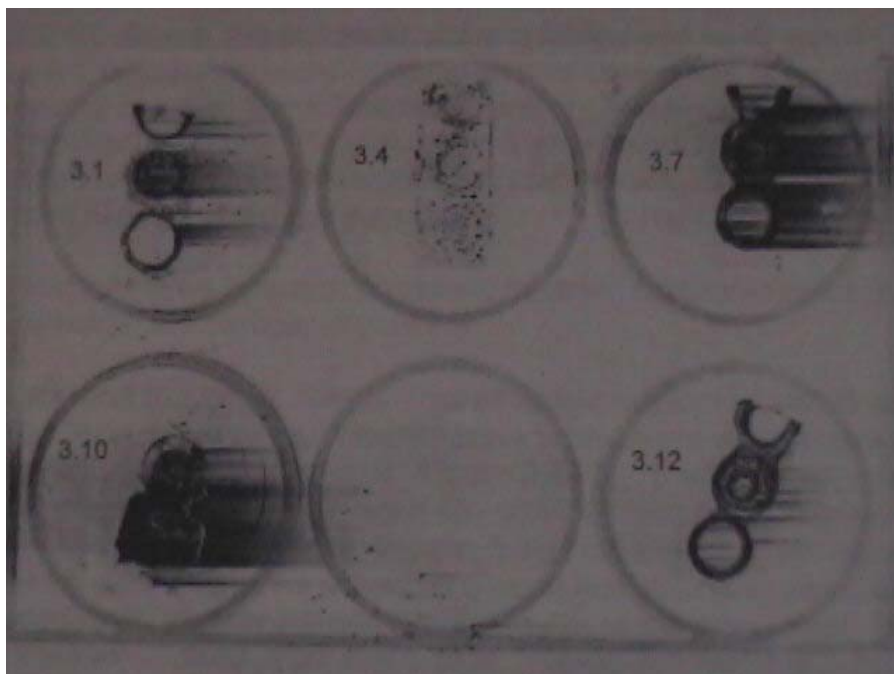


Figure 5.3.6B: FluorImager image of SBH oligomers 3.1, 3.4, 3.7, 3.10 and 3.12 labeled with Fluorescein using a normal sensitivity scan. 40  $\mu$ L aliquots (in 5:2 DMF:water solutions) on NCO treated silicon wafers.

It is difficult to determine the significance of the data obtained by the FluorImager due to the "leaking" of the sample solution into bordering wells. Although it is easy to "see" the fluorescence on the surface, it is hard to determine the difference between the isocyanatopropyl triethoxysilane treated silicon wafers and the IPA, acid / base washed cleansed wafers.

Sample SBH 3.4, which was partially soluble in ethanol, had a very random drying pattern in both samples. However, the other samples all tend to have higher fluorescence concentrations in circular patterns regardless of "leaking". These circles are essentially the same diameters as the well plate holes, which suggest that the solutions are adhering to the well plate sides, thus resulting in higher fluorescence concentration after drying.

### 5.3.7 Experiment 7: Re-establishing the Wettability of Silicon Wafers Using DMF: H<sub>2</sub>O (5:2) as a Solvent

Due to leakage problems in Experiment 5.3.6, a DMF: H<sub>2</sub>O (5:2) solvent composition was again used for its wettability properties. Again, sample SBH 3.4 containing ethanol as a solvent did not seem to be very concentrated when looking at Figure 5.3.7A.

In the case of the other samples where DMF: H<sub>2</sub>O (5:2) was used, the droplets formed a circular pattern and had the highest fluorescent concentration in the middle of the droplet. This was an expected result, since the DMF: water ratio was used to deter sample concentrations around the edge of the droplet.

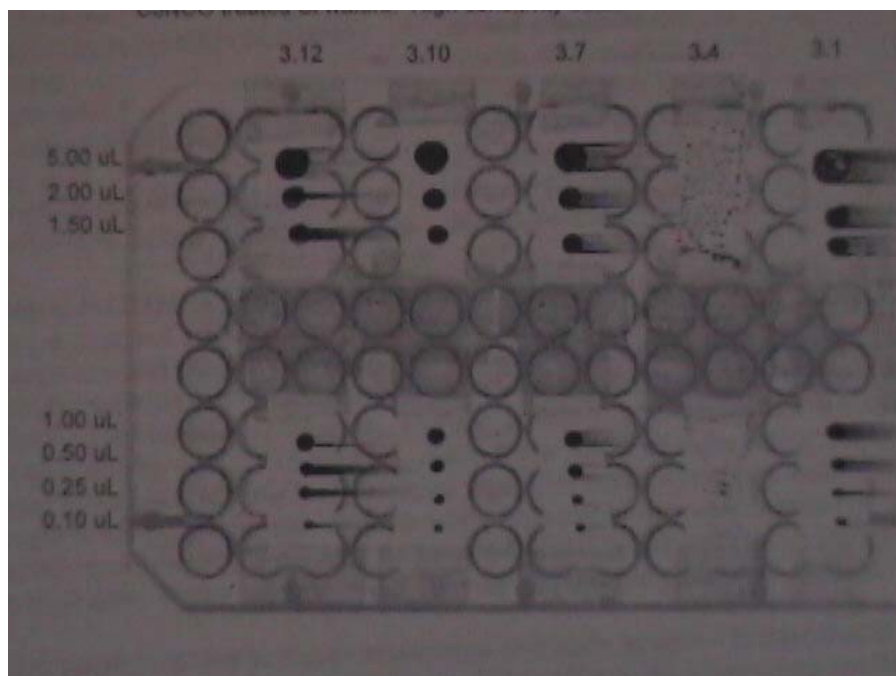


Figure 5.3.7A: FluorImager image of Fluorescein labeled SBH oligonucleotides 3.1, 3.4, 3.7, 3.10, and 3.12 covalently tethered to NCO treated silicon wafers. Various aliquot sizes are visible on each wafer (5.0 to 0.10  $\mu\text{L}$  top to bottom). Samples were dissolved in a DMF/water (5:2) solution and secured to a 96-well plate using tape prior to aliquot deposition and imaging.

"Streaks" visible from the FluorImager image (Figure 5.3.7A) suggests that the sample solution was either not dried thoroughly or a result of sample transference through leaching. A high sensitivity scan was performed to attempt to decrease the scan lines produced. Although this did not enhance the image from the FluorImager, it is reasonable to assume that the scan lines are a result of instrumentation factors since these "streaks" are parallel and noticeably extend over open well holes.

Sample SBH 3.4 has an irregular, unordered pattern. It appears that the sample is not very concentrated due to the decreased fluorescence intensity compared to the other samples.

This sample solution contains 95% ethanol and as a solvent, it did not disperse the solid completely. This would decrease the overall concentration of the solution considerably and may also explain why there are only "patches" of fluorescence visible. Also, only 4 sample aliquots were transferred onto the wafers. This was due to a very high hydrophilic interaction between the silicon surface and the ethanol solution. On the upper wafer, a 5.0  $\mu\text{L}$  aliquot covered the entire silicon surface. On the lower wafer, only 1.0, 0.25, and 0.10  $\mu\text{L}$  aliquots were possible.

In all cases except SBH 3.4, the sample droplets formed very ordered circular patterns and tended to dry with the highest fluorescent concentration in the middle of the droplet. This is completely opposite to previous experiments (Experiment 5.3.6), where the sample solution dried with the highest fluorescent concentrations around the edges.

More data will need to be obtained to determine if the modified well plate enhances (encourages) fluorescent accumulation at the edges. At this point, however, it appears to influence this phenomenon.

In all cases except sample SBH 3.4, fluorescence was detectable in all volumes regardless of sample concentration. Therefore, a 0.10  $\mu\text{L}$  aliquot using these oligonucleotides labeled with fluorescein would be detectable in the FluorImager at various concentrations.

### 5.3.8 Experiment 8: A Fluorescein Labeled Oligonucleotide (SBH 3.1) on Treated and Untreated Silicon Wafers to Verify Covalent Attachment

Experiment 5.3.7 proved successful from a wettability perspective and it was necessary to confirm that the oligonucleotide was covalently bonded to the SAM-treated silicon wafer. Therefore, SBH 3.1 solution from Experiment 5.3.6 with a fluorescein label was attached to treated and untreated silicon wafers and rinsed with varying quantities of DMF: water (5:2)



solvent. Fluorescent measurements were conducted during the process to monitor fluorescence loss, if any, due to washing.

The silicon wafers without NCO SAM attachment initially demonstrated a similar amount of fluorescence as those with the SAM linker (Figure 5.3.8A). However, after the wash with DMF: H<sub>2</sub>O (5:2 volume to volume ratio), the fluorescence of the non-SAM treated wafers declined at a greater rate than the fluorescence of the SAM-treated silicon wafers (Figures 5.3.8B and C).

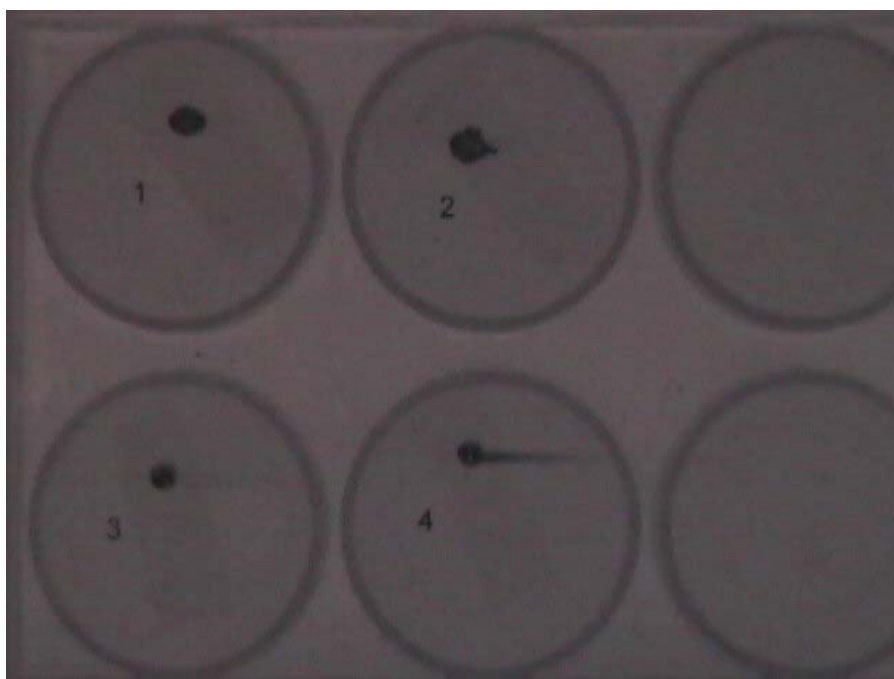


Figure 5.3.8A: FluorImager image of Fluorescein-labeled SBH 3.1 oligonucleotide on silicon wafers. Dry labeled samples 1 and 2 are cleansed wafers while labeled samples 3 and 4 are NCO treated wafers. A 2.0  $\mu$ L aliquot is visible on each wafer using a normal sensitivity scan in ambient air.

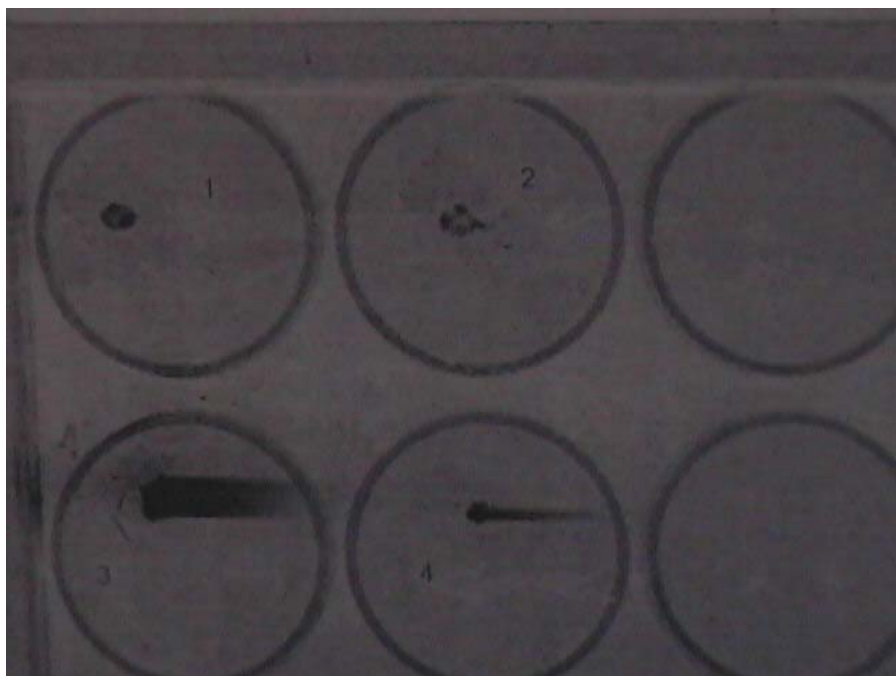


Figure 5.3.8B: FluorImager image of Fluorescein-labeled SBH 3.1 oligonucleotide on silicon wafers after a 5 mL DMF/water (5:2) washing. Dry labeled samples 1 and 2 are cleansed wafers while labeled samples 3 and 4 are NCO treated wafers. A 2.0  $\mu\text{L}$  aliquot is visible on each wafer using a normal sensitivity scan in ambient air.

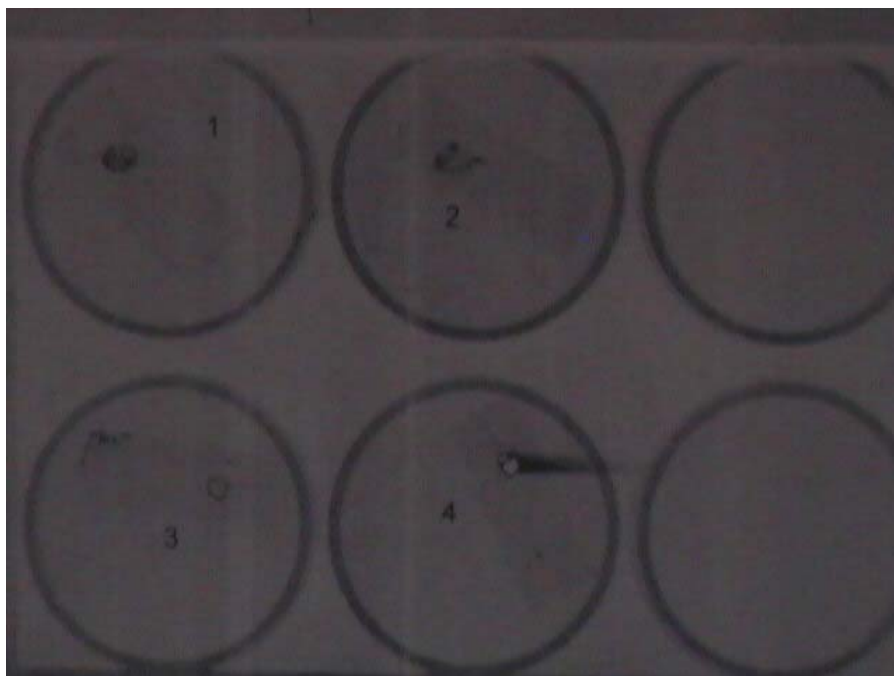


Figure 5.3.8C: FluorImager image of Fluorescein-labeled SBH 3.1 oligonucleotide on silicon wafers after a 20 mL DMF/water (5:2) washing. Dry labeled samples 1 and 2 are cleansed wafers while labeled samples 3 and 4 are NCO treated wafers. A 2.0  $\mu\text{L}$  aliquot is visible on each wafer using a normal sensitivity scan in ambient air.

From Figure 5.3.8A, the cleansed wafers (1 and 2) as well as the NCO treated wafers (3 and 4), all exhibit strong fluorescence prior to any rinsing with DMF: water solvent. The fluorescent images are very visible and dark. This may, however, be attributed to sample "shadowing" which results in the appearance of fluorescence due to sample thickness. This is unlikely, though, since only a 2.00  $\mu\text{L}$  aliquot of sample was used for analysis which significantly reduces the sample amount. Samples 1 and 2 possess slightly larger fluorescent diameters than samples 3 and 4, which can be attributed to increased wetting on the silicon surface. This is expected, since previous experiments (Experiment 5.3.1) showed that untreated,

cleansed silicon wafers have a ~21 degree wetting contact angle, whereas NCO treated wafers had wetting contact angles of approximately 71 degrees.

There is also slight "smearing" on sample 4 fluorescence picture. This may be due to contamination on the well plate or possibly sample photobleaching of the fluorescent tag.

After rinsing with ~5 mL of DMF: water solvent (5:2) the fluorescence in samples 1 and 2 reduced slightly (Figure 5.3.8B). The overall shape did not change but the intensity of fluorescence declined. Samples 4 remained about the same although sample 3 fluorescence increased. It also produced a large scan line across the image. This may be due to instrumentation errors or photo bleaching of the sample due to over-exposure to light. It is also possible that sample 3 was partially wet upon transference onto the well plate, thus transferring the sample onto the plate. Sample 4 scan line also darkened slightly. This, however, may be a contrast difference the two images.

From Figure 5.3.8C, samples 1 and 2 show significant fluorescence loss after rinsing with 20 mL of DMF: water solvent, as expected. It is interesting to note that sample 3 also exhibits little fluorescence. This may be due to photo bleaching or excessive rinsing. There is slight fluorescence in the area where the original aliquot (sample 3) was placed and also toward the bottom of the wafer. This area may have accumulated sample due to migration during rinsing of the sample. Sample 4 fluorescence increased slightly, despite the increase in scan lines. All of these samples were nitrogen dried after being washed.

Despite not having NCO SAM attachment to the silicon surface, samples 1 and 2 displayed similar characteristics as samples 3 and 4, which were NCO treated. This is not uncommon, since silane chemistry allows for very strong interaction with similar compounds such as oligonucleotides.

Samples 3 and 4 repeatedly exhibited strong fluorescence throughout the experiment, with the exception of Figure 5.3.8C, sample 3. Instrument error, contamination, or photo bleaching may have caused the streaks in the images obtained (Figures 5.3.8A – C). The latter is more likely to have occurred since the samples were exposed to a marginal amount of direct light. Therefore, this experiment was repeated to verify the data results.

### 5.3.9 Experiment 9: Repeat of Fluorescein Labeled SBH 3.1 Oligonucleotide on Treated and Untreated Silicon Wafers

Experiment 5.3.8 was repeated to validate the results of the data obtained and to determine the reproducibility of the data. SBH 3.10 with a fluorescein label was also used. The solvent used to dissolve SBH 3.1 oligonucleotide was a DMF: H<sub>2</sub>O (5:2) mixture (wafer dimensions: 1 inch x 1 cm). The cleansed silicon wafer again exhibited high hydrophilic interactions with the solvent in the sample, so the sample droplet was not uniform in shape (Figures 5.3.9A-C). The cleansed silicon samples lost fluorescence in proportion to the amount of solvent used to wash the wafers.

In Figures 5.3.9D-F, SBH 3.10 oligonucleotide was studied. The cleansed silicon wafer displayed very little fluorescence after 15 minutes of washing, which suggests that the oligonucleotide sample was probably physisorbed to the surface. The NCO-treated wafer

showed greater fluorescence after the washing in two of the aliquots, which suggests that the oligonucleotide sample was covalently attached to the silicon surface.

It can be assumed that the fluorescent-labeled oligonucleotide is bound to the NCO-treated silicon surface, since after two separate washes with DMF: water (5:2), there was no significant reduction in fluorescence. It was not possible to quantify the fluorescence with the instrument used in this experiment under experimental conditions.

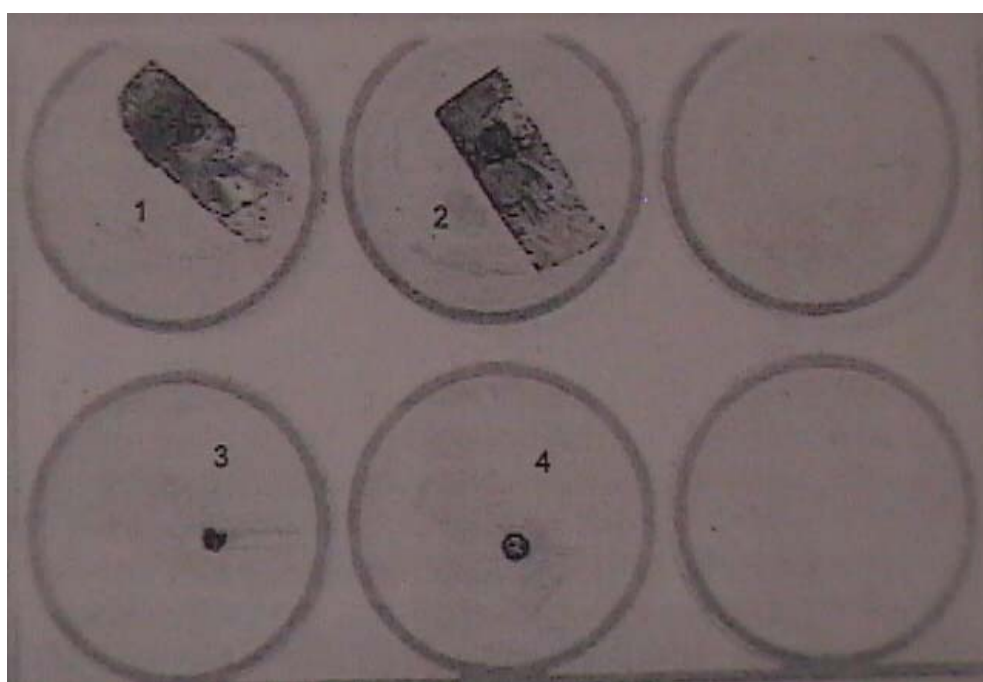


Figure 5.3.9A: FluorImager image of Fluorescein-labeled SBH 3.1 oligonucleotide on silicon wafers. Dry labeled samples 1 and 2 are cleansed wafers while labeled samples 3 and 4 are NCO treated wafers. A 2.0  $\mu\text{L}$  aliquot is visible on each wafer using a normal sensitivity scan in ambient air.

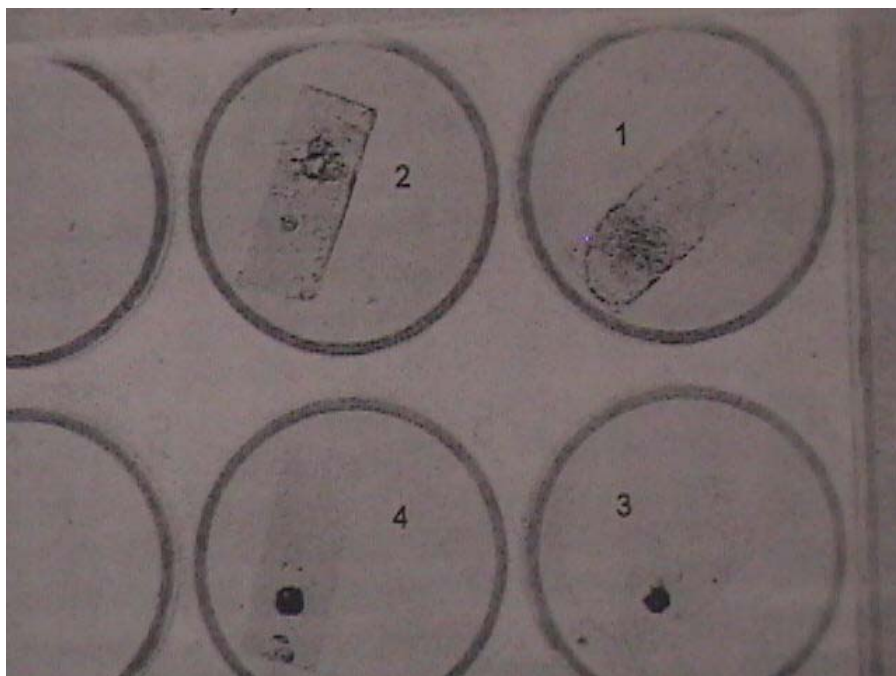


Figure 5.3.9B: FluorImager image of Fluorescein-labeled SBH 3.1 oligonucleotide on silicon wafers after a ~5 mL DMF: water (5:2) washing. Dry labeled samples 1 and 2 are cleansed wafers while labeled samples 3 and 4 are NCO treated wafers. A 2.0  $\mu$ L aliquot is visible on each wafer using a normal sensitivity scan in ambient air.

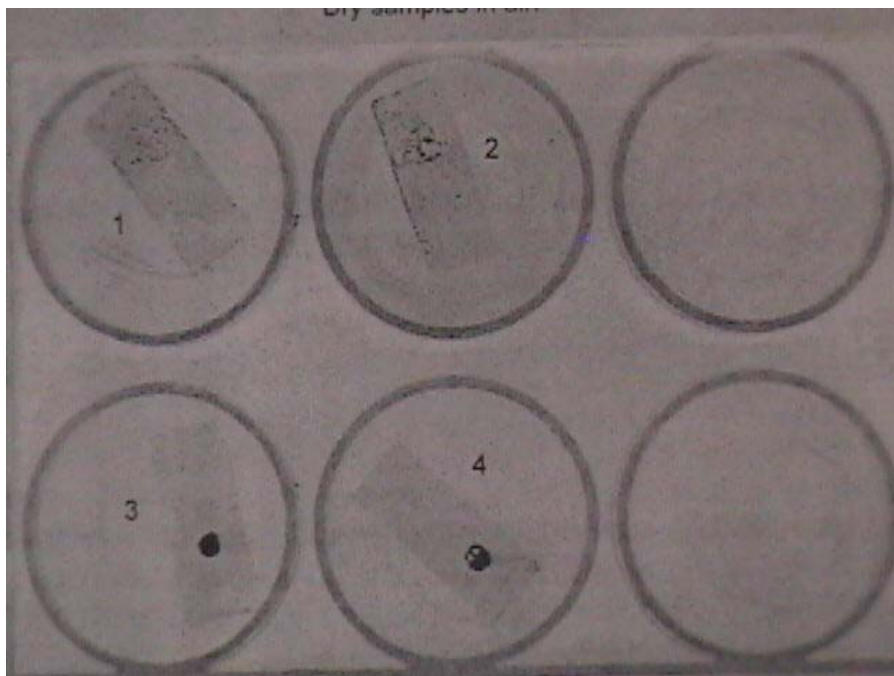


Figure 5.3.9C: FluorImager image of Fluorescein-labeled SBH 3.1 oligonucleotide on silicon wafers after a 20 mL DMF: water (5:2) washing. Dry labeled samples 1 and 2 are cleansed wafers while labeled samples 3 and 4 are NCO treated wafers. A 2.0  $\mu\text{L}$  aliquot is visible on each wafer using a normal sensitivity scan in ambient air.

From Figure 5.3.9A, samples 1 and 2 aliquot dispersed on the cleansed silicon wafer, covering the majority of the surface. There is a slightly darker circle in the upper half portion of the wafer where the initial aliquot was placed. Sample surface coverage implies a highly hydrophilic attraction of the sample solvent and the silicon surface. Samples 3 and 4 have very distinct, dark, circular patterns and is not dispersed throughout the surface. This would suggest that the interaction between the SAM surface and the solvent is very hydrophobic.

From Figure 5.3.9B, samples 1 and 2 have considerably less fluorescence noticeable on the wafer as a whole. There is still a large, random, slightly dark area in one-half of the wafer. Most of the sample appears to have rinsed away after the 5 mL rinsing with solvent. Samples 3



and 4 still exhibit the same distinct, dark, circular pattern in the lower portion of the wafer. This suggests that 5 mL solvent wash rinsed away none, or very little, of the sample from the surface. This would imply that there is a covalent bond between the SAM and the oligonucleotide and chemisorbed material is minimal.

Samples 1 and 2 from Figure 5.3.9C are almost completely undetectable. There is very light fluorescence visible in the upper-half portion of the wafer but it is not uniform and has a "blotchy" pattern. It appears that the 20 mL wash rinsed the majority of the sample off the surface suggesting that the sample was only physisorbed to the surface. Samples 3 and 4 continue to exhibit strong fluorescence and a very localized pattern. The 20 mL washing does not appear to rinse any of the oligonucleotide off the surface. Due to the strong fluorescence, a covalent bond is probable.

From the data obtained in Figures 5.3.9A-C, it appears that the fluorescent labeled oligonucleotide is covalently bound to the NCO treated silicon surface. Washing with 5 and then 20 mL of DMF / water (5:2) did not reduce the visible fluorescence which suggests that the oligonucleotide was not rinsed away with the solvent. Although it is not possible to quantify the fluorescence with the instruments utilized in this experiment, it is possible to qualify fluorescence by intensity alone.

Due to the high hydrophilic interactions between the cleansed silicon surface and the sample, the solvent spread over a large portion of the wafer. The sample aliquot droplet was not very uniform and was extremely random. The cleansed silicon samples appear to lose fluorescence proportionally to the amount of solvent used to wash the wafers. This is apparent in Figures 5.3.9A-C. This also suggests that the sample was possibly physisorbed to the surface.

### 5.3.10 Experiment 10: Attachment of SBH 3.1 and 3.10 Oligonucleotides With a Fluorescent Label on 3 x 1 Inch Silicon Wafers

An array was prepared by spotting 2.00  $\mu\text{L}$  aliquots of the SBH 3.1 and 3.10 oligonucleotides (dissolved in DMF:  $\text{H}_2\text{O}$  (5:2) solvent) on SAM-treated silicon wafers. The array consisted of four, 3 x 2 aliquots alternating from SBH 3.1 to 3.10, evenly spaced throughout the silicon surface (Figure 5.3.10A). The 2.00  $\mu\text{L}$  aliquots placed on the cleansed silicon wafers were not uniform and trickled together to form large “puddles”. This is due in part to the hydrophilic surface of the cleansed silicon wafer and was expected.

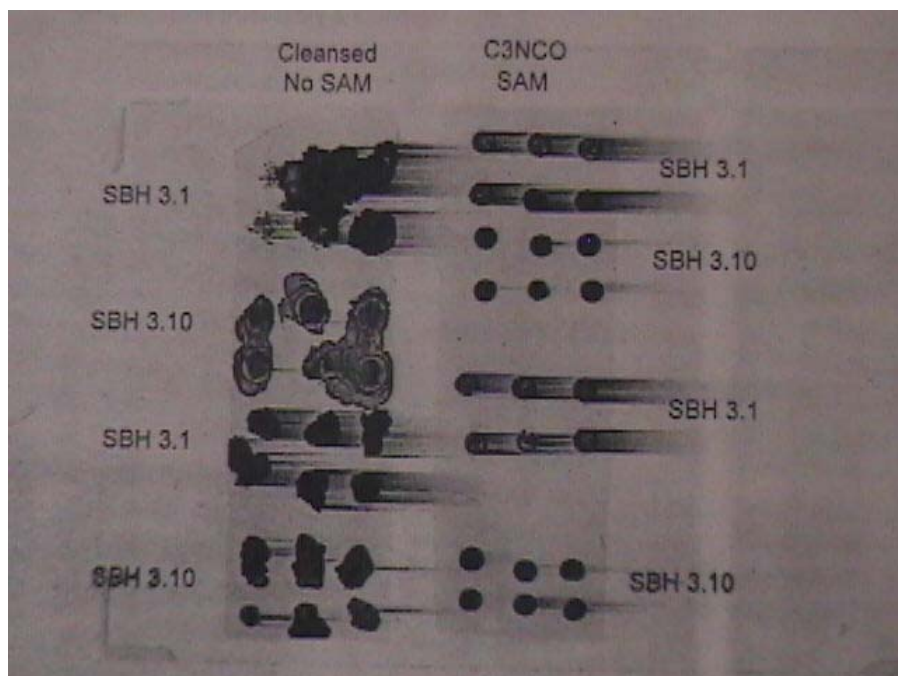


Figure 5.3.10A: FluorImager image of Fluorescein-labeled SBH oligonucleotides 3.1 and 3.10 on silicon wafers producing a 3 x 2 array which alternates from SBH 3.1 to SBH 3.10. The left 3x1 inch wafer sample is cleansed while the right 3x1 inch wafer sample is a NCO treated wafer. 2.0  $\mu$ L aliquot “dots” are visible on each wafer using a normal sensitivity scan in ambient air.

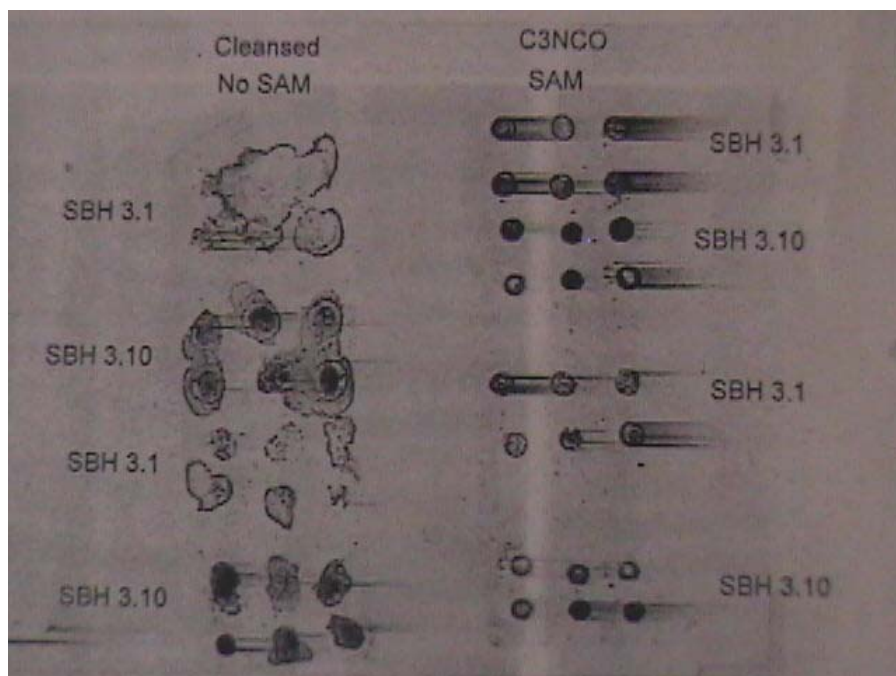


Figure 5.3.10B: FluorImager image of Fluorescein-labeled SBH oligonucleotides 3.1 and 3.10 on silicon wafers producing a 3 x 2 array which alternates from SBH 3.1 to SBH 3.10 after a 20 mL DMF/water (5:2) washing. The left 3x1 inch wafer sample is cleansed while the right 3x1 inch wafer sample is a NCO treated wafer. 2.0  $\mu$ L aliquot “dots” are visible on each wafer using a normal sensitivity scan in ambient air.

After washing with 20 mL of deionized water, the treated silicon wafer retained the majority of its fluorescence while the cleansed wafer lost a significant amount of fluorescence (Figure 5.3.10B). This again suggests that the oligonucleotide was covalently attached to the SAM-treated silicon surface. The aliquots that were placed on the NCO-treated silicon wafers, also retained their circular shapes after drying and again after rinsing with deionized water, which was also expected.

There was a noticeable streaking associated with the images obtained from the FluorImager SI. This may be attributable to quenching or photo bleaching of the sample during

transference from sample holder to instrument. It should be noted, however, that the intensity of the streaks coincided with the intensity of the sample “droplets” prepared.

### 5.3.11 Experiment 11: Attachment of SBH 3.1 and 3.10 Oligonucleotides (no label) on 3 x 1 Inch Silicon Wafers

Experiment 10 was repeated without using a fluorescently labeled oligonucleotide. New SBH 3.1 and 3.10 oligonucleotides were obtained and prepared with a concentration similar to that described in Experiment 5.3.6 (Table 5.3.11A). Ellipsometry measurements were conducted on the wafers after washing with deionized water for 5 minutes with continuous shaking (Table 5.3.11B). The ellipsometry results suggest that a multi-layer attachment may have occurred. However, these results were obtained using a different ellipsometer than previous measurements (UVISEL Spectroscopic Phase Modulated Ellipsometer from ISA Jobin-Yvon-Spex Groupe Instruments). The reproducibility and accuracy of these measurements are therefore unknown. Therefore, caution should be used when trying to compare these results to previous results obtained.

Table 5.3.11A: SBH 3.1 and 3.10 Mass (mg) and Concentration ( $\mu\text{g}/\mu\text{L}$ ).

<b>Samples</b>	<b>Mass (mg)</b>	<b>Concentration (<math>\mu\text{g}/\mu\text{L}</math>)</b>
SBH 3.1	1.534	15.34
SBH 3.10	1.020	10.20

Table 5.3.11B: Attachment of SBH 3.1 and 3.10 Average Ellipsometry Measurements ( $\text{\AA}$ ) after two consecutive washings with deionized water for 5 minutes with continuous shaking.

Samples	Thickness ( $\text{\AA}$ )
SBH 3.1	$250.92 \pm 104.04$
SBH 3.10	$283.85 \pm 111.38$

Although the ellipsometry measurements made on these samples could not be directly compared with previous results which have been obtained from the Gaertner Ellipsometer due to an instrumental problem, the measurements conducted on the UV/SEL Spectroscopic Phase Modulated Ellipsometer was calibrated and in fine working condition. It is therefore assumed that the ellipsometry measurements obtained are accurate. When taking the averages and standard deviations of the measurements into account, the minimal thickness value for SBH 3.1 and 3.10 would still be approximately 14 and 40  $\text{\AA}$ , respectively, after the average NCO SAM and oxide coating thickness is subtracted. These values are in fair agreement with previous experimental discussion results (Experiment 4, 5.3.4) if the oligonucleotides are in a “lying-down” conformation and thus are considered valid.

## 5.4 Conclusion

The objective of this work was to tether oligonucleotides onto a solid flat surface with a low background intrinsic fluorescence. The results demonstrate that it was possible to covalently attach an oligonucleotide to a derivatized silicon wafer substrate using isocyanatopropyl triethoxysilane (NCO) as the tethering SAM. Covalent attachment of the oligonucleotide was monitored using ellipsometry, contact wetting angle measurements, and fluorescence. The developed method could be made adaptable to automated liquid handling systems (such as Biomek 2000) to create an array.

## **CHAPTER SIX**

### **6 COMPOSITES**

#### **6.1 Introduction**

Self-assembled monolayer fiber coating can greatly increase the bond strength between the fiber and the resin matrix of a composite material. Composite munitions components molded from such materials may exhibit higher strength than current materials and can provide a major improvement in the performance of composites in military applications. Use of composite materials in military applications is desirable because of the lighter weight of the materials and their high strength. The development of new self-assembled monolayer fiber coatings was consequently explored.

The core of the project was to modify the covalent interface of glass fibers or glass substrates (or other reinforcing fibers) to induce strong, uniform, defect-free adhesion between the fiber's surface and the polymer matrix, thus increasing the strength or toughness of composite materials. Installing a self-assembled monolayer tailored to the specific matrix resin can accomplish this. Simply, the self-assembled monolayer modifies the fiber to make it appear to have the same chemical composition as the resin matrix. The self-assembled monolayer creates a receptive, hydrophobic interface that the thermoset resin (or polymer precursors) would wet more effectively, leading to a higher contact surface area and more efficient adhesion.

Glass fiber composites and their bulk properties were also a focal point. The bulk properties testing of composite laminates were made from different glass fiber surface treatments



that were done on tensile, flexural, and short-beam shear specimens. The SAM treatments on glass fibers have demonstrated an improved affect in the overall composite bulk properties. The matrix materials for a thermoset system can be chemically bonded to the glass fiber surface. The chemical bond takes place through the curing mechanism called cross-linking. The epoxy resin can be cross-linked to the surface of the chemically prepared surface or epoxide groups on the glass fiber surfaces can be cross-linked with the curing agent that has been mixed in with the epoxy resin. The research included applying various SAM treatments to the glass fiber mats and compared them to a non-surface treated glass fiber system and a commercially available glass fiber. The SAM affects the adhesion to the surface of the glass fiber as well as the modulus in the interphase region once the resin system is cross-linked and cured. Once the resin system is cross-linked and cured, the SAM affects the adhesion to the surface of the glass fiber and as well as the modulus in the interphase region. The different types of SAMs can control the modulus of the material in the interphase area. The tensile test shows the effect that the SAMs have on the strength of the material. The 3-(3',4'-epoxycyclohexyloxy)-3-propyltrimethoxysilane SAM showed the highest tensile strength as well as the highest short-beam shear.

Installation of 4 self-assembled monolayers (SAMs) was tailored to the specific epoxy matrix resin used. The 4 SAMs used were 3-aminopropyltrimethoxysilane (APS); glycidoxypropyltrimethoxysilane (GLY); 3-(3',4'-epoxycyclohexyloxy)-3-propyltrimethoxysilane (ECH); and 3-isocyanatopropyltrimethoxysilane (NCO). Fiber, diatomaceous earth, and glass slides were modified to provide a surface that looks to the resin matrix as if it had the same chemical composition as the matrix resin.

The surface energy of glass was measured to the thermoset resin before and after surface modifications and the result was surprising, but explainable.

As mentioned previously in Section 2.4.2, one method for characterizing the chemical behavior of a surface is to measure its wettability. This can be done using a solvent such as water, pH buffers or non-volatile organic solvents, as a way of gauging the different components (acid/base properties, permanent dipole moment, and polarizability) of the overall interfacial wettability. The most common of these measurements is the water contact angle measurement, in which a droplet of water is placed on the surface and the angle formed between the edge of the droplet and the surface is measured precisely. A hydrophilic surface will wet very nicely with water and the droplet will “wick out” across the surface, resulting in a very low contact angle (<10 degrees). A hydrophobic surface will cause the droplet to “bead up”, and the contact angle will be high (>90 degrees).

While these measurements are useful to the surface scientist, they don’t directly address the question as to how well these SAM-coated surfaces wet with an epoxy resin. This epoxy wettability has a direct influence on the contact area, and hence the interfacial adhesion, between the two phases of the resulting composite. Thus, measuring the contact angle formed by the epoxy resin on the monolayer-coated substrates was chosen.

The results of these water contact angle measurements for monolayer coated substrates are summarized in Table 6.1A (these results were obtained by Warren Schimpf of Advanced Fiber Technologies, Inc.):

Table 6.1A: Contact Wetting Angle Measurements (in degrees) for Monolayer Coated Substrates

NCO	22°
APS	16°
ECH	24°
GLY	16°
None	6°

Note that the native glass slides are more wettable (by the epoxy mix) than these coated surfaces. Therefore, it can safely be concluded that whatever strength enhancement is observed in the lap-shear tests is in fact due to covalent attachment between the two phases, and not simply due to increased interfacial contact.

The complete and uniform coverage of the SAM formation spreads the adhesion between the fiber and the matrix evenly over a larger area of the glass fiber relative to an uncoated fiber. This will reduce composite failure due to fiber/matrix interfacial shear. This application should enhance high fatigue components or in cases where severe environments could affect the physical properties of the composite. Using SAM coatings to control the physical properties of the interphase region, the tailored monolayer can improve composite strength or toughness. A rigid interphase will enhance composite strength and a flexible interphase will promote composite toughness.

## 6.2 Methodology

The project consisted of one phase- the thermoset phase- to be accomplished within four tasks each. The four tasks within the thermoset phase encompassed fabrication of SAMs on glass fabrics, fabricating panels, fabricating test specimens, and a testing task.

## 6.3 General Procedure

### 6.3.1 Procedure for Fabrication of SAMs on Glass Fabrics

Formation of SAMs on fiberglass cloth follows a general procedure. Fiberglass cloth (15 cm x 250 cm; CS-724 grade; Style 7781; Advanced Composites) was carefully accordion folded onto the internal pin assembly of the reaction vessel. The loaded rack was then submerged in isopropanol and stirred magnetically for 20-30 min to remove superficial impurities from the surface of the glass weave. After washing, the rack was removed and the isopropanol was decanted from the vessel. The rack was replaced and the vessel purged with a vigorous flow of dry nitrogen for at least 2 hours to remove all traces of solvent. The nitrogen line was then routed through a water bubbler, so that the resulting nitrogen stream would be saturated with water vapor. This 100% relative humidity nitrogen stream was then routed through the reaction vessel for 1 hour to ensure that the clean glass surface was adequately (and uniformly) hydrated (interfacial water is critical to the success of good monolayer formation). At this point, the top of the apparatus was removed and approximately 6 L of toluene added and the top replaced. The headspace was flushed with dry nitrogen for 15 minutes and then 25 mL of the appropriate silane (NCO, GLY, ECH, APS) was added via syringe through the septum in the vessel lid. The vessel

was placed on a hot plate/stirrer and stirring and heating initiated. The reaction mixture was equilibrated at approximately 70° Celsius for 18 hours, then allowed to cool to ambient temperature. Once cool, the reaction mélange was decanted off and the vessel refilled with isopropanol and the coated glass fiber were once again washed for 20-30 min in isopropanol. When the washing was completed, the isopropanol was decanted off and the glass cloth was once again dried under a stream of dry nitrogen for at least 1 hour.

Figure 6.3.1A shows how the silicon surface is derivatized with reactive ends of a SAM molecule that reacts and cross-links to the thermoset materials.

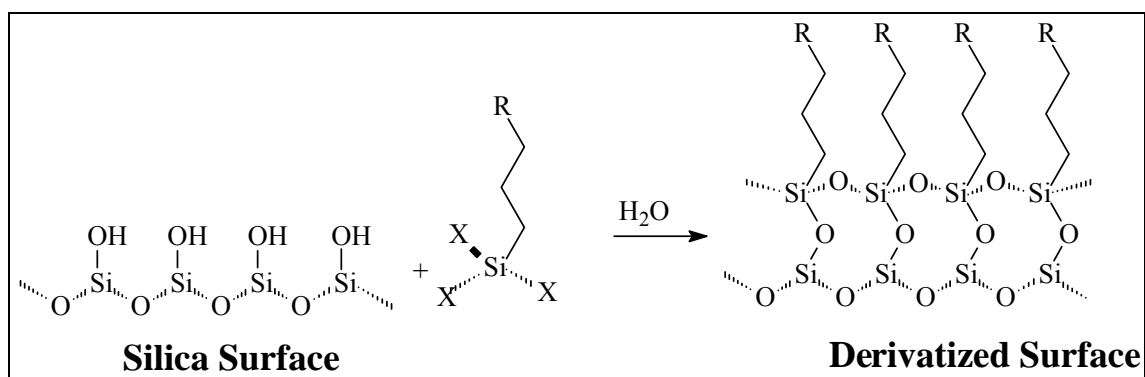


Figure 6.3.1A: Silicon surface derivatized with reactive ends of a SAM molecule, which reacts and cross-links with thermoset materials.

### 6.3.2 Panel Fabrication<sup>100</sup>

The lay-up process consisted of mixing the REFCOA epoxy and Diethylenetriamine (DETA) curing agent at the calculated proportions and placing it in a vacuum to degas. First, a small amount of epoxy was brushed on the bottom of the mold, followed by the first layer of glass. A paintbrush was used to wet each piece of glass and blot the epoxy. After the desired number of layers was achieved, the top of the mold was replaced and the whole mold was placed

in a heated press and left for 1 h at 100°C with an internal pressure of 38 kPa. Figure 6.3.2A shows the difference of the chemical interaction with the glass surface with and without SAM treatment. Figure 6.3.2B shows the interaction of the epoxy in the cured state and how the epoxy chemically mixes and cures to the SAM surface.

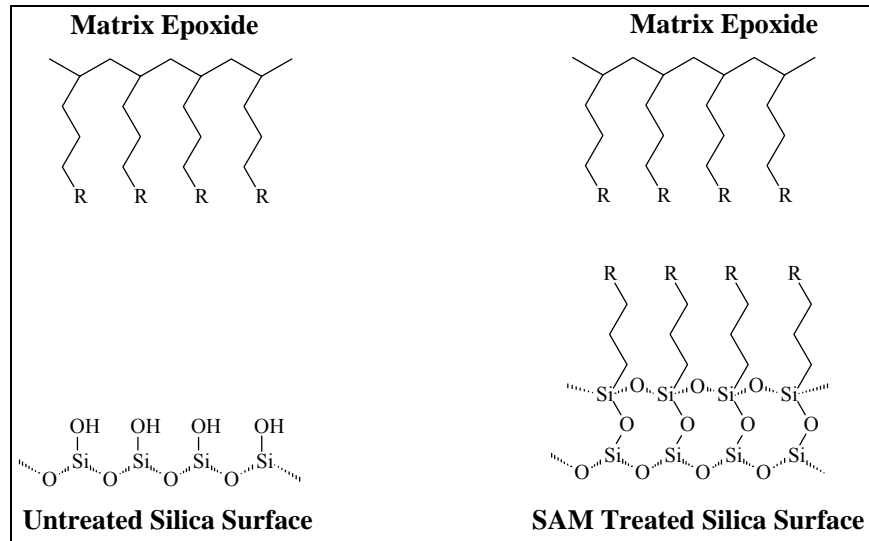


Figure 6.3.2A: Interaction of the epoxy resin with the untreated vs. treated surfaces.

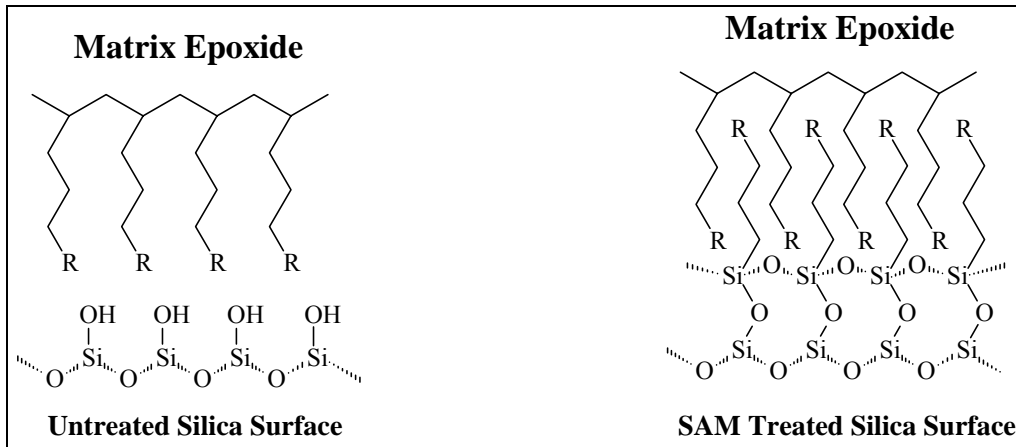


Figure 6.3.2B: Interaction of cured epoxy matrix with untreated versus treated surfaces.

### 6.3.3 Test Specimen Part Fabrication<sup>100</sup>

The tensile test specimens were cut from the 15.2-cm x 15.2-cm x 1.6-mm panels. The specimens were cut so that the unidirectional fiber lay in the longitudinal direction. Originally, the specimens were cut in 25.4-mm widths, to duplicate the standards used in the ASTM D3039 testing method. Tabs (2.54 cm x 3.81 cm x 4.0 mm) were bonded to the specimens as prescribed in the test method. However, when attempting to test them, the tabs would detach before the specimens could fail. The specimens were cut in half to approximately 1.27 cm wide and tested. Again the tabs detached from the specimens. A 6.35-mm radius was cut into the specimen on both sides at the mid-point of the specimen. This created a smaller cross-sectional area (roughly half) and allowed the sample to fail before the tabs detached.

The samples for the flex modulus test were cut out of the 4.0-mm-thick panels to a dimension of 1.27 cm x 3.18 cm long. ASTM 790 was used as guidance in the sample prep for flexural modulus and strength. Again the direction of the fibers was in the longitudinal direction for both the flex modulus samples and the short beam shear samples. The short beam shear

samples were also cut out of the 4.0-mm-thick panels, and their dimensions were 4.0 mm wide x 2.54 cm long.

#### 6.3.4 Testing<sup>101</sup>

The flexural modulus and short beam shear strength of sixty composite samples were measured. The results are summarized in the following Tables and Figures of Section 6.3.4.

##### 6.3.4.1 Flexural Modulus Measurements

The flexural testing is the simplest of the tests to perform. In general, it is considered an intrinsic property and is also inexpensive to run. However, flexural testing does not provide the basic material properties. This is due to the fact that when a beam is under load, it will have compression on one side, tension on the other, and pure shear in the neutral axis of the specimen. The flexural measurement gives a combination of these three properties. Thus, depending on the values of each of the three components in a composite material, any one of the values may actually be measured. Usually the shear component is kept small by making the test specimen relatively long compared to the thickness. The ASTM 790 standard gives guidance to the sample size and test parameters.

The flexural moduli of the composite materials were measured on a Rheometrics RMS-605. The samples were placed in a three-point bend tool with knife-edges. A room temperature (approximately 22° C) frequency sweep was used to measure the flexural modulus of each sample. The frequency was varied from 0.693-100 Hz in two different tests, with the frequency increasing in the first test and decreasing in the second test. The values reported in Table



6.3.4.1A are for 1 Hz. The modulus was approximately constant over this frequency range and the forward and reverse frequency sweeps gave excellent agreement. The average readings for each set are plotted in Figures 6.3.4.1A, B, and C.

Table 6.3.4.1A: Flexural Modulus Data including sample identification (Id), width, thickness, and flexural modulus (dynes/cm<sup>2</sup>) and (psi) values.

Sample ID	Width (in)	Thickness (in)	Flexural Modulus (dyn/cm <sup>2</sup> )	Flexural Modulus (psi)
FM9-01	0.5035	0.1555	2.63E+10	3.81E+05
FM9-02	0.5015	0.155	2.76E+10	4.00E+05
FM0-03	0.5015	0.156	2.70E+10	3.92E+05
FM9-04	0.504	0.155	2.40E+10	3.48E+05
FM9-05	0.5035	0.156	2.66E+10	3.86E+05
		Average	2.63E+10	3.81E+05
		St Deviation	1.36E+09	1.97E+04
FM10-01	0.502	0.155	2.05E+10	2.97E+05
FM10-02	0.502	0.1545	2.08E+10	3.02E+05
FM10-03	0.5015	0.1545	2.40E+10	3.49E+05
FM10-04	0.501	0.1535	2.09E+10	3.04E+05
FM10-05	0.504	0.155	2.17E+10	3.14E+05
		Average	2.16E+10	3.13E+05
		St Deviation	1.43E+09	2.07E+04
FM14-01	0.5025	0.156	2.65E+10	3.85E+05
FM14-02	0.5025	0.156	2.48E+10	3.59E+05
FM14-03	0.503	0.156	2.38E+10	3.45E+05
FM14-04	0.503	0.156	2.30E+10	3.34E+05
FM14-05	0.501	0.156	2.46E+10	3.57E+05
		Average	2.45E+10	3.56E+05
		St Deviation	1.32E+09	1.91E+04
FM17-01	0.5015	0.1545	2.55E+10	3.70E+05
FM17-02	0.503	0.1545	2.72E+10	3.94E+05
FM17-03	0.501	0.155	2.88E+10	4.18E+05
FM17-04	0.5015	0.155	2.66E+10	3.85E+05
FM17-05	0.502	0.1555	2.87E+10	4.16E+05
		Average	2.73E+10	3.96E+05
		St Deviation	1.42E+09	2.05E+04
FM18-01	0.4995	0.154	1.72E+10	2.49E+05
FM18-02	0.4995	0.154	2.14E+10	3.11E+05
FM18-03	0.5015	0.154	1.75E+10	2.54E+05
FM18-04	0.5015	0.1535	1.78E+10	2.58E+05
FM18-05	0.5	0.1545	2.32E+10	3.37E+05
		Average	1.94E+10	2.82E+05
		St Deviation	2.73E+09	3.96E+04
FM21-01	0.5015	0.154	2.46E+10	3.57E+05
FM21-02	0.5005	0.155	2.68E+10	3.89E+05
FM21-03	0.4995	0.1545	2.50E+10	3.62E+05
FM21-04	0.5005	0.154	2.47E+10	3.59E+05
FM21-05	0.4995	0.154	2.54E+10	3.69E+05
		Average	2.53E+10	3.67E+05
		St Deviation	9.03E+08	1.31E+04

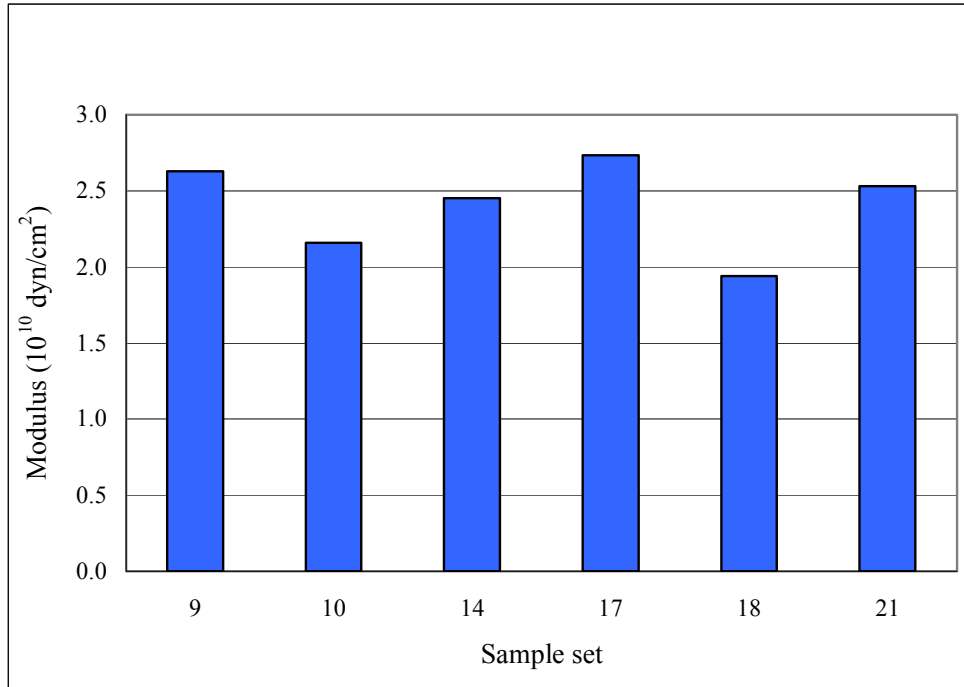


Figure 6.3.4.1A: Flexural modulus average values.

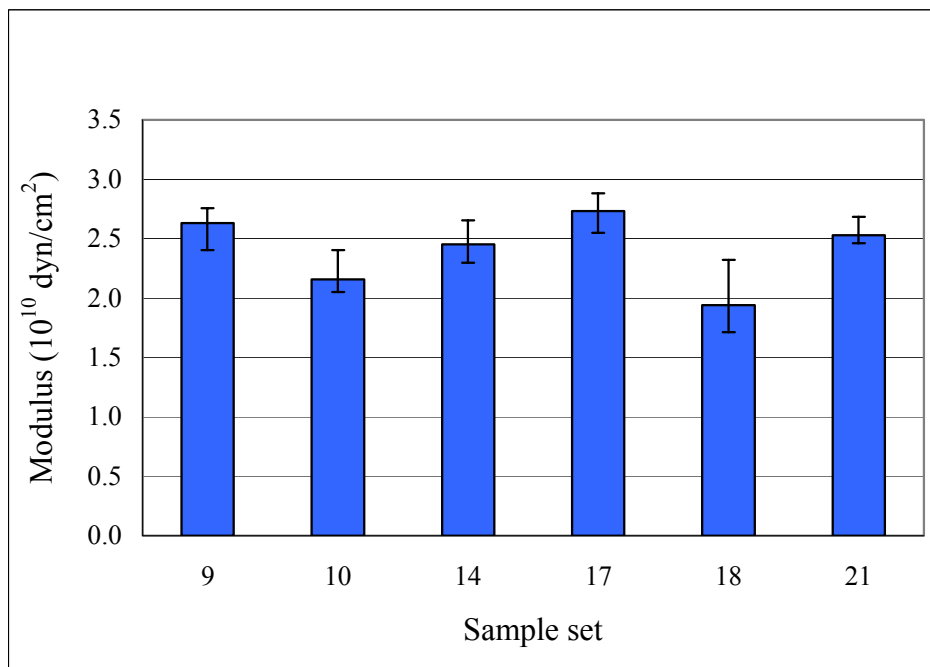


Figure 6.3.4.1B: Flexural modulus average values including maximum and minimum bars.

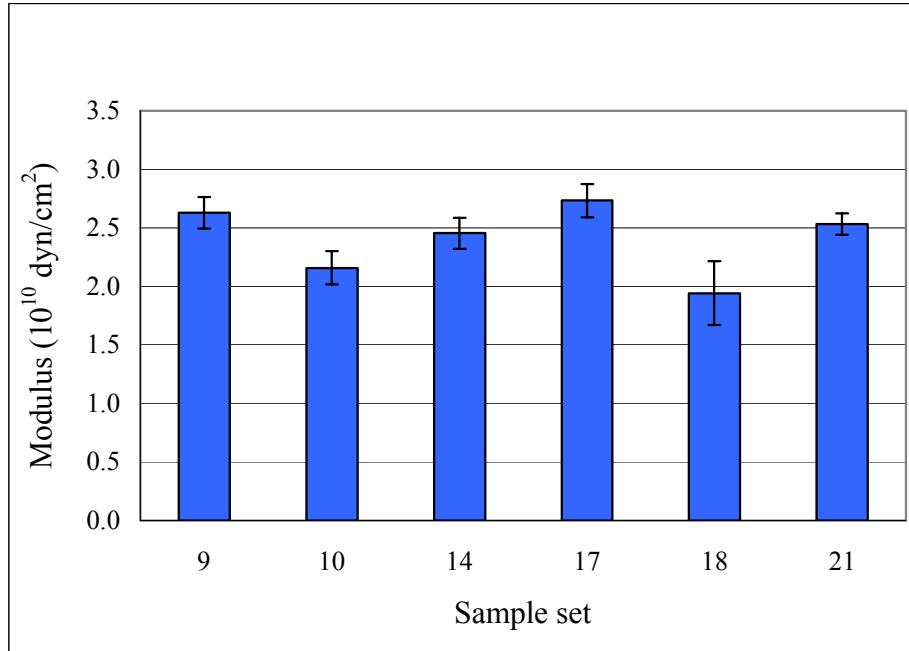


Figure 6.3.4.1C: Flexural modulus average values including +/- standard deviation error bars.

### 6.3.4.2 Short Beam Shear Testing

The apparent interlaminar shear strength was measured by the short beam method as per ASTM D2344. The samples were tested on an Instron 4505 with a crosshead speed of 1.3 mm per min. The maximum load was recorded and used to determine the shear strength of the materials, as shown in Table 6.3.4.2A. The force versus displacement plots for the tests were similar, with a drastic drop in force after the initial break. The test was continued after the initial break, and the force again rose until a subsequent break ruined the integrity of the sample. Often, the initial break was accompanied by an audible crack. The average readings for each set are plotted in Figures 6.3.4.2A, B, and C.

Table 6.3.4.2A: Short beam shear data. Sample identification, width, thickness, load at failure, displacement maximum load, strain at maximum load, apparent shear strength values and description of break information included.

Sample ID	Width (in)	Thickness (in)	Load at Failure (lbs)	Displacement Max Load (in)	Strain at Max Load (in/in)	Apparent Shear Strength (psi)	Description of Break
SBS9-01	0.1540	0.1560	99.07	0.0346	0.0278	3092.8	De-Lamination into 3 plys, one side only, 2 audible breaks
SBS9-02	0.1555	0.1555	109.30	0.0919	0.0735	3390.2	De-Lamination into 4 plys, one side only
SBS9-03	0.1580	0.1560	111.10	0.0647	0.0519	3380.6	De-Lamination into 3 plys, one side -possibly both sides, beginning of separation
SBS9-04	0.1560	0.1550	115.10	0.0636	0.0507	3570.1	De-Lamination into 2 plys, one side only, possible fracturing, vertical failure
SBS9-05	0.1575	0.1560	120.10	0.0616	0.0495	3666.1	De-Lamination into 3 plys, substantial separation of top ply, one side only
					<b>Average</b>	3420.0	
					<b>St. Dev</b>	219.4	
SBS10-01	0.1555	0.1550	137.90	0.0626	0.0499	4291.0	De-Lamination into 2 plys, separation of plys, one side only
SBS10-02	0.1570	0.1545	155.00	0.0598	0.0475	4792.5	De-Lamination into 2 plys, slight separation of plys, one side only
SBS10-03	0.1570	0.1555	131.10	0.0443	0.0354	4027.5	De-Lamination into 2 plys, minimal separation, one side only
SBS10-04	0.1575	0.1545	145.10	0.0593	0.0472	4472.2	De-Lamination into 2 plys, separation of plys, one side only
SBS10-05	0.1570	0.1545	149.60	0.0511	0.0406	4625.6	De-Lamination into 2 plys, no separation, one side only
					<b>Average</b>	4441.8	
					<b>St. Dev</b>	296.7	
SBS14-01	0.1560	0.1560	129.70	0.0579	0.0464	3997.2	De-Lamination, both sides into two plys, Large decrease in force, 2 audible cracks
SBS14-02	0.1625	0.1560	151.20	0.0609	0.0488	4473.4	De-Lamination, separation into 2 plys, one side
SBS14-03	0.1580	0.1560	143.70	0.0617	0.0495	4372.6	De-Lamination into 2 plys on one side w/separation, 3 plys on other w/no separation
SBS14-04	0.1575	0.1560	129.30	0.0601	0.0482	3946.9	De-Lamination into 4 plys
SBS14-05	0.1570	0.1560	118.50	0.0616	0.0494	3628.7	De-Lamination on both sides, 3 plys on one side, 2 plys on the other
					<b>Average</b>	4083.7	
					<b>St. Dev</b>	342.2	
SBS17-01	0.1565	0.1555	138.50	0.0650	0.0520	4268.4	De-Lamination into 2 plys, a lot of cracking/fracturing
SBS17-02	0.1570	0.1560	126.50	0.0890	0.0712	3873.7	De-Lamination/separation into 4 plys
SBS17-03	0.1570	0.1555	126.90	0.0766	0.0614	3898.5	De-Lamination into 3 plys
SBS17-04	0.1565	0.1555	120.40	0.0473	0.0378	3710.6	De-Lamination into 3 plys
SBS17-05	0.1555	0.1565	107.10	0.0827	0.0666	3300.7	De-Lamination into 2 plys, cracks throughout
					<b>Average</b>	3810.4	
					<b>St. Dev</b>	350.5	
SBS18-01	0.1555	0.1550	132.80	0.0630	0.0502	4132.4	De-lamination into 3 layers
SBS18-02	0.1560	0.1550	113.10	0.0346	0.0276	3508.1	De-lamination into 2 layers
SBS18-03	0.1555	0.1540					BROKEN SAMPLE
SBS18-04	0.1560	0.1540	150.80	0.0638	0.0505	4707.8	De-lamination into 3 layers
SBS18-05	0.1555	0.1550	141.90	0.0657	0.0524	4415.5	De-lamination into 3, possibly 4 layers
					<b>Average</b>	4190.9	
					<b>St. Dev</b>	512.3	
SBS21-01	0.1550	0.1555	145.60	0.0568	0.0454	4530.7	Delamination on both ends, Both sides two layers
SBS21-02	0.1555	0.1550	154.00	0.0583	0.0465	4792.0	Delamination into 3 layers on one side, 2 on other
SBS21-03	0.1555	0.1550					BROKEN SAMPLE
SBS21-04	0.1555	0.1550	138.90	0.0588	0.0469	4322.2	Delamination on one side into possibly 4 layers
SBS21-05	0.1555	0.1550	143.20	0.0687	0.0548	4456.0	De-Lamination into three layers
					<b>Average</b>	4525.2	
					<b>St. Dev</b>	197.7	

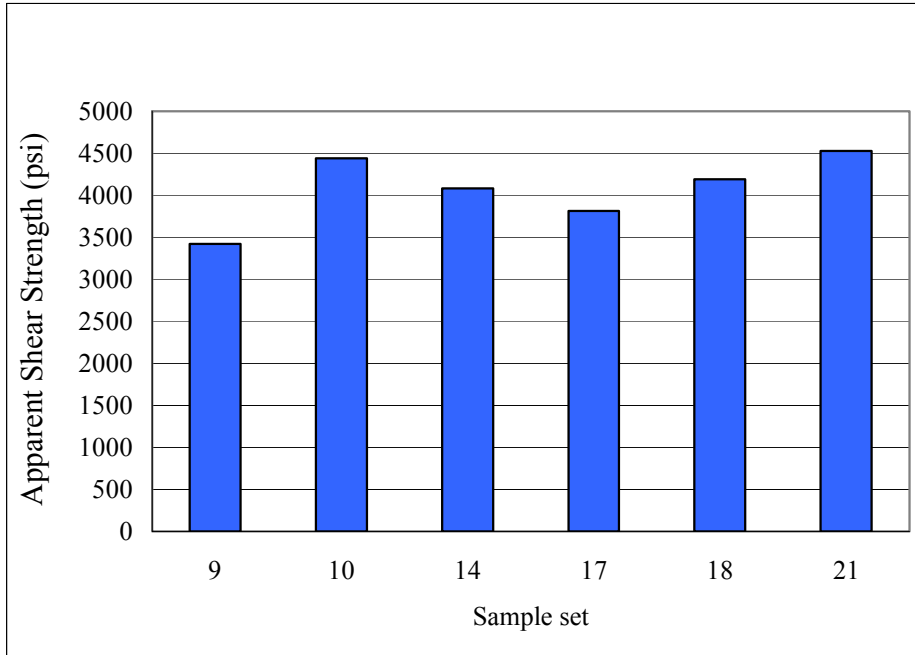


Figure 6.3.4.2A: Short beam shear average values (psi).

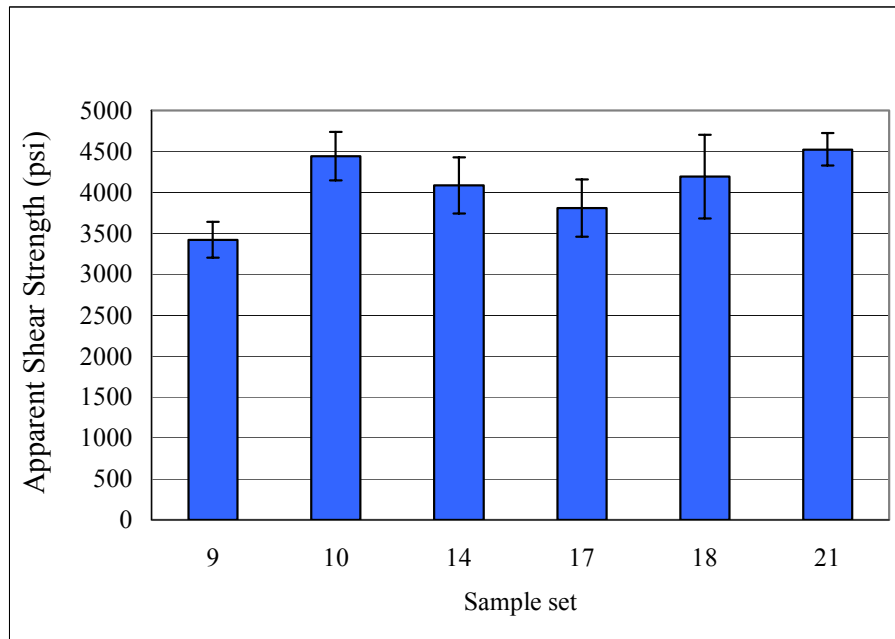


Figure 6.3.4.2B: Short beam shear average values (psi) including +/- standard deviation error bars.

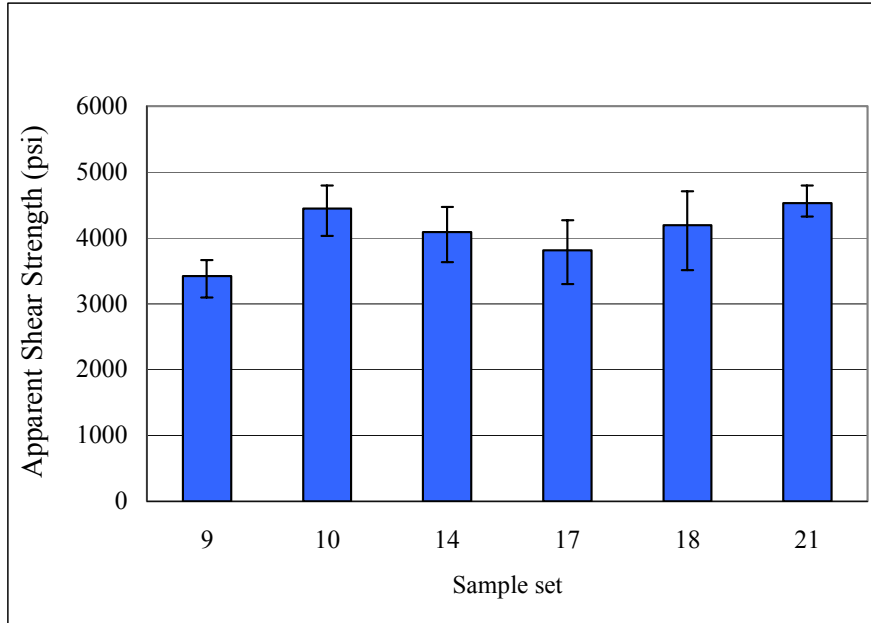


Figure 6.3.4.2C: Short beam shear average values (psi) including maximum and minimum bars.

### 6.3.4.3 Tensile Testing

The tensile testing was based on guidance from ASTM D-3039 and the use of a 4505 Instron Universal Testing machine. The samples were prepared as outlined in the previous section and tested in tension at 1 mm per min. Table 6.3.4.3A shows the measured geometries and maximum loads at failure. A statistical analysis was performed on the data and Figures 6.3.4.3A and B the mean tensile strength and modulus. SEM images of the tensile fracture specimens are shown in Figures 6.3.4.3C through H.

Table 6.3.4.3A: Tensile Test Data (1/4" R Notched Specimens). Sample identification (Id), width, thickness, sample area (inch<sup>2</sup>), maximum load, maximum stress, modulus, mean, standard error (S.E.), median, standard deviation (st. dev.), sample variance (variance), range, minimum and maximum sample range, sum and sample count values given.

	Sample ID	Width	Thickness	Area (In2)	Max Load	Max Stress	Modulus	Max Stress		Modulus
Greige	T7-01	0.2510	0.0605	0.01519	720.1	47420	14517	Mean	47234	12579
	T7-02	0.2550	0.0605	0.01543	732.7	47493	10288	S.E.	509	497
	T7-03	0.2545	0.0605	0.01540	753.4	48931	12292	Median	47493	12562
	T7-04	0.2530	0.0615	0.01556	693.0	44539	12562	St. Dev.	1346	1316
	T7-05	0.2540	0.0615	0.01562	731.5	46828	13499	Variance	1812159	1731741
	T8-01	0.2620	0.0610	0.01598	762.8	47729	11988	Range	4392	4229
	T8-02	0.2590	0.0615	0.01593	759.8	47701	12907	Minimum	44539	10288
								Maximum	48931	14517
							Sum	330640	88053	
							Count	7	7	
CS724	T11-05	0.2500	0.0610	0.01525	671.1	44007	17260	Mean	42351	14161
	T11-06	0.2520	0.0610	0.01537	665.6	43300	14085	S.E.	698	995
	T12-02	0.2585	0.0605	0.01564	638.1	40801	11125	Median	43079	14085
	T12-03	0.2480	0.0610	0.01513	613.7	40567	14869	St. Dev.	1562	2226
	T12-04	0.2240	0.0605	0.01355	583.8	43079	13464	Variance	2439230	4953486
								Range	3440	6135
								Minimum	40567	11125
								Maximum	44007	17260
							Sum	211754	70803	
							Count	5	5	
APS	T13-01	0.2560	0.0615	0.01574	766.6	48692	12123	Mean	47201	11463
	T13-02	0.2445	0.0615	0.01504	730.9	48608	11920	S.E.	841	382
	T13-03	0.2570	0.0610	0.01568	691.3	44096	10161	Median	47670	11920
	T13-04	0.2540	0.0610	0.01549	727.3	46941	12087	St. Dev.	1879	855
	T13-05	0.2535	0.0605	0.01534	731.1	47670	11022	Variance	3532208	730877
								Range	4596	1962
							Minimum	44096	10161	
							Maximum	48692	12123	
							Sum	236006	57313	
							Count	5	5	
NCO	T16-01	0.2505	0.0615	0.01541	746.8	48475	11711	Mean	47275	11793
	T16-02	0.2480	0.0625	0.01550	730.5	47129	12360	S.E.	452	277
	T16-03	0.2510	0.0625	0.01569	717.0	45705	12485	Median	47415	11711
	T16-04	0.2500	0.0615	0.01538	729.0	47415	11071	St. Dev.	1011	619
	T16-05	0.2500	0.0615	0.01538	732.6	47649	11340	Variance	1021423	383392
								Range	2770	1414
								Minimum	45705	11071
								Maximum	48475	12485
							Sum	236373	58967	
							Count	5	5	
GLY	T19-01	0.2540	0.0630	0.01600	739.6	46219	12421	Mean	47760	13009
	T19-02	0.2500	0.0620	0.01550	715.6	46168	13581	S.E.	833	201
	T19-03	0.2510	0.0625	0.01569	736.0	46916	13076	Median	46916	13076
	T19-04	0.2515	0.0620	0.01559	782.2	50164	12728	St. Dev.	1863	450
	T19-05	0.2495	0.0625	0.01559	769.3	49334	13241	Variance	3469543	202550
								Range	3996	1160
							Minimum	46168	12421	
							Maximum	50164	13581	
							Sum	238801	65047	
							Count	5	5	
ECH	T20-01	0.2500	0.0620	0.01550	709.5	45774	13074	Mean	48325	13256
	T20-02	0.2495	0.0620	0.01547	748.8	48406	13600	S.E.	724	322
	T20-03	0.2500	0.0625	0.01563	757.2	48461	12265	Median	48461	13129
	T20-04	0.2485	0.0615	0.01528	768.4	50279	13129	St. Dev.	1620	719
	T20-05	0.2505	0.0625	0.01566	762.5	48703	14214	Variance	2623414	516858
								Range	4505	1949
							Minimum	45774	12265	
							Maximum	50279	14214	
							Sum	241623	66282	
							Count	5	5	



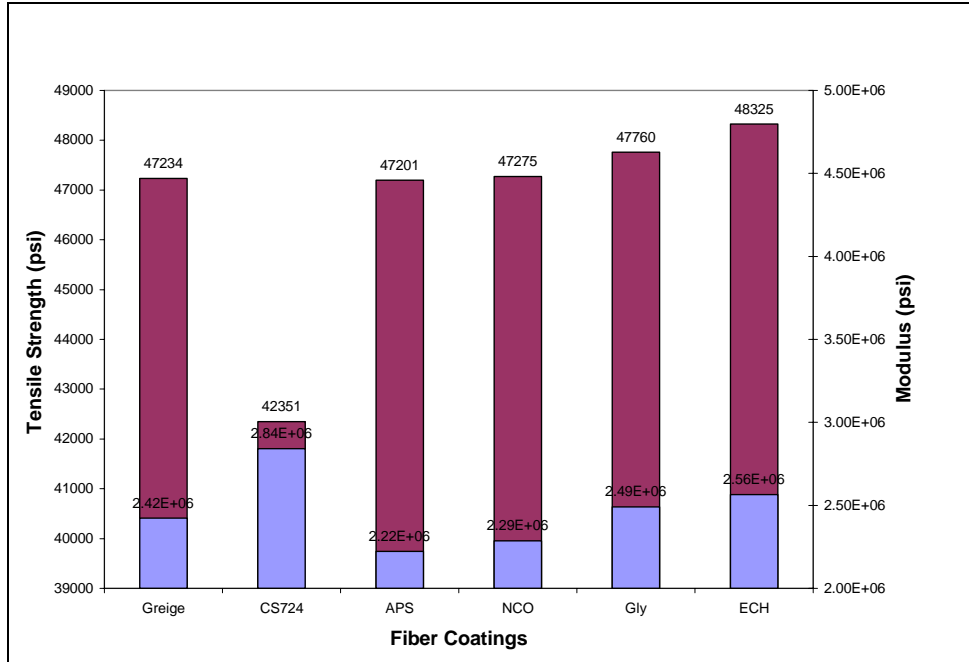


Figure 6.3.4.3A: Comparison of Modulus and Strength.

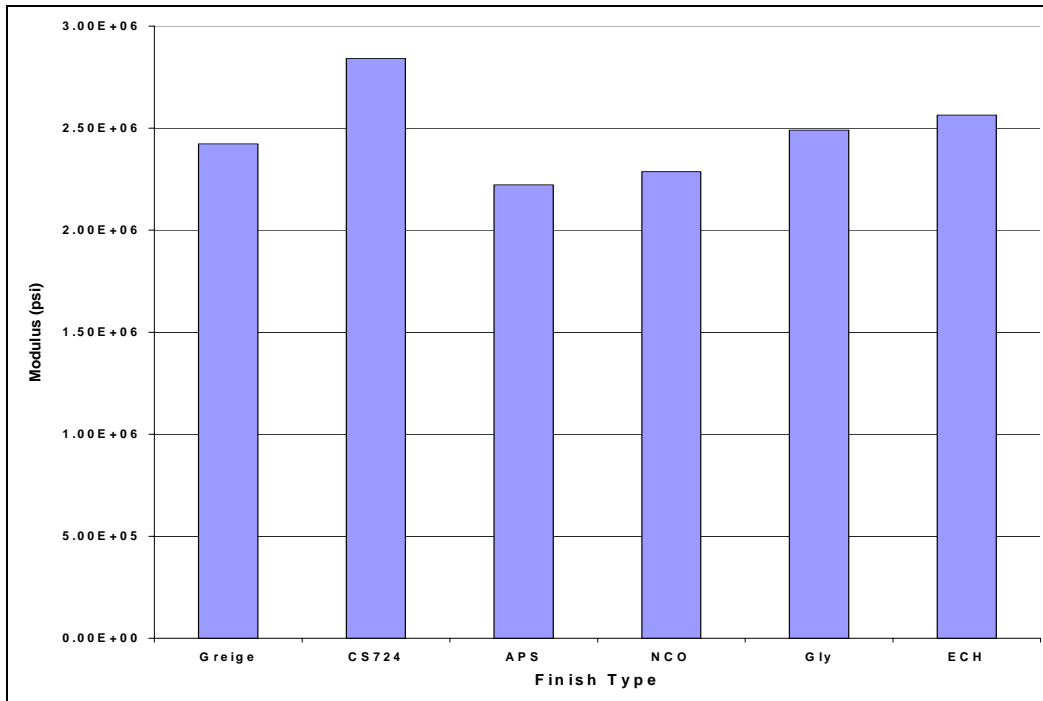


Figure 6.3.4.3B: Tensile Modulus.



Figure 6.3.4.3C: Scanning electron microscopy (SEM) of Greige Fiber tensile fracture.

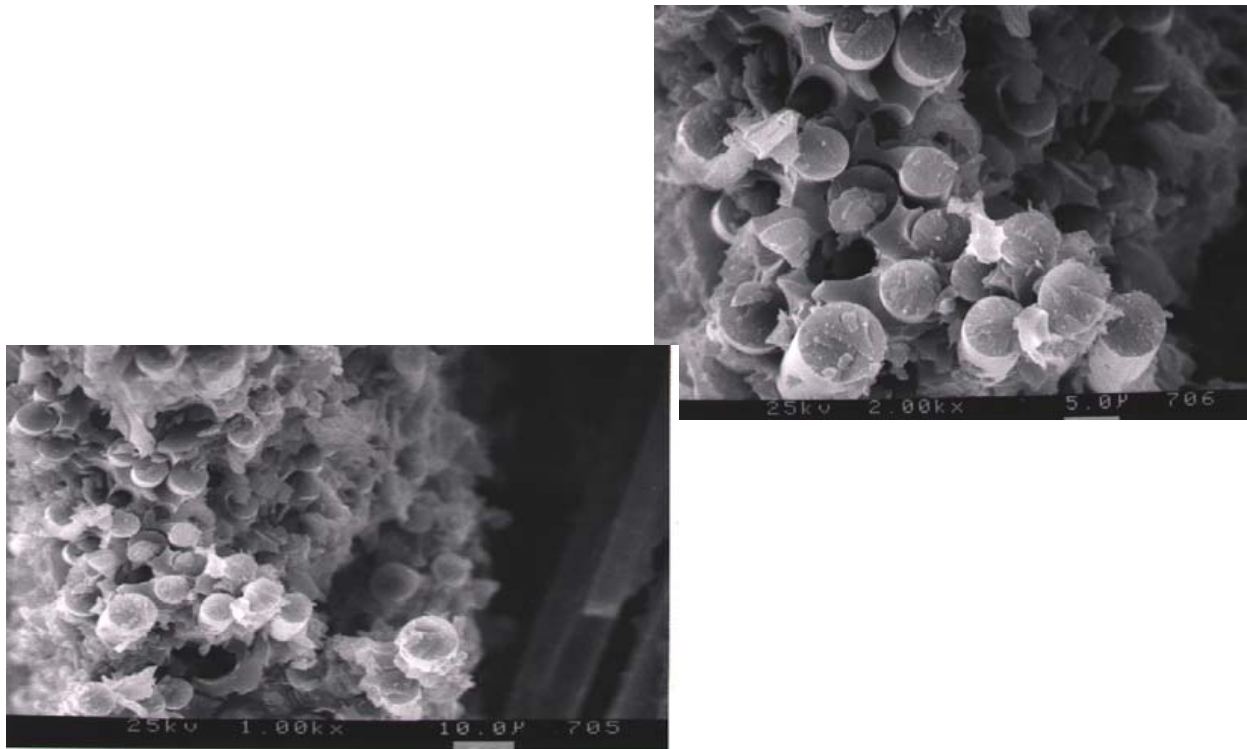


Figure 6.3.4.3D: Scanning electron microscopy (SEM) of Commercial Treatment tensile fracture.

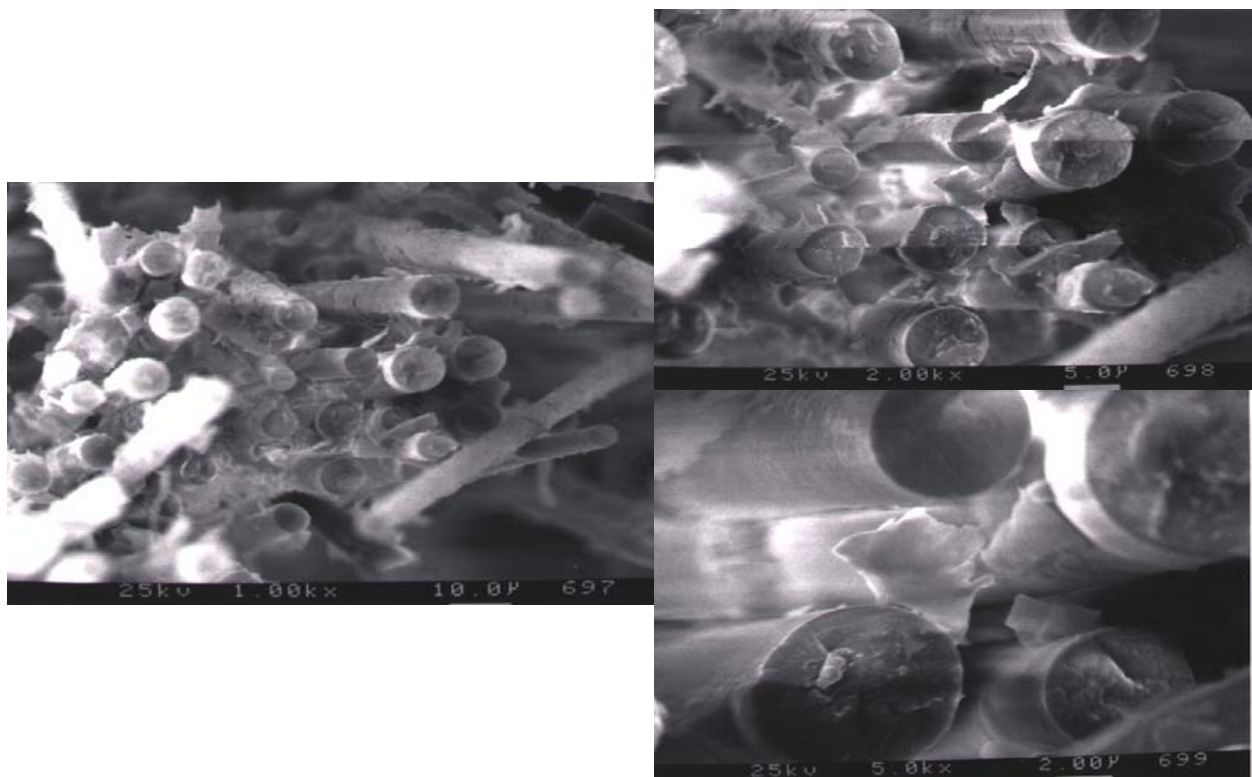


Figure 6.3.4.3E: Scanning electron microscopy (SEM) of ECH SAM tensile.



Figure 6.3.4.3F: Scanning electron microscopy (SEM) of NCO SAM tensile.

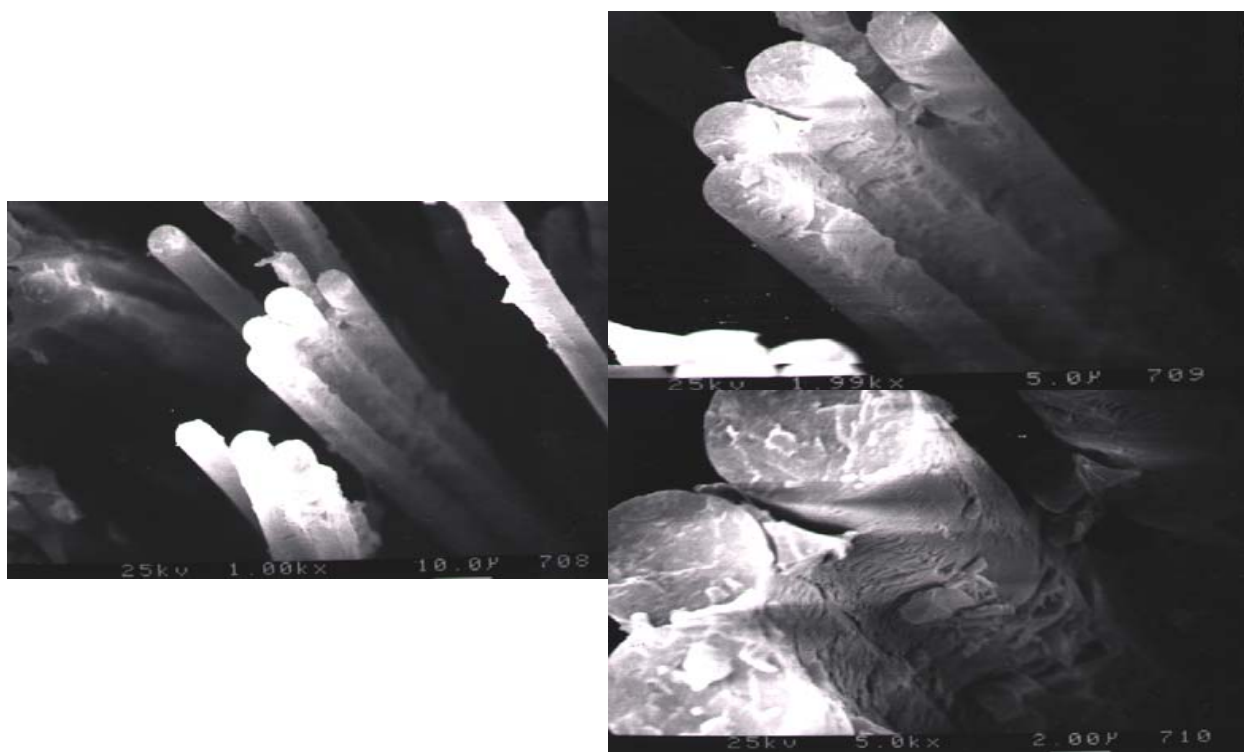


Figure 6.3.4.3G: Scanning electron microscopy (SEM) of APS SAM tensile.

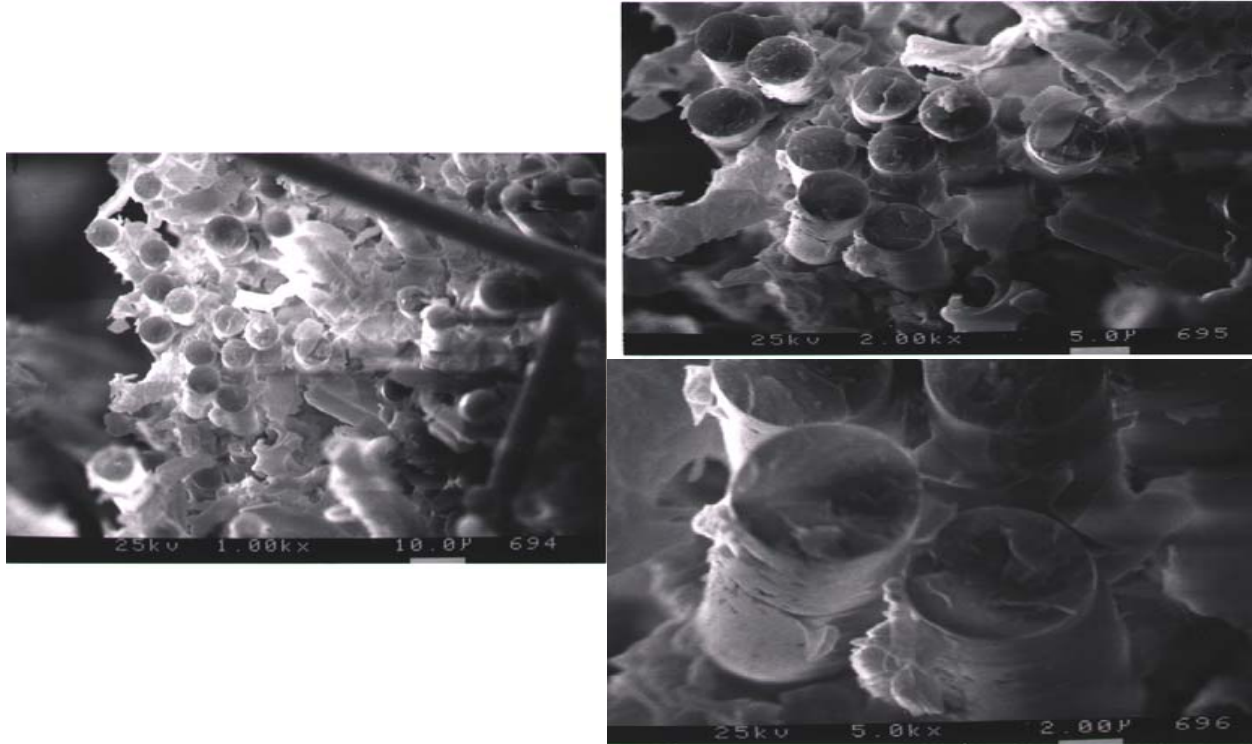


Figure 6.3.4.3H: Scanning electron microscopy (SEM) of GLY SAM tensile fracture.

## 6.4 Results and Conclusions

This research demonstrated that it is possible to increase the adhesive strength, as well as increase the heat deflection temperature through the use of SAMs on glass fiber composite laminates. The bulk properties testing of composite laminates were made from different glass fiber surface treatments that were done on tensile, flexural, and short-beam shear specimens.

Figure 6.4A(a) shows the load transfer mechanism for a single glass fiber embedded in a matrix material that is subjected to axial loading. The matrix material that is typically between the single fibers transfers the subjected load to the fibers. Upon the load transfer from the matrix to the glass fiber, shear stresses build at the fiber/matrix interface. The interface is the key to developing a strong composite material. The shear stresses have high values near the ends of

fibers, such as a fiber break, and decrease as function of distance from the fiber end. The tensile stress in the glass fiber does just the opposite. The tensile stress increases as a function of distance from the glass fiber end and if the tensile strength of the fiber is exceeded, the fiber fails and delamination from shear stress begins, as shown in Figure 6.4A(c).

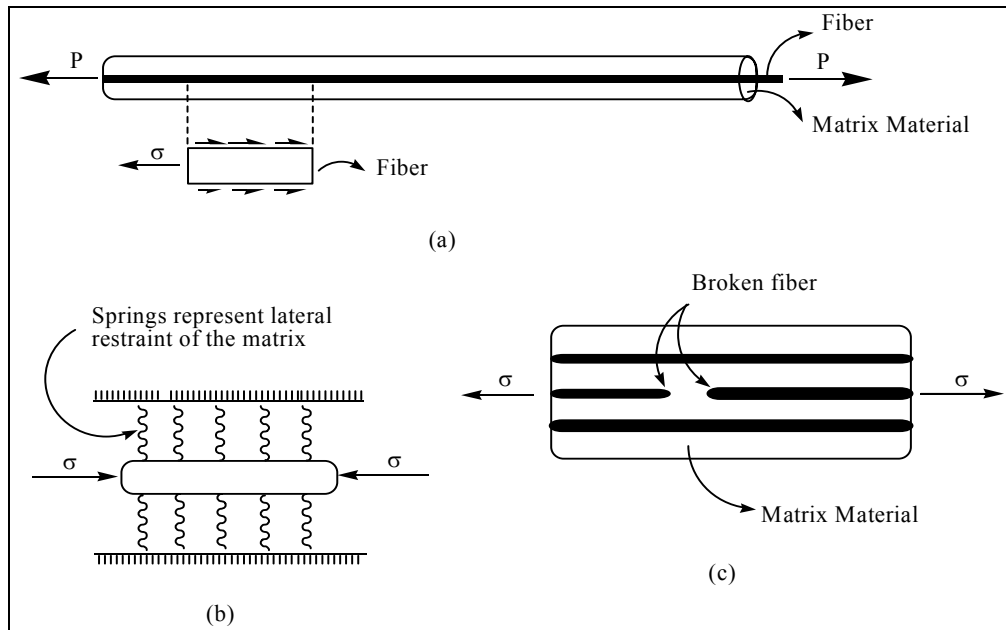


Figure 6.4A: Load transfer stress distributions in a single fiber embedded in a matrix material and subjected to an axial load.

The SAM treatments on glass fibers have demonstrated an improved affect in the overall composite bulk properties. The improvements can be explained by Figures 6.3.2B and 6.4A(b) in how it works and why. Figure 6.3.2B shows how the matrix material for a thermoset system can be chemically bonded to the glass fiber surface. The chemical bonding takes place through the curing mechanism called cross-linking. The epoxy resin can be cross-linked to the surface of the

chemically prepared surface or epoxide groups on the glass fiber surfaces can be cross-linked with the curing agent that has been mixed in with the epoxy resin.

This research applied various SAM treatments to the glass fiber mats and compared them to a non-surface treated glass fiber system and a commercially available glass fiber. The SAM affects the adhesion to the surface of the glass fiber as well as the modulus in the interphase region once the resin system is cross-linked and cured. Figures 6.3.4.3C through H shows Scanning Electron Microscopy (SEM) images of a non-surface treated glass fiber system, commercially available glass fiber, and various SAM-treated glass fibers after exposure to the epoxy resin. From these images, it is possible to view the bond of the epoxy resin to the glass fiber surface, if one exists. This is also another validation that the epoxy resin and glass fiber surface is indeed chemically bonded together.

Figure 6.4A(b) demonstrates how the interphase works as springs. The different types of SAMs can control the spring constants or modulus of the material. The tensile test shows the effect that the SAMs have on the strength of the material. The ECH SAM showed the highest tensile strength as well as the highest short-beam shear. The other SAMs show some improvements but the properties were anticipated to be different. The other SAMs testing data demonstrates that by controlling the chemical interface with the SAM system, the properties can be tailored to what is desired. For instance, if a toughened system is desired, a lower modulus interface can be applied.



## 6.5 References

100. Majority of sample panel preparation and analysis was performed by Kevin Simmons, Roger Voise, and Kirk Bigelow.

101. Performed by Kevin Simmons, Kirk Bigelow, and Roger Voise.

## CHAPTER SEVEN

### 7 EXPERIMENTAL SECTION

#### 7.1 General SAM Deposition Procedure

Silicon wafers (18 Å) were cut into 1 inch by 1 cm rectangles using a diamond etching pen. Cut wafer pieces were placed in a plastic holder, reflective side out using polypropylene forceps to avoid contact with skin, submersed in isopropanol, and ultrasonicated for 5 minutes. Plastic holder was then transferred into a glass beaker and covered with 0.1 N KOH for approx. 2 minutes then transferred into another beaker and covered with 0.1 M HNO<sub>3</sub> for at least 10 minutes. Wafers were washed with deionized water, dried with nitrogen, and stored under continuous nitrogen flow for 1-2 hours. Samples were then placed in a reaction kettle, covered with toluene, and stir bar added. Before the system was closed, it was flushed with nitrogen for 5-10 minutes to displace water vapor in air. Roughly 1 mL of isocyanatopropyl triethoxysilane (NCO) was added using a syringe. System was then closed and allowed to react for at least 4 hours at 70 degrees. After heating, samples were cooled to room temperature and the wafers were ultrasonicated in toluene for ~10 minutes, nitrogen dried, and stored under a constant stream of nitrogen until used.

## 7.2 Enzymes and Proteins

### 7.2.1 Experiment 1

The general method described in 7.1 was used as the procedure in this experiment. Place desired number of wafers into respective labeled 20mL glass vials containing 2 mg  $\beta$ -Amyloid 20 mer and 1 mL Catalase with water as a solvent. Be sure to place wafers in solution that will maximize surface area (reflective surface) interaction with solution. Leave overnight. Extract silicon wafers and dry with nitrogen to minimize possible “spots”. Place in new, dry 20 mL vials and analyze.

Ellipsometry measurements were obtained using a Gaertner Ellipsometer and contact angle measurements were obtained using a NRL C.A. Goniometer Model #100-00 115. Ellipsometry readings were produced using Gaertner Automatic Ellipsometry Program.

NCO SAM wafers were placed in dilute solutions of either  $\beta$ -Amyloid or a Catalase enzyme for 24-hours. The wafers were then washed and dried under nitrogen. Ellipsometry and contact angle measurements were obtained.

### 7.2.2 Experiment 2

The general method described in 7.1 was used as the procedure in this experiment. Each peptide was dissolved in either water or dimethylformamide (DMF) and was placed into 20 mL glass vials. The treated silicon wafers were then submersed in the solution

## 7.3 Antimicrobials

### 7.3.1 Materials

Silicon wafers (Wafernet), Isocyanatopropyl triethoxysilane (NCO) (United Chemical Co.), Toluene (Aldrich), Isopropanol (Aldrich), Potassium hydroxide (KOH) (Aldrich), Nitric acid (HNO<sub>3</sub>) (J. T. Baker). Antimicrobials tested can be found in Chapter 4.

### 7.3.2 Antimicrobial Preparation and Attachment

Approximately 20 mg of each antimicrobial agent was weighed and individually placed in labeled, 20 mL glass vials. In each vial, 2.00 mL of solvent was added and shaken until the antimicrobial was completely dissolved. A SAM treated wafer was removed from nitrogen container and broken into the desired 1.5 by 1.5 cm dimensions using the polypropylene coated forceps. The wafer was placed into the 20 mL glass vial containing the antimicrobial solution, with the reflective side facing the bottom of the glass vial. Wafers remained in solution for at least 20 hours. The wafer was then removed, placed in a clean 20 mL glass vial, and washed with respective solvent while continuously shaking for 5 minutes. The wafer was removed, dried using a constant stream of nitrogen, and placed in a labeled, clean glass (or plastic) vial. Ellipsometric measurements of antimicrobial coating thickness were then performed. Wafer samples were stored in the refrigerator until further testing and/or use.

### 7.3.2.1 Bacterial Growth and Assessment

Three grams of Tryptic Soy Broth (TSB) was placed in a 250 mL volumetric flask and 100 mL of deionized water was added. Solution was stirred using a magnetic stir bar until the TSB was completely in solution. The solution was autoclaved at 121°C for 15 minutes, allowed to cool to room temperature and then a ~10 mL extract of TSB solution was placed in a beaker. Two “loops” of desired bacteria (*E. coli* P175 alpha) was placed into the ~10 mL TSB aliquot. The solution was stirred, or shaken, for roughly 2 minutes to disperse the *E. coli* throughout the TSB solution. Solution was then inoculated in a 37° Celsius heating bath with shaking and with periodic optical density measurements at 600 nm taken to confirm viable cell content. Three mL of non-inoculated TSB solution was placed in each of the vials containing an antimicrobial-coated wafer. Next, 1 mL of the inoculated TSB solution was added to each vial and immediately placed in an incubated heating bath at 37° Celsius with shaking. An optical density measurement (absorbance) at various time intervals at a wavelength of 600 nm was then taken.

### 7.3.3 Experimental Detail

#### 7.3.3.1 Experiment 1

The general method described in 7.1 was used as the procedure in this experiment with the following additions or modifications. Antimicrobials were dissolved in a solution of dimethylformamide (DMF) and water at a ratio of 5:2. The silicon wafers were washed with copious amounts of water after attachment of the antimicrobial. Ellipsometry measurements were conducted to verify covalent attachment of the antimicrobial to the NCO SAM functionality. The

silicon wafers were then submersed for sixteen hours in an E.coli media and photographed. Real-time measurement of biofilm formation was conducted with a Leica Ergolux AMC Microscope with Kodak Megaplug digital camera attached. The image was processed with Image Pro Plus Software (Media Cybernetics) to determine the amount of bacterial growth. These images were only used as “proof-of-concept” to determine antimicrobial effectiveness after covalent attachment to the NCO SAM and were not saved.

Baseline ellipsometry and contact angle measurements were conducted on the silicon wafers as-received, after cleansing, and after NCO SAM deposition. The results are below in Tables 1-4. Ellipsometry measurements are in Å and contact angle are in degrees.

Table 7.3.3.1A: Antimicrobial Solution Concentration

<b>Antimicrobial</b>	<b>Solvent</b>	<b>Concentration (mg/mL)</b>
Polymyxin β	H <sub>2</sub> O	10.0
Tetracycline	DMF/H <sub>2</sub> O	11.5
Nalidixic Acid	Chloroform	10.0
Kanamycin	H <sub>2</sub> O	9.5

Table 7.3.3.1B: Ellipsometry measurements on Silicon Wafers As-Received

	1	2	3	4	5	6	7	8	Ave	Std. Dev.
Sample 1	18.22	17.95	19.35	19.31	18.64	18.12	18.11	18.08	18.47	0.57
Sample 2	18	17.82	17.67	18.38	17.69	17.71	17.65	18.22	17.89	0.28
<b>Overall</b>									<b>18.18</b>	<b>0.53</b>

Table 7.3.3.1C: Ellipsometry measurements on Silicon Wafers after Cleansing

	1	2	3	4	5	6	7	8	Ave	Std. Dev.
Wafer #1	20.23	20.28	20.33	18.88	20.23	20.69	18.23	20.21	19.89	0.85
Wafer #2	19.69	19.65	25.14	28.79	29.38	22.95	24.31	25.91	24.48	3.66
Wafer #3	17.79	23.43	21.39	23.87	18.83	20.08	19.76	19.92	20.63	2.13
Overall									<b>21.67</b>	<b>3.15</b>

Table 7.3.3.1D: Static Contact Angle measurements on Silicon Wafers after Cleansing

	1	2	3	4	5	6	Ave	Std. Dev.
Wafer #1	29	28	28	27	26	28	27.7	1.03
Wafer #2	29	25	35	32	30	33	30.7	3.50
Overall							<b>29.2</b>	<b>2.92</b>

Table 7.3.3.1E: Ellipsometry measurements on NCO Wafers

	1	2	3	4	5	6	7	8	Ave	Std. Dev.
Wafer #1	33.20	34.65	34.84	34.72	34.76	34.66	33.96	34.59	34.42	0.56
Wafer #2	34.72	36.37	33.63	34.38	35.15	35.01	35.82	34.15	34.90	0.89
Wafer #3	33.75	36.46	35.11	34.95	34.75	38.17	36.48	34.83	35.56	1.39
Wafer #4	35.15	35.37	35.89	34.48	35.25	33.28	34.52	35.19	34.89	0.79
<b>Overall</b>									<b>34.95</b>	<b>1.00</b>

### 7.3.3.2 Experiment 2

The general method described in 7.1 was used as the procedure in this experiment with the following additions or modifications. The antimicrobial solutions used in the previous experiment (7.1.3.1 Experiment 1) was recovered and re-used for this experiment. Antimicrobial agents used were Nalidixic acid, Polymyxin  $\beta$ , Chloramphenicol, Kanamycin monosulfate, and

Tetracycline. Ellipsometry measurements were performed on the treated wafers after antimicrobial attachment.

A NCO treated silicon wafer and NCO wafers treated with Nalidixic acid, Polymyxin  $\beta$ , Chloramphenicol, Kanamycin monosulfate, and Tetracycline were placed into 20 mL glass vials. A solution consisting of 100 mL of deionized water and 3.0 g tryptic soy broth (TSB) was stirred for approximately 5 minutes and autoclaved at 121° Celsius for 15 minutes. The solution was allowed to cool to room temperature and inoculated with three (3) loopfuls of E.Coli P175 (non-pathogenic) bacteria and allowed to dissipate throughout the solution for 15 minutes. Four (4) mL of the TSB-E. coli solution was transferred into each of the vials containing antimicrobial coated wafer and place on a pre-heated water bath shaker (37° Celsius) and allowed to shake at 60 oscillations/minute. Absorbance measurements were conducted at various time intervals.

### 7.3.3.3 Experiment 3

The general method described in 7.1 was used as the procedure in this experiment with the following additions or modifications. The antimicrobial solutions used in the previous experiments (7.1.3.1 and 2) was recovered and re-used for this experiment. Antimicrobial agents used were Nalidixic acid, Polymyxin  $\beta$ , Chloramphenicol, Kanamycin monosulfate, and Tetracycline. Ellipsometry measurements were performed on the treated wafers after antimicrobial attachment.



**Materials.**

Silicon wafers	Wafernet 451, 450.04.10
Isocyanatopropyl triethoxysilane	United Chemical Technologies
Toluene	Aldrich Chemical Company
Isopropanol	Aldrich Chemical Company
Potassium Hydroxide	Aldrich Chemical Company
Nitric Acid	J.T. Baker
Nalidixic Acid	Sigma Chemical
Polymyxin $\beta$ , sulfate	Calbiochem
Chloramphenicol	Sigma Chemical
Kanamycin Monosulfate	Sigma Chemical
Tetracycline Hydrochloride	Sigma Chemical

A NCO treated silicon wafer and NCO wafers treated with Nalidixic acid, Polymyxin  $\beta$ , Chloramphenicol, Kanamycin monosulfate, and Tetracycline were placed into 20 mL glass vials. A solution consisting of 100 mL of deionized water and 3.0 g tryptic soy broth (TSB) was stirred for approximately 5 minutes and autoclaved at 121° Celsius for 15 minutes. The solution was allowed to cool to room temperature and inoculated with three (3) loopfuls of E.Coli P175 (non-pathogenic) bacteria and allowed to dissipate throughout the solution for 15 minutes. Four (4) mL of the TSB-E. coli solution was transferred into each of the vials containing antimicrobial coated wafer and place on a pre-heated water bath shaker (37° Celsius) and allowed to shake at 60 oscillations/minute. Absorbance measurements were conducted at various time intervals.

## 7.4 Oligonucleotides

For all experiments in this section, the general SAM deposition procedure (7.1) was used as the procedure unless otherwise mentioned with the following additions or modifications.

### 7.4.1 Experiment 1

Same procedure as described in Section 7.1.

#### 7.4.2 Experiment 2

Two treated silicon wafers for each nucleotide sample were placed in each of the nucleotide/ deionized water solutions for 7 days. One of the two wafers was rinsed with deionized water after the 7 days. Both wafer samples were nitrogen dried and analyzed for fluorescence and deposition thickness using ellipsometry.

#### 7.4.3 Experiment 3

**Well Plate Modification and Usage.** A Corning round bottom 96 cell well made of polystyrene was modified to accommodate silicon wafers treated with isocyanatopropyl triethoxysilane for nucleotide attachment. The round bottom portion of the cell wells were shaved off (beveled) using a router. The well edges were then smoothed using a Kimwipe<sup>®</sup> towel and cleansed in isopropanol.

The NCO treated silicon wafer samples were then placed on the cell wells (reflective sides down) and kept in place using scotch tape. The wafers were positioned to maximize the area completely covering the most well cells. These cell wells were then filled with the appropriate sample solution. A minimal amount of solution was used; enough to cover the entire silicon surface. The well plate was then placed in an aluminum foil covered Tupperware<sup>®</sup> container and left for a 24 hour period.

**Procedure.** The round-bottom portion of the cell wells was shaved (beveled) level using a router. The well edges were then smoothed using Kim-wipe<sup>®</sup> paper towels and cleansed using isopropanol. Four (4) treated silicon wafers and two (2) cleansed silicon wafers were secured to the non-beveled side of the well plate using scotch tape. The wafers were positioned such that

the scotch tape ran across the etched, non-reflective side of the wafers and taped to the well plate on the non-beveled side, which held the smooth, reflective side snugly to the well plate. An approximate 2.0-mL aliquot of Fmly 2.1 – 2.4 sample solution from Experiment 2 was pipetted into each cell well through the beveled-side opening that covered the silicon surface (one aliquot per wafer). Two untreated, but cleansed, silicon wafers were used as controls. Two wells for each cleansed wafer were used to place the approximate 2.0-mL aliquot into the wells. Fmly 2.1 and 2.2 control samples were labeled 1/2 and Fmly 2.3 and 2.4 were labeled 3 /4. The cell plate was covered with aluminum foil and then placed in aluminum foil-covered Tupperware<sup>®</sup> container and left to bind to the silicon surface for 48 hours at ambient temperature and atmosphere.

The samples were taken out of the Tupperware<sup>®</sup> container, removed from the well plate, rinsed with deionized water, and nitrogen dried. Silicon wafer samples were then placed in aluminum foil-covered glass vials (labeled as control or sample). Due to a 48-hour reaction time, the sample solution had evaporated leaving only a noticeable ring (circle) on the silicon surface. After rinsing with deionized water and nitrogen drying, however, the circles were not as apparent. Samples were analyzed using ellipsometry and fluorescence (FluorImager).

#### 7.4.4 Experiment 4

A Corning round bottom 96 cell well made of polystyrene was modified to accommodate the silicon wafers. The round bottom portion of the cell wells were shaved (beveled) level using a router. The well edges were then smoothed and cleansed using isopropanol.

The treated silicon wafers were secured to the non-beveled side of the well plate using scotch tape. The wafers were positioned such that the scotch tape ran across the etched, non-

reflective side of the wafers and taped to the well plate on the non-beveled side, which held the smooth, reflective side snugly to the well plate. The wafers were positioned over the cell well to maximize the surface area completely covering the most well cells. 100  $\mu$ L of deionized water was pipetted into each SBH sample vial and shaken lightly. After approximately 20-30 seconds of shaking, sample vials were centrifuged for one minute. The 100  $\mu$ L sample solution was then transferred from the vial into marked cell wells using a pipet to completely cover the exposed silicon surface area. The well plate was then placed in aluminum foil-covered Tupperware<sup>®</sup> container and left to bind to the silicon surface for 24 hours at ambient temperature and atmosphere. The samples were then nitrogen dried, placed in separate labeled vials, and analyzed.

Ellipsometry measurements were obtained using a Gaertner Ellipsometer and fluorescence measurements were obtained on a FluorImager II. Ellipsometry readings were produced using Gaertner Automatic Ellipsometry Program.

#### 7.4.5 Experiment 5

Four silicon wafers were used in this experiment. Two were treated with isocyanatopropyl triethoxysilane and two were cleansed with isopropanol, potassium hydroxide and nitric acid. All wafers were dried with nitrogen. The silicon wafers were not immersed in a diluted sample solution. Instead they were secured to a modified 96 well plate by using scotch tape and the sample solution was pipetted onto the surface.

Two sample solutions were prepared in a dark room with minimal light exposure to the fluorescein sample. 1.5 mg of fluorescein was transferred into 1 mL of deionized water and 4.4

mg was transferred into 1 mL of dimethylformamide (DMF). The solutions were contained in 10 mL glass vials covered with aluminum foil.

Aliquots of various amounts were pipetted onto the secured silicon surface using an eppendorf pipet (0-2  $\mu\text{L}$ ) or syringe (25  $\mu\text{L}$ ). This was performed in a photography dark room using only a yellow bulb for the source of light. Both sample solutions were placed on treated and non-treated substrates and stored in an aluminum foil covered Tupperware<sup>®</sup> container for a 24 hour period to allow the solution to dry completely. A detailed description of solution size and observations will be discussed in the data and conclusion sections of this report.

When transferring the samples from the container to the FluorImager SI, light exposure was kept to a minimum. Fluorescence measurements were conducted using a FluorImager SI.

After performing the fluorescence measurements on the 4 fluorescein treated silicon wafers, they were rinsed with approximately 10 mL of solvent (water or DMF depending on the solution solvent). This process was conducted in a short time span with minimal light exposure. The wafers were quickly nitrogen dried (~10 seconds) and then placed in a 6 well plastic tray with a lid overnight (approx. 18 hours). The tray was placed in the aluminum foil covered Tupperware<sup>®</sup> container for storage to reduce light exposure.

#### 7.4.6 Experiment 6

Five NCO treated wafers and 5 cleansed wafers were labeled and secured to the modified 96 well plate with scotch tape. Wafers were secured with the shiny (reflective) side down and orientated in such a fashion that maximum well hole coverage was available.

Sample 3.1 was dissolved with 500  $\mu\text{L}$  DMF and 200  $\mu\text{L}$  water in sample vial. Five hundred  $\mu\text{L}$  ethanol was added to sample number 3.4 vial. A solution of DMF and water (ratio 5:2) containing 4.0 mL of DMF and 1.6 mL of water was prepared and refrigerated until used. Five hundred  $\mu\text{L}$  of this solution was transferred into samples 3.7, 3.10, and 3.12 vials and allowed to sit in a refrigerator over a 3 day period. Samples were gently vortexed for 10 seconds and centrifuged for 30 seconds.

Twenty  $\mu\text{L}$  of sample 3.1 solution was placed into the well containing the labeled silicon wafer cleansed with IPA, KOH, and  $\text{HNO}_3$ . This was repeated for SBH 3.4, 3.7, 3.10, and 3.12 solutions. Forty  $\mu\text{L}$  of sample 3.1 solution was transferred into the well containing the labeled silicon wafer treated with NCO. This was repeated for SBH 3.4, 3.7, 3.10, and 3.12 solutions. Well plate was then placed in aluminum foil covered Tupperware<sup>®</sup> container for a period long enough to allow the solution to evaporate.

#### 7.4.7 Experiment 7

The general SAM deposition procedure (7.1) was used as the procedure in this experiment; however, the SAM deposition reaction occurred in a glass jar. The solution was covered with aluminum foil and sealed with a jar lid. The reaction ran for over a  $\sim 72$  hours at room temperature.

Ten NCO treated wafers were labeled and secured to the modified 96 well plate with scotch tape. The wafers were taped with the reflective side upward while maximizing the silicon surface area unexposed to the tape. SBH 3.1, 3.4, 3.7, 3.10, and 3.12 sample solutions previously prepared from Experiment 5.3.6 were used. A 25  $\mu\text{L}$  syringe was used to transfer 5.0

$\mu\text{L}$  of SBH 3.1 to the upper corner section of one wafer. The aliquot was as uniform and circular as possible. Using a 2.0  $\mu\text{L}$  Eppendorf pipette, 2.0 and 1.5  $\mu\text{L}$  aliquots were made to the same wafer. To another wafer, 1.0, 0.50, 0.25, and 0.10  $\mu\text{L}$  droplets in a row (top to bottom) were transferred using the Eppendorf pipette.

This process was repeated for the remaining 8 wafers using SBH 3.4, 3.7, 3.10, and 3.12 solutions. The syringe was thoroughly cleansed after each use by rinsing it in the following manner: twice with deionized water, twice with ethanol, and twice with deionized water. Also, a new pipette tip was used after each sample transference. The well plate was placed into an aluminum foil covered Tupperware<sup>®</sup> container and allow to air dry over an 18 hour period.

#### 7.4.8 Experiment 8

##### **Materials**

Silicon wafer	Wafernet
Isocyanatopropyl triethoxysilane	United Chemical Co.
Toluene	Aldrich Chemical Co.
Isopropanol	Aldrich Chemical Co.
Potassium Hydroxide	Aldrich Chemical Co.
Nitric Acid	J.T. Baker
Dimethylformamide	Aldrich Chemical Co.
EconoPURE SBH 3.1 oligonucleotide	Keystone Labs

Labeled and transferred two, cleansed and nitrogen dried silicon wafers to a 6 well plate with the reflective sides upward. Repeated for two NCO treated silicon wafers. Pipetted a 2.00  $\mu\text{L}$  aliquot of sample SBH 3.1 solution obtained previously (Experiment 7) onto the cleansed silicon surface under minimal light exposure. The aliquot was transferred such that a uniform, circular droplet was obtained. This was repeated again for the remaining cleansed wafer and two

treated wafers. The well plate was placed into an aluminum foil covered Tupperware<sup>®</sup> container and allowed to air dry over an 18 hour period. Samples were analyzed for fluorescence.

All wafers were then rinsed with ~5 mL of DMF / water (5:2) solution in a dark room (photography room) and allow to air dry momentarily (2 - 5 minutes) and re-analyzed. This process was repeated with a rinse of 20 mL of the same solution while keeping light exposure to a minimum. Wafers were dried with nitrogen immediately following rinsing and transferred into a clean 6 well plate. Samples were again re-analyzed.

#### 7.4.9 Experiment 9

The same procedure that was used for Experiment 8 (7.4.8) was used except that a photography room (dark room) was used when administering the aliquot of oligonucleotide and subsequent washing and drying.

#### 7.4.10 Experiment 10

Labeled and transferred one, cleansed and nitrogen dried silicon wafer and one, NCO-treated silicon wafer onto a Kim-wipe in the aluminum foil covered Tupperware<sup>®</sup> container in dark room using only yellow light to reduce photo bleaching or quenching of the Fluorescein. Wafers were arranged such that the orientation of the 1 inch side is at the top and the 3 inch side is on the sides (i.e. 1 inch at North-South and 3 inch is at East-West directions). A 2.0  $\mu$ L aliquot of SBH 3.1 solution previously prepared in Experiment 9 was placed onto the upper left hand corner of the cleansed silicon wafer. The aliquot was transferred so that a uniform, circular droplet was obtained. This was continued in such a fashion as to create a 3 x 2 aliquot array in



the upper  $\frac{1}{4}$  section of the wafer. This procedure was repeated using SBH 3.10 in the next  $\frac{1}{4}$  section of the wafer, SBH 3.1 in the following  $\frac{1}{4}$  section of the wafer, and ending using SBH 3.10 in the lower  $\frac{1}{4}$  section of the wafer. This procedure was repeated for the 3 x 1 inch NCO-treated silicon wafer. The samples were left in the dark room and kept in a Tupperware<sup>®</sup> container after replacing and securing the lid. Samples were air dried at ambient temperature and atmosphere over an 18 hour period.

The 2, 3x1 inch samples were placed in a cleaned plastic holder tray, reflective side face down and analyzed on the FluorImager SI. After the fluorescence measurement, the samples were rinsed one time with 20 mL of deionized water in the darkroom using only yellow light as the light source. Samples were allowed to air dry at ambient temperature and atmosphere and then were re-analyzed on the FluorImager for fluorescence intensity. The samples were then placed back into the aluminum foil covered plastic holder tray and stored.

#### 7.4.11 Experiment 11

Experiment 10 was repeated without using a fluorescent labeled oligonucleotide. New SBH 3.1 and 3.10 oligonucleotides with the same sequence were obtained and prepared with a concentration similar to that described in Experiment 6 (5.3.6). A stock solution of DMF: deionized water with a ratio of 5:2 (volume:volume) was made and 100  $\mu$ L was transferred into each of the oligonucleotide sample vials. The solvent and solute were shaken by hand to expedite complete solubility.

The cleansed silicon wafer and the NCO-treated silicon wafer were labeled “clean” and “C<sub>3</sub>NCO”, respectively, on the non-reflective sides of the wafers. The wafers were arranged such that the orientation of the 1 inch side is at the top and the 3 inch side is on the sides (i.e. 1 inch at

North-South and 3 inch is at East-West directions). A 2.0  $\mu\text{L}$  aliquot of SBH 3.1 solution was placed onto the upper left hand corner of the cleansed silicon wafer. The aliquot was transferred so that a uniform, circular droplet is obtained. This process was continued in such a fashion as to create a 3 x 1 aliquot array in the upper  $\frac{1}{4}$  section of the wafer. This was repeated using SBH 3.10 in the next  $\frac{1}{4}$  section of the wafer, SBH 3.1 in the following  $\frac{1}{4}$  section of the wafer, and ending using SBH 3.10 in the lower  $\frac{1}{4}$  section of the wafer. This was repeated for the 3 x 1 inch NCO-treated silicon wafer as well. Samples were placed in a clean, aluminum foil-covered Tupperware<sup>®</sup> container and secured with lid. Samples were air dried at ambient temperature and atmosphere over an 18 hour period.

The 2, 3 x 1 inch samples were washed with deionized water by pouring deionized water into the Tupperware<sup>®</sup> container and shaking for 5 minutes. The deionized water was then decanted and the wafers were again submersed in fresh deionized water for another 5 minutes with shaking. The samples were then removed, nitrogen dried, and placed in a clean, dry plastic holder tray. Samples were measured for oligonucleotide thickness coating using an ellipsometer (UV/SEL Spectroscopic Phase Modulated Ellipsometer by ISA Jobin-Yvon-Spex Groupe Instruments S.A.).